Untersuchungen zum Einfluss der Chemokinrezeptoren CCR7 und CCR9 auf die Migration von Immunzellen

Von der Naturwissenschaftlichen Fakultät
der Gottfried Wilhelm Leibniz Universität Hannover
zur Erlangung des Grades eines

DOKTORS DER NATURWISSENSCHAFTEN
Dr. *rer. nat.*

genehmigte Dissertation
von

Dipl.-Biol. Meike Wendland
geboren am 09. Dezember 1976 in Burgwedel

2009

Referent: Prof. Dr. Reinhold Förster

Korreferent: Prof. Dr. Reinhard Schwinzer

Tag der Promotion: 02.02.2009

Erklärung

Hiermit versichere ich, dass ich die vorliegende Arbeit eigenständig verfasst und keine anderen als die angegebenen Quellen und Hilfsmittel verwendet habe, und diese Dissertation nicht schon als Diplomarbeit oder ähnliche Prüfungsarbeit verwendet habe.

Hannover, im Oktober 2008

Zusammenfassung

Leukozyten zirkulieren nach ihrer Entstehung durch das Blut- und das lymphatische System des ganzen Körpers, um möglichst schnell körperfremde Antigene aufzuspüren und eine entsprechende Immunantwort auslösen zu können. Dabei erfolgt die Migration in die lymphatischen Organe nicht zufällig, sondern unterliegt einer direkten Steuerung, an der Chemokine maßgeblich beteiligt sind. Chemokine sind chemotaktische Cytokine, die die Wanderung der Zellen entlang eines Chemokingradienten zum Ort der höchsten Chemokinkonzentration steuern können.

Naive T-Zellen exprimieren den Chemokinrezeptor CCR7 und migrieren unter anderem durch postkapilläre Venolen mit hohem Endothel in sekundäre lymphatische Gewebe.

Um den genauen Einfluss des Chemokinrezeptors CCR7 auf das Migrationsverhalten von Lymphozyten in den Lymphknoten zu studieren, wurde im Rahmen dieser Arbeit eine Maus generiert, in der durch homologe Rekombination das murine CCR7 Gen durch das humane CCR7 Gen ersetzt wurde.

Mit der homologen Rekombination des CCR7 Allels wurde gleichzeitig die als Selektionsmarker fungierende PgK-NEO-Kassette in das Genom der Maus integriert. Die PgK-NEO-Kassette unterdrückte die Expression des humanen CCR7 und führte so in der Maus zu einem CCR7 Knock-out Phänotyp.

Die PgK-NEO-Kassette wird beidseitig von LoxP-Erkennungssequenzen flankiert, die es ermöglichten, die PgK-NEO-Kassette mit Hilfe des Cre/LoxP-System zu entfernen.

Durch Verpaarungen dieser transgenen Mäuse mit einem zweiten transgenen Mausstamm, im dem die Cre-Rekombinase unter Kontrolle des CD4 Promotors exprimiert wird, konnten Mäuse erzeugt werden, die den humanen Chemokinrezeptor CCR7 selektiv nur auf T-Zellen exprimieren, während alle anderen Zellen CCR7-defizient bleiben.

In dieser Arbeit wurde herausgefunden, dass die Expression von CCR7 auf den T-Zellen alleine nicht ausreicht, um die Homöostase der Wanderung zu gewährleisten. Vielmehr zeigte sich in den peripheren Lymphknoten der Mäuse eine verminderte Konzentration des Chemokins CCL21, Ligand des Chemokinrezeptors CCR7. Dies könnte darauf zurück geführt werden, dass die CCR7-defizienten dendritische Zellen nicht in den Lymphknoten einwandern können, um dort das von den Stromazellen gebildete CCL21 zu binden.

Die geringe Konzentration des Chemokins CCL21 führt dazu, dass die T-Zellen den Lymphknoten schneller verlassen, als dass neue T-Zellen einwandern können. Dies führt zu einer Reduktion von T-Zellen im Lymphknoten.

Ein weiterer Chemokinrezeptor, CCR9, ist dagegen ein wichtiger Migrationsfaktor für die Wanderung von Immunzellen in den Darm.

Der Ligand des Rezeptors CCR9, das Chemokin CCL25, wird unter anderem im Epithel des Dünndarms exprimiert. Das Oberflächenepithel des Darms stellt eine der wichtigsten Kontaktstellen des Körpers mit Bakterien, Viren und anderen körperfremden Antigenen dar. Um einer Infektion vorzubeugen, benötigt es daher einen effektiven Schutz. Dazu liegen in der *Lamina propria* und im Epithel der Mukosa eine Vielzahl von Immunzellen vor.

In dieser Studie wurde insbesondere eine Subpopulation der dendritischen Zellen genauer untersucht. Dabei handelt es sich um die intestinalen plasmazytoiden dendritischen Zellen (pDC). Es stellte sich heraus, dass CCR9 eine entscheidende Rolle bei der Migration der pDC in den Dünndarm spielt. Zusätzlich konnte die wichtige Bedeutung der pDC zur schnellen Mobilisierung der in der *Lamina propria* ansässigen myeloiden dendritischen Zellen (mDC) entschlüsselt werden.

Stichwörter: CCR7, CCR9, plasmazytoide dendritische Zellen

Abstract

After their development leucocytes circulate through the blood and the lymphatic system to track down foreign antigens as fast as possible and to induce an immune response. The migration into the lymphatic organs underlies a strict control that is caused by chemokines. These chemokines are small chemotatic molecules that effect the migration of leucocytes by means of a chemokine gradient.

Naïve T-cells express CCR7 and migrate via high endothelial venules (HEV) into secondary lymphatic tissue. To investigate the influence of CCR7 on the migration of lymphocytes, mutant mice were generated. The murine CCR7 gene was substituted by the human CCR7 gene by homologous recombination.

Together with the homologous recombination of the CCR7 allel, the PgK-NEO-cassette used as a selection marker, was integrated into the genome of the mouse. The PgK-NEO-cassette disabled the expression of human CCR7. This in turn led to knock-out phenotype of the mouse.

The PgK-NEO-cassette is flanked on both sides by LoxP-sites. This allowed the removal of the PgK-NEO-cassette by means of the cre/LoxP-system.

Breeding the mutant mice with CD4-Cre-deleter mice generated mice that expressed the human CCR7 chemokine receptor selectively on T-cells while all other cells possessed a knock-out phenotype.

It was concluded that the expression of CCR7 on T-cell is not sufficient to ensure the homeostasis of migration. Rather, this study has shown that there is less CCL21 concentraion in the lymph node. This might be due to the interruption of the CCR7-dependent migration of dendritic cells into the lymph node where the dendritic cells bound the CCL21. The low concentration of CCL21 leads to a rapid departure of T-lymphocytes out of the lymph node. The immigration of T-cells into the lymph node is not fast enough, and new T-cells are, thus, not able to enter the lymph node.

In contrast, CCR9 is an important factor for the migration of cells into the small intestine. The ligand of CCR9, the chemokine CCL25, is mainly expressed by the epithelium of the small intestine. Since the surface of the intestine is one of the largest ports of entry for bacteria, viruses, and other foreign antigens, this epithelium needs well organized protection. For that purpose a variety of immune cells are present in the *lamina propria* and in the epithelium of the mucosa.

In this study, plamacytoid dendritic cells were particulary investigated. It was discovered that CCR9 plays a crucial role in migration of pDC to the small intestine. Additionally, the important role of pDC for rapid mobilization of *lamina propria* mDC could be identified.

Keywords: CCR7, CCR9, plasmacytoid dendritic cells

Inhaltsverzeichnis

Zusammenfassung I

Abstract III

Inhaltsverzeichnis V

Abkürzungsverzeichnis VII

1. Einleitung 1

1.1 Chemokine und Chemokinrezeptoren 1

1.1.1 Der Chemokinrezeptor CCR9 2

1.1.2 Der Chemokinrezeptor CCR7 4

1.2 CCR7-vermittelte Migration naiver T-Zellen 5

1.2.1 Einwanderung der T-Zellen in den Lymphknoten mittels der mehrstufigen Adhäsionskaskade 5

1.2.2 CCR7-abhängige Verweildauer von T-Zellen im Lymphknoten 6

1.3 Dendritische Zellen 9

1.3.1 CCR7 organisiert die Migration Dendritischer Zellen aus der Peripherie in die T-Zellzone der Lymphknoten 9

1.3.2 Plasmazytoide dendritische Zellen 9

1.4 Aufgabenstellung 10

2. Diskussion 11

2.1 Der Chemokinrezeptor CCR9 trägt zur Lokalisation von Plasmazellen in den Dünndarm bei 11

2.2 CCR9 ist ein Migrationsfaktor, der plasmazytoide dendritische Zellen in den Dünndarm leitet 11

2.2.1 Charakterisierung und Lokalisation der pDC im Dünndarm der Maus 11

2.2.2 Die Migration der pDC in den Dünndarm ist CCR9-abhängig 13

2.2.3 pDC-abhängige Mobilisierung von myeloiden mDC aus der Lamina propria 14

2.2.4 Ausblick 16

2.3 Die Einwanderung naiver T-Zellen ist CCR7/CCL21-abhängig………………. 17

2.3.1 Humanes CCR7 kann die Funktion des murinen CCR7 übernehmen 17

2.3.2 Generierung eines konditionalen CCR7-*Knock-ins* auf CCR7-defizientem Hintergrund 18
2.3.3 Eingeschränkte Migration von T-Zellen in T-CCR7-*Knock-in* Mäusen 18
2.3.4 Reduzierte Größe der Lymphknoten in T-huCCR7ki Mäusen 18
2.3.5 Die Zellzahl in den Lymphknoten ist abhängig von der Einwanderung dendritischer Zellen 20
2.3.6 Das Chemokin CCL21 hält T-Zellen im Lymphknoten zurück 21
2.3.7 Ausblick 23

3. Anhang

3.1 Referenzen 25
3.2 Danksagung 31
3.3 Eigene Publikationen 33

1. Chemokine Receptor CCR9 Contributes to the Localization of Plasma Cells to the Small Intestine
2. CCR9 is a homing receptor for plasmacytoid dendritic cells to the small intestine
3. A CCR7-dependent steady state homing of dendritic cells essentially required for lymph node T cell homeostasis

3.4 Lebenslauf

Abkürzungsverzeichnis

CCL	CC-Chemokinligand
CCR	CC-Chemokinrezeptor
CD	cluster of differentiation - Differenzierungscluster
CpG	Cytosin-phosphatidyl-Guanosin
CXCR	CXCR-Chemokinrezeptor
DNS	Desoxyribonukleinsäure
GAG	Glykosaminoglykane
HEV	High endothelial venule - postkapilläre Venolen mit hohem Endothel
i.v.	intravenös
ICAM	intercellular adhesion molecule – interzelluläres Adhäsionsmolekül
IEL	Intraepitheliale Lymphozyten
LPL	*Lamina propria* Lymphozyten
IFN	Interferon
IgA	Immunglobulin A
IL	Interleukin
IPC	Interferon producing cell – Interferon produzierende Zelle
kDa	Kilo Dalton
ki	Knock-in
LFA	lymphocyte function-associated antigen – funktionelle Leukozytenantigene
LPS	Lipopolysaccharide
mDC	myloid dendritic cell - Myeloide dendritische Zelle
MHC	Major Histocompatibility Complex - Haupthistokompatibilitätskomplex
M-Zelle	Microfold cell
NEO	Neomycin
PBS	hosphate buffered saline - Phosphat-gepufferte Salzlösung
pDC	Plasmacytoid dendritic cell – plasmazytoide dendritische Zelle
PgK	Phosphoglycerate Kinase
PNAd	peripheral node adressin - peripheres Lymphknotenaddressin
RNS	Ribonukleinsäure
S1P1	Sphingosin-1-Phosphat Rezeptor 1
TCR	T-cell receptor – T-Zellrezeptor

TLR	Toll-like-Rezeptor
TNF	Tumornekrosefaktor
VEGF	Vascular Endothelial Growth Factor - vaskulo-endothelialer Wachstumsfaktor

1. Einleitung

Immunzellen sind migratorische Zellen, die im ganzen Körper verteilt vorliegen. Das ständige Zirkulieren durch den Körper und die damit verbundene große Präsenz in den unterschiedlichen lymphatischen und nicht-lymphatischen Geweben ist wichtig, weil Pathogene und fremde Antigene jederzeit an den unterschiedlichsten Orten in den Körper eindringen können. Dies wird besonders bei den mukosalen Oberflächen, wie z.B. der Darmschleimhaut, deutlich, in der eine Vielzahl von Bakterien, die in ihrer Anzahl die Zellen des Körpers deutlich übersteigen, nur durch eine einzige Schicht von Epithelzellen vom Körperinneren getrennt wird (1). Immunzellen sind nicht zufällig im Körper verstreut: Insbesondere Zellen des adaptiven Immunsystems füllen ein komplexes System sekundärer lymphatischer Organe, wie Lymphknoten, Milz und Peyersche Platten, in denen die Immunantwort kontrolliert wird (2).

Naive T-Zellen reifen in den primären lymphatischen Organen und zirkulieren danach mit dem Blut durch die sekundären lymphatischen Organe. Dort treffen sie auf Antigene, die von Antigen-präsentierenden Zellen in der Peripherie aufgenommen und in die sekundären lymphatischen Organe transportiert wurden (3). Dies ermöglicht die Aktivierung der antigenspezifischen Lymphozyten und ein Ingangsetzen der adaptive Immunantwort, mit dem Ziel, die gebildeten Effektorzellen gezielt zum Entzündungsherd zu führen.

Für alle Wanderungsschritte benötigt die Zelle Chemokine als Wegweiser, die ihnen nicht nur den Weg in die lymphatischen und nicht-lymphatischen Organe zeigen, sondern die ihnen auch ihren Platz in den Kompartimenten innerhalb der Organe und deren Mikrostruktur zuweisen.

1.1 Chemokine und Chemokinrezeptoren

Chemokine und ihre Rezeptoren sind die Schlüsselfaktoren bei der fein abgestimmten Migration von Leukozyten in lymphatisches und nicht-lymphatisches Gewebe (4, 5).

Sie sind chemotaktischen Cytokine von etwa 8 –14 kDa, die von unterschiedlichen Zellen des Körpers freigesetzt werden können. Chemokine werden, wie die Cytokine, von Leukozyten und Gewebezellen unter konstitutiven oder inflammatorischen Bedingungen sezerniert und können auf diese Weise eine auto-, para- oder endokrine Wirkung entfalten (6, 7).

Dabei werden die Chemokine von den entsprechenden Chemokinrezeptoren der Zielzellen erkannt und tragen auf diese Weise zur Entwicklung, Homöostase und Funktion des Immunsystems bei (4, 8, 9).

Das Zusammenspiel der großen Anzahl von Chemokinen mit ihren Rezeptoren bildet ein komplexes Netzwerk, das nicht nur die Einwanderung der verschiedenen Zellpopulationen in die Makrostrukturen, wie z.B. Lymphknoten oder Milz organisiert, vielmehr kontrollieren die Chemokin-vermittelten Signale zusätzlich die Positionierung der Immunzellen in definierte, funktionelle Kompartimente (Mikroarchitekturen).

Die meisten Chemokinrezeptoren verfügen über mehr als einen Liganden. Der Chemokinrezeptor CCR9 jedoch interagiert, soweit bisher bekannt, lediglich mit einem einzigen Linganden: dem Chemokin CCL25 (10).

1.1.1 Der Chemokinrezeptor CCR9

Die Expression des Chemokins CCL25 wurde erstmals bei dendritischen Zellen in der Medulla des Thymus nachgewiesen (11). Es konnte jedoch kurz darauf gezeigt werden, dass es auch von den Epithelzellen in Kortex und Medulla des Thymus und von den Epithelzellen des Dünndarms exprimiert wird (12), nicht jedoch vom Dickdarmepithel oder anderem Gewebe (12).

Im Thymus trägt die Mehrzahl der CD4/CD8-doppeltpositiven Thymozyten CCR9, während beim Wechsel der Zellen zum Stadium der CD4- oder CD8-einzelpositiven Thymozyten CCR9 herab reguliert wird (12).

Der Dünndarm beinhaltet in jeder einzelnen Zotte eine Vielzahl von Immunzellen. Dabei unterscheidet man zum einen die Immunzellen, die zwischen den Enterozyten liegen, die intraepithelialen Lymphozyten (IEL; Abb.1), und zum anderen die Immunzellen, die unterhalb des Epithels in der *Lamina propria* liegen, den *Lamina propria* Lymphozyten (LPL; Abb.1).

Es besteht eine direkte Korrelation zwischen der Expression von CCR9 auf intestinalen Immunzellen und dem Migrationsverhalten dieser Zellen in den Darm (10, 13).

Auf nahezu allen T-Zellen der IEL und LPL der *Lamina propria* wird der Chemokinrezeptor CCR9 exprimiert, wohingegen im Blut nur von einem sehr geringen Teil der T-Zellen CCR9 gebildet wird (14, 15). Die Rolle der Wechselwirkung zwischen CCR9 und CCL25 wird deutlich, wenn CCL25 durch die Verabreichung von Antikörpern blockiert wird. T-Zellen können in diesem Fall nicht mehr effizient in den Darm wandern (16).

CCR9-defiziente Mäuse weisen eine Reduktion an intraepithelialen T-Zellen auf. Die große Mehrheit der CD8αα $TCR\alpha\beta^+$ und CD8αα $TCR\gamma\delta^+$ IEL exprimiert CCR9 und migriert in chemotaktischen *in vitro* Migrationsexperimenten auf CCL25 (17). Des Weiteren konnte gezeigt werden, dass IgA-produzierende Plasmazellen aus Milz, Peyerschen Platten und mesenterischen Lymphknoten in hohem Maße auf CCL25 migrieren (15). Plasmazellen werden in großer Anzahl in die *Lamina propria* des Darms rekrutiert. Dabei wird zwischen IgA^+ $B220^{int}$ und IgA^+ $B220^-$ Plasmazellen unterschieden. Plasmazellen, die B220 in intermediärem Maße exprimieren, wandern deutlich besser auf CCL25 als Plasmazellen ohne B220-Expression. Bowman et al. führen dies darauf zurück, dass IgA^+ $B220^-$ Plasmazellen ihr endgültiges Ziel erreicht haben und dadurch kein Bedarf mehr an dem Migrationsrezeptor besteht (15).

Die ausgereiften B-Zellen verlassen die Peyerschen Platten oder den mesenterischen Lymphknoten und migrieren mit Hilfe von CCR9 in die *Lamina propria* des Dünndarms.

Bereits vor über 40 Jahren konnte festgestellt werden, dass IgA den Hauptanteil des Immunglobulin-Isotyps ausmacht (18).

Den größten Teil der *Lamina propria* Zellen machen die dendritischen Zellen und die Makrophagen aus (19). Es wird sogar beschrieben, dass die mDC der *Lamina propria* in der Lage sind die *Tight Junctions* zwischen den Epithelzellen durchdringen, um Dendriten in das Lumen des Darms zu senden (Abb.1). Mit diesen sind sie in der Lage von dort direkt z.B. Bakterien aufzunehmen und zu prozessieren. Diese Eintrittsroute für Bakterien ist völlig unabhängig von den auf transzytotische Transportfunktionen spezialisierten M-Zellen der Peyerschen Platten (20).

Zusammenfassend lässt sich sagen, dass CCR9 ein wichtiger Migrationsfaktor ist, um Immunzellen in peripheres Gewebe, wie es der Darm darstellt, zu leiten. Die Einwanderung der Zellen in die sekundären lymphatischen Gewebe wie Lymphknoten wird jedoch von einem anderen wichtigen homöostatisch exprimierten Chemokinrezeptor gesteuert. Dabei handelt es sich um den Chemokinrezeptor CCR7 und seine konstitutiv exprimierten Liganden CCL19 und CCL21.

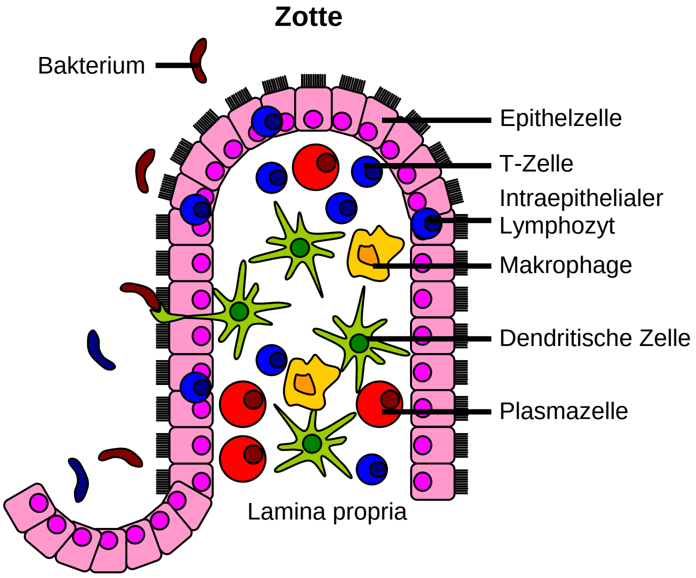

Abbildung 1: Schema einer murinen Dünndarmzotte. Das Lumen des Darms wird durch nur eine Schicht Epithelzellen vom Körper getrennt. Zwischen den Epithelzellen finden sich Immunzellen, fast ausschließlich T-Zellen, die in ihrer Gesamtheit IEL (Intraepitheliale Lymphozyten) genannt werden. In der *Lamina propria* dagegen befinden sich Blut- und Lymphgefäße und eine Vielzahl verschiedener Zellen.

1.1.2 Der Chemokinrezeptor CCR7

Der Chemokinrezeptor CCR7 und seine beiden einzigen Liganden, die konstitutiv exprimierten Chemokine CCL19 und CCL21, regulieren die Zellwanderung während der Homöostase (21). Sie werden von einer Reihe verschiedener Zellpopulationen, wie den Stromazellen der T-Zellzone (22), den Thymozyten, während bestimmter Stadien ihrer Entwicklung (23), naiven B- und T-Zellen (24, 25) und Subpopulationen von Gedächtnis-T-Zellen (25) exprimiert.

CCR7 und seine Liganden konnten als entscheidende Migrationsfaktoren bei der Einwanderung von T-Zellen und dendritischen Zellen in die Lymphknoten identifiziert werden (26).

In CCR7-defizienten Mäusen zeigt sich eine gravierende Reduktion der T-Zellen in Lymphknoten und Peyerschen Platten (26). Auch die Aufteilung in strukturierte Kompartimente, wie B-Zellzone und T-Zellzone, ist gestört. Transferiert man CCR7-defiziente T-Zellen in Wildtyp-Empfänger, sind sie nicht in der Lage in die Lymphknoten einzuwandern. In der Milz lassen sich die transferierten Zellen in der roten Pulpa, jedoch nicht in der weißen Pulpa finden (26).

Die Migration von T-Zellen in den Lymphknoten findet über postkapilläre Venolen mit hohem Endothel (HEV – high endothelial venules) statt (27).

1.2 CCR7-vermittelte Migration naiver T-Zellen

1.2.1 Einwanderung von T-Zellen in den Lymphknoten mittels der mehrstufigen Adhäsionskaskade

Die Migration von T-Zellen in den Lymphknoten wird am besten anhand eines Mehrstufenmodells beschrieben, in dessen Ablauf verschiedene Adhäsionsmoleküle sowie Chemokine involviert sind. Sie erlauben den Eintritt der T-Zellen aus dem Blut über HEV in den Lymphknoten (27, 28). Die HEV sind postkapilläre Venolen, die sich durch einen sehr kleinen Gefäßdurchmesser auszeichnen (29). Da die Fließgeschwindigkeit in diesen dünnen Gefäßen sehr hoch ist und somit ernorme Scherkräfte auf den Zellen lasten, ist ein einfacher Durchtritt der Zellen durch die Gefäßwand nicht möglich. Daher wird eine Abbremsung der Zellen im Blutstrom über Adhäsion benötigt, was zu einem Rollen entlang der Gefäßwand führt. Dadurch ist die Aktivierung und feste Bindung möglich, die letztendlich zum Durchtritt der Zelle durch die Gefäßwand führt (30).

Die Adhäsion der Lymphozyten an das Endothel der HEV wird von Selektinen vermittelt (31). Alle Selektine sind Zelloberflächenmoleküle, die eine Grundstruktur gemeinsam haben. Diese unterscheidet sich nur in den extrazellulären Abschnitten der Lektindomänen. Diese Domänen binden jeweils an ein spezifisches Kohlenhydratmolekül (sulfatisiertes Sialyl-Lewis^{x}) der Zelloberfläche (32). L-Selektin bindet im peripheren Lymphknoten an das Adressin PNAd (peripheral-node addressin; ref. 30, 33). Allerdings ist die Bindung zu locker, um eine feste Adhäsion an die Gefäßwand zu garantieren (Abb.2, Abbremsen und Rollen). Die Zellen lösen sich und gehen gleichzeitig neue Bindungen ein, was zu einem langsamen Rollen entlang der Gefäßwand führt. Eine feste Bindung und somit eine Arretierung der Zellen kann erst durch Integrine, wie LFA-1 vermittelt werden (Abb.2; ref. 34). Diese müssen jedoch zuvor Signale zur Konformationsänderung erhalten, um eine feste Bindung mit den Liganden ICAM-1,2 eingehen zu können (35). Das benötigte Signal kann von dem Chemokine CCL21, das an der Endotheloberfläche der Gefäßwand gebunden ist und von Stromazellen in der T-Zellzone sezerniert wird, ausgelöst werden (Abb. 2, Aktivierung; ref. 36). Das Chemokin wird von dem Chemokinrezeptor CCR7 der migrierenden Zellen erkannt und führt dort zu einer erhöhten Affinität der Integrine zu ihren Liganden an der

Endothelwand (Abb.2, Bindung; ref. 37). Nachdem die Zelle an der Endothelwand festen Halt über die Integrine gefunden hat, kann sie das Endothel durchdringen und dem Chemokingradienten im Inneren des Lymphatischen Gewebes zu ihrem Bestimmungsort folgen (Abb.2, Transmigration).

CCR7 ist nicht nur an der Einwanderung von Lymphozyten in Lymphgewebe beteiligt, sondern begünstigt auch die Beweglichkeit von T-Zellen innerhalb der T-Zellzone (38, 39).

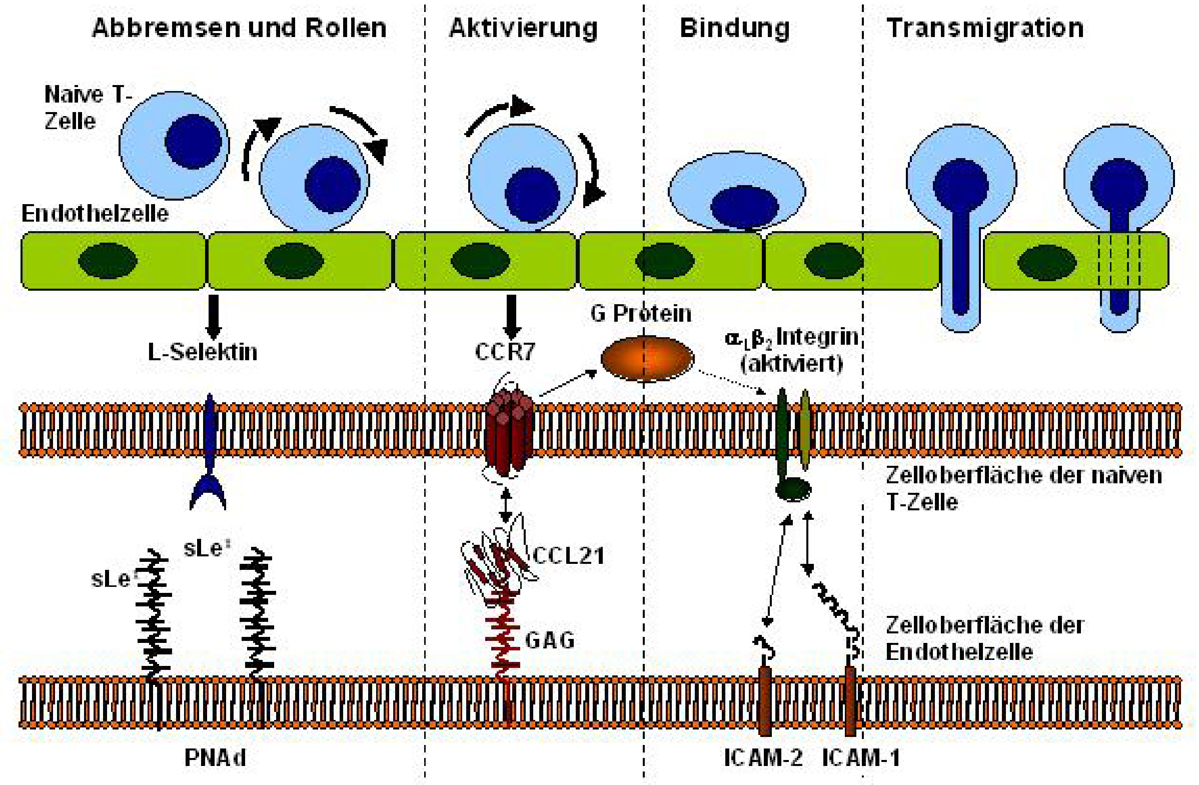
Abbremsen und Rollen
Aktivierung
Bindung
Transmigration
Naive T-Zelle
Endothelzelle
L-Selektin
CCR7
G Protein
$\alpha_L\beta_2$ Integrin (aktiviert)
Zelloberfläche der naiven T-Zelle
sLe^x
sLe^x
CCL21
GAG
Zelloberfläche der Endothelzelle
PNAd
ICAM-2
ICAM-1

Abbildung 2: Modifiziertes Schema der mehrstufigen Adhäsionskaskade (nach Ulrich H. von Andrian und Charles R. Mackay, The New England Journal of Medicine, 2000). Das Bild zeigt naive T Lymphozyten, die durch die HEV in die peripheren Lymphknoten einwandern. Dabei werden sie von Selektinen locker gebunden, was zu einer Abbremsung und einem langsamen Rollen der Zellen entlang des Endothels führt. Im weiteren Verlauf werden die Zellen durch Chemokine aktiviert, was zu einer Konformationsänderung der Integrine führt. Infolgedessen werden die Zellen fest an die HEV gebunden und können in den Lymphknoten einwandern. Dabei können die Lymphozyten zwischen zwei Wegen der Transmigration wählen: der parazellulären Migration zwischen den Endothelzellen hindurch und der transzellulären Migration, bei der sie durch das Zytoplasma der Endothelzellen stoßen.

1.2.2 CCR7-abhängige Verweildauer von T-Zellen im Lymphknoten

Während die Einwanderung der Zellen in den Lymphknoten gut untersucht ist, ist die Kenntnis über deren Auswanderung bisher begrenzt. Die Lymphozyten verlassen die Lymphknoten und die Peyerschen Platten durch die efferente Lymphe, während die Auswanderung aus der Milz zusammen mit dem Blut erfolgt (40). Die Austrittspforte der Immunzellen aus dem Lymphknoten sind efferente Lymphgefäße, die sich an den Marksinus anschließen (Abb.3; ref. 41, 42).

Als ein wichtiger Faktor, der bei der Emigration von Immunzellen eine Rolle spielt, konnte Sphingosin-1-Phosphat (S1P) identifiziert werden (43, 44). Dabei wurde in Studien festgestellt, dass der S1P Rezeptor-1 ($S1P_1$) für die Auswanderung von Lymphozyten aus dem Thymus und aus peripheren lymphatischen Organen notwendig ist (43, 44). $S1P_1$ ist ein Rezeptor, der Signale mittels der Gαi-Untereinheit der G-Proteine weiterleitet (45).

Cyster et al. konnten kürzlich nachweisen, inwiefern $S1P_1$ die Auswanderung von Lymphozyten unterstützt. Dabei ist wichtig zu wissen, dass die Verweildauer der Lymphozyten im Lymphknoten CCR7-abhängig ist (46). CCR7 hält die Lymphozyten im Lymphknoten zurück und verhindert deren Emigration. Dies zeigte sich in Experimenten mit CCR7-defizienten Immunzellen. Nach dem Transfer von CCR7-defizienten Zellen und Wildtyp-Zellen in Wildtyp-Mäuse, konnte gezeigt werden, dass CCR7-defiziente Lymphozyten die peripheren Lymphknoten deutlich schneller wieder verlassen, als es bei den ko-transferierten Kontrolllymphozyten der Fall war (46). Damit ist CCR7 ein direkter Gegenspieler zu $S1P_1$. Pham et al. nehmen an, dass die $S1P_1$-vermittelte Auswanderung durch die Herabregulierung des CCR7, wie sie in aktivierten T-Zellen stattfindet, und durch die Inhibierung der Gα1-Proteine unterstützt wird (46). Zusammenfassend lässt sich sagen, dass die Entscheidung darüber, ob der Lymphozyt den Lymphknoten verlässt oder noch länger in ihm verweilt, davon abhängig ist, welches Signal zu dem jeweiligen Zeitpunkt stärker auf die Zelle wirkt.

CCR7 ist aber nicht nur ein wichtiger Migrationsfaktor für T- und B-Zellen, sondern vermittelt auch die Migration reifer dendritischer Zellen in den Lymphknoten (26, 47).

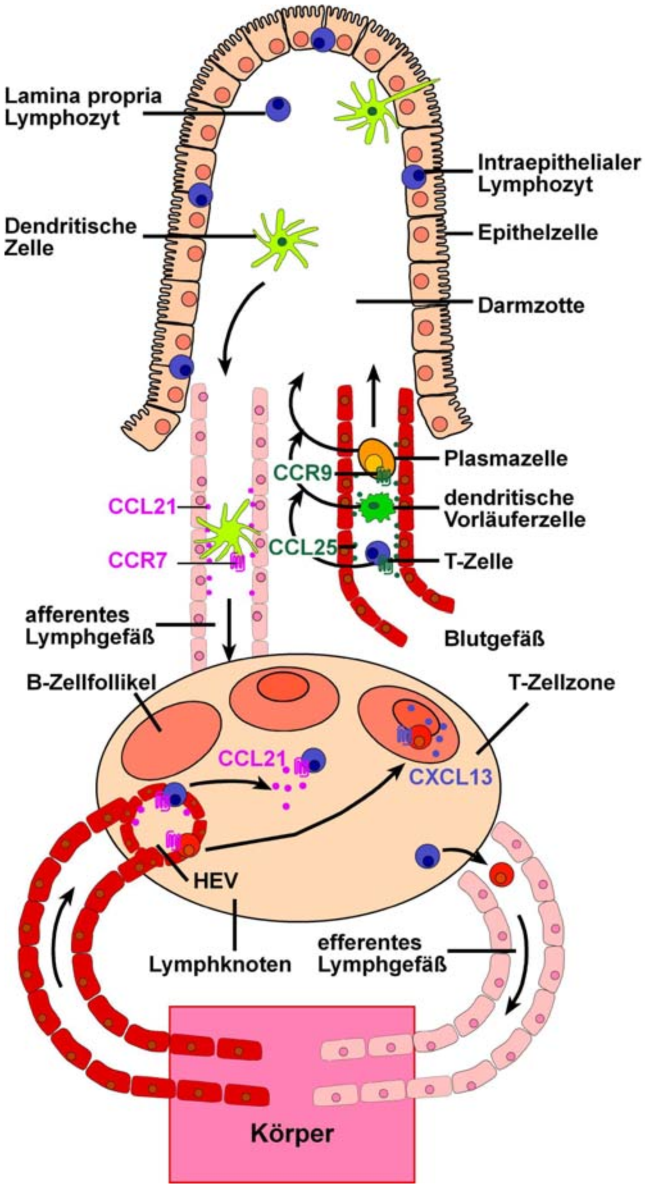
Lamina propria
Lymphozyt
Intraepithelialer
Lymphozyt
Dendritische
Zelle
Epithelzelle
Darmzotte
CCR9
Plasmazelle
CCL21
dendritische
Vorläuferzelle
CCL25
CCR7
T-Zelle
afferentes
Lymphgefäß
Blutgefäß
B-Zellfollikel
T-Zellzone
CCL21
CXCL13
HEV
Lymphknoten
efferentes
Lymphgefäß
Körper

Abbildung 3: Schematisch dargestellte Funktion der homöostatisch exprimierten Chemokine CCL21 und CCL25 in der Migration von Immunzellen im intestinalen Immunsystem. CCR9 leitet die Migration verschiedener Immunzellen über die Blutgefäße in die Darmmukosa, während CCR7 aktivierte dendritische Zellen durch Lymphgefäße in den drainierenden Lymphknoten leitet. In den Lymphknoten selbst gelangen B- und T- Zellen durch die CCR7-vermittelte Migration durch die HEV, wohingegen sie ihn durch efferente Lymphgefäße wieder verlassen.

1.3 Dendritische Zellen

1.3.1 CCR7 organisiert die Migration Dendritischer Zellen aus der Peripherie in die T-Zellzone der Lymphknoten

Dendritische Zellen sind auf das Präsentieren von Antigen spezialisierte Zellen, die Antigen in nicht-lymphatischen Gewebe aufnehmen, prozessieren und in die drainierenden Lymphknoten wandern, um es dort den T-Zellen zu präsentieren (48).

Die unreifen mDC finden sich in nicht-lymphatischen Geweben und auf der Oberfläche von Organen, um ihre Umgebung nach Antigenen abzusuchen. Auch in der Kuppelregion der Peyerschen Platten findet man mDC, die dort Antigen aufnehmen, das via Transzytose von den M-Zellen aus dem Lumen an sie weitergegeben wird (49).

Im Gewebe nehmen mDC über Pinozytose, Endozytose und Phagozytose Antigene auf, bauen diese zu Proteinen um und laden diese auf Haupthistokompatibilitätskomplex (major histocompatibility complex – MHC), um diesen Peptid-MHC-Komplex zur Zellmembran zu schicken (49).

Haben die mDC einmal Antigen aufgenommen, beginnen sie zu reifen. Durch die Reifung wird der Chemokinrezeptor CCR7 hochreguliert, was eine Migration in das sekundäre lymphatische Gewebe ermöglicht (Abb.3; ref. 50). Anders als Lymphozyten, die mittels der HEV in den Lymphknoten gelangen, migrieren mDC durch das afferente Lymphgefäßsystem in den Lymphknoten und weiter in die T-Zellzone des lymphatischen Gewebes (Abb. 3).

Dort treffen sie auf die ständig durch die Lymphknoten zirkulierenden naiven T-Zellen. Erkennen die T-Zellen ihr spezifisches Antigen auf den mDC, werden sie aktiviert und reifen zu Effektor-T-Zellen heran.

1.3.2 Plasmazytoide dendritische Zellen

Vor einigen Jahren konnte eine neue Subpopulation der mDC identifiziert werden. Dieser Subpopulation wurde später der Name „plasmazytoide dendritische Zellen“ gegeben. Sie wurden erstmals 1958 von den beiden Pathologen Lennert und Remmele als eine Zellpopulation in der T-Zellzone humaner Lymphknoten beschrieben, die zwar eine plasmazellartige Morphologie aufwiesen, jedoch keine bekannten Marker für Plasmazellen oder B-Zellen exprimierten (51).

Im weiteren Verlauf wurden diesen Zellen verschiedene Namen gegeben, wie „T-Zell-assoziierte Plasmazellen“ (52), „plasmazytoide T-Zellen“ (53) und „plasmazytoide

Monozyten“ (54). Doch erst in den späten 1990er Jahren kam man der Funktion der Zellen auf die Spur, nachdem es gelungen war, sie zu isolieren und zu kultivieren. So fand man erstmals heraus, dass sie in der Lage waren, große Mengen Interferon-alpha (IFN-α) nach viraler Infektion zu produzieren und *in vitro* zu mDC zu differenzieren (55, 56).

Heute wird die Zelle aufgrund ihrer Morphologie als plasmazytoide dendritische Zelle (pDC; ref. 57) oder auch basierend auf ihrer Eigenschaft große Mengen an INF-α zu produzieren „IFN-produzierende Zelle“ (IFN-producing cell, IPC; ref. 58) genannt.

Zunächst wurden pDC nur im Menschen beschrieben. Ihre Abstammung wurde als lymphoid und nicht myeloid angesehen, da sie viele der typischen myeloiden Antigene wie CD11b, CD13, CD14 und CD33 nicht exprimierten und keine phagozytotische Aktivität aufwiesen (59). Im Menschen werden pDC als CD4^{+} CD11c^{-} lin^{-} (CD3, CD14, CD16, CD19, CD56) Zellen mit plasmazellartiger, glatter und runder Morphologie mit einem nierenförmigen Zellkern beschrieben (59, 60).

Im Jahr 2001 wurden pDC dann erstmals auch im lymphatischen Gewebe der Maus gefunden (57, 58). Murine pDC zeigen die gleichen morphologischen Eigenschaften wie humane pDC, sie werden jedoch am besten durch die Expression der Marker CD11c^{int}B220^{+}Ly6c^{+} beschrieben (57). Ähnlich wie B- und T-Zellen migrieren pDC durch die HEV, um sich in der T-Zellzone zu positionieren.

1.4 Aufgabenstellung

Es gibt bereits viele Untersuchungen zur Migration von Immunzellen in lymphatisches und nicht-lymphatisches Gewebe. Sie liefern einen guten Überblick, jedoch ist die Aufgabe der Chemokinrezeptoren CCR7 und CCR9 im Detail noch nicht verstanden.

Ziel dieser Arbeit war es, die Funktion des Chemokinrezeptors CCR7 bei der Migration von T-Zellen zu entschlüsseln. Dabei sollte insbesondere untersucht werden, wie sich CCR7-positive T-Zellen in einem CCR7-defizienten Organismus verhalten. Um dies zu klären, sollte eine Maus generiert werden, die ausschließlich auf den T-Lymphozyten CCR7 exprimiert, während alle übrigen Zellen defizient für CCR7 sind.

Der zweiter Teil dieser Arbeit befasste sich mit der CCR9-abhängigen Migration von Immunzellen in den Dünndarm der Maus. Hierbei wurde insbesondere eine Subpopulation der dendritischen Zellen untersucht, die plasmazytoiden dendritischen Zellen.

2. Diskussion

2.1 Der Chemokinrezeptor CCR9 trägt zur Lokalisation von Plasmazellen in den Dünndarm bei

Es konnte gezeigt werden, dass Plasmazellen CCR9 exprimieren und *in vitro* auf CCL25 migrieren (15). Pabst et al. konnten nun verdeutlichen, dass die Einwanderung von Plasmazellen in die *Lamina propria* des Dünndarms von CCR9-defizienten Mäusen gestört ist. Dies führt zu einer reduzierten Anzahl von IgA-produzierenden Plasmazellen innerhalb der *Lamina propria*. Als unmittelbare Folge der Reduktion von IgA^+-Plasmazellen kann in diesen Tieren keine ausreichende Immunantwort auf orale Antigene erzielt werden.

Der Aufbau und die Zellzusammensetzung der Peyerschen Platten sind in CCR9-defizienten Tieren jedoch nicht beeinträchtigt. Die Mobilisierung von mDC in der subepithelialen Region der Peyerschen Platten durch die orale Verabreichung von Choleratoxin ist in Mutanten und Wildtypen gleichermaßen möglich. Die Aktivierung naiver B-Zellen sollte demnach auch in CCR9-defizienten Tieren möglich sein. Es konnte gezeigt werden, dass die Bildung von IgA^+ Plasmazellen unbeeinflusst von der CCR9-Defizienz ist (61).

2.2 CCR9 ist ein Migrationsfaktor, der plasmazytoide dendritische Zellen in den Dünndarm leitet

2.2.1 Charakterisierung und Lokalisation der pDC im Dünndarm der Maus

Wie bereits in der Einleitung beschrieben, konnten plasmazytoide Zellen bereits 2001 in der Maus identifiziert werden (58). Die Arbeitsgruppe um Giorgio Trinchieri konnte zeigen, dass eine Zellpopulation mit plasmazytoider Morphologie in der Milz und im Knochenmark für die Virus-induzierte IFN-α Produktion verantwortlich ist. Diese Zellen exprimierten CD11c, Ly6G/C und B220 und ähnelten den humanen plasmazytoiden DC stark (58).

Im Rahmen der vorliegenden Arbeit ist es gelungen, pDC im Darm der Maus nachzuweisen. Die Zellen ließen sich über die oben beschrieben Marker und ihre plasmazytoide Morphologie identifizieren. Darüber hinaus exprimierten die Zellen die pDC-Marker PDCA-1 und 120G8. Obwohl der größte Anteil der pDC im Bereich der *Lamina propria* zu liegen schien und nur ein vergleichsweise kleiner Teil der pDC direkt am oder im Epithel lag, konnte in durchflusszytometrischen Untersuchungen gezeigt werden, dass sich in den Isolationen von *Lamina propria* und Epithel in etwa gleich viele pDC finden ließen. Diese Beobachtung gab Grund zur Annahme, dass sich die pDC des Epithels leichter und erfolgreicher isolieren lassen, als die der *Lamina propria*. Würden die pDC der Epithelfraktion aus der *Lamina propria* stammen und durch unpräzise Isolation vermehrt in die Epithelfraktion gelangen, so müssten auch andere Zellen der *Lamina propria*, wie etwa die mDC, in der Epithelfraktion nachweisbar sein. Dies war aber nicht der Fall.

Die weiteren Untersuchungen dieser Studie bezogen sich auf Grund der einfacheren und sanfteren Gewinnung weitgehend nur noch auf die pDC des Epithels.

Die selektive Expression von Adhäsionsmolekülen auf unterschiedlichen Zellpopulation entscheidet über die Positionierung der Zellen an bestimmten physiologischen Orten. Diese Orte können die Lymphknoten, aber auch der Darm sein. Wie es bereits im Abschnitt 1.1 beschrieben wurde, spielen bei diesem Prozess Chemokine eine wichtige Rolle. 1999 konnte gezeigt werden, dass der Chemokinrezeptor CCR9 von allen intestinalen *Lamina propria* und intraepithelialen Lymphozyten exprimiert wird (10). In der vorliegenden Studie konnte gezeigt werden, dass auch die intestinalen pDC und die pDC des Knochenmarks in hohem Maße CCR9 exprimieren, während pDC aus anderen lymphatischen Organen dies nur zu einem geringen Anteil tun.

In diesem Zusammenhang stellt sich die Frage, ob pDC, die bereits im Knochenmark CCR9 exprimieren, ausschließlich in den Darm wandern, oder ob das darmspezifische Expressionsmuster erst an anderer Stelle induziert wird. Dies ist beispielsweise bei T-Zellen und Plasmazellen der Fall. Effektor T-Zellen, die in unterschiedlichen lymphatischen Organen generiert werden, zeigen einen spezifischen Gewebetropismus. Effektor T-Zellen, die im mesenterischen Lymphknoten aktiviert werden, regulieren ihre Expression der darmspezifischen Moleküle, das Integrin $\alpha 4\beta 7$ und der Chemokinrezeptor CCR9, hoch. Die Regulation dieser beiden Moleküle wird durch Retinsäure induziert, die wiederum von Darm-assoziierten dendritischen Zellen aus Retinol (Vitamin A) produziert wird (62). Es besteht die Möglichkeit, dass pDC nach der Auswanderung aus dem Knochenmark CCR9 herunterregulieren, und dass erst im mesenterischen Lymphknoten die Expression von CCR9 durch den oben beschriebenen Mechanismus induziert wird, was eine Lokalisation im Dünndarm zur Folge hat.

Eine weitere Möglichkeit ist, dass die pDC aus dem Knochenmark auf Grund der CCR9-Expression zunächst in den Dünndarm wandern, um sich von dort aus im gesamten Körper zu verteilen. Beide Annahmen gehen mit der Beobachtung konform, dass pDC auch in anderen lymphatischen Geweben zu finden sind. Zudem tragen pDC bereits im Knochenmark eine

Vielzahl anderer Chemokinrezptoren, wie die inflammatorisch exprimierten Rezeptoren CCR5 und CXCR3, was die Wanderung der Zellen zu Entzündungsherden ermöglicht (63-65).

2.2.2 Die Migration der pDC in den Dünndarm ist CCR9-abhängig

Bereits Agace et al. konnten zeigen, dass CCR9 vorzugsweise von murinen $\alpha_E\beta_7$ CD8$\alpha\beta^+$ Lymphozyten exprimiert wird, und dass die CCR9-Expression auf einem Teil dieser Zellen nach Aktivierung im mesenterischen Lymphknoten beibehalten wird. Die aktivierten CCR9$^+$ CD8$\alpha\beta^+$ Lymphozyten lokalisieren sich daraufhin in der Dünndarmmukosa. Durch die Gabe eines spezifischen Antikörpers, der den CCR9-Liganden CCL25 neutralisiert, konnte die Lokalisation dieser Zellen in der Dünndarmmukosa blockiert werden. Auf diese Weise wurde gezeigt, dass CCL25 eine wichtige Rolle bei der Lokalisation der CD8$\alpha\beta^+$ Lymphozyten in der Dünndarmmukosa spielt (16).

Die vorliegende Studie zeigt durch Experimente zur chemotaktischen *in vitro* Migration, dass auch pDC in hohem Maße auf CCL25 migrieren.

Die CCR9-Abhängikeit der Migration von pDC in den Dünndarm wurde durch Analysen von CCR9-defizienten Mäusen bestätigt. Diese Tiere weisen ein massives Fehlen von pDC im Epithel und der *Lamina propria* des Dünndarms auf. Auch in den Peyerschen Platten ist die Anzahl der pDC reduziert, während in anderen lymphatischen Organen, wie der Milz oder in Lymphknoten, kein Unterschied zwischen CCR9 Knock-out Mäusen und Wildtyptieren zu finden war.

In Transferexperimenten konnte außerdem gezeigt werden, dass CCR9-defiziente Zellen nicht in der Lage waren, in den Dünndarm einzuwandern. Diese Ergebnisse verdeutlichen, dass pDC in ähnlicher Weise wie es für CD8$\alpha\beta^+$ Lymphozyten bereits gezeigt wurde, CCR9-abhängig in die Dünndarmmukosa einwandern.

Anjuere et al. konnten in ihrer Studie zeigen, dass es nach der oralen Applikation von Choleratoxin zu einer massiven Akkumulation dendritischer Zellen in der subepithelialen Mukosa der Dünndarmzotten und des drainierenden mesenterischen Lymphknotens kommt. Die Autoren nehmen an, dass Choleratoxin dendritische Zellen in das mukosale Epithel lockt und deren Reifung, mit anschließender Wanderung in den mesenterischen Lymphknoten, stimuliert (66).

In der vorliegenden Studie reagierten pDC nach oraler Gabe von Choleratoxin ähnlich wie die oben beschriebenen mDC mit einer Akkumulation in der Dünndarmmukosa.

Zusammengefasst verdeutlichen diese Ergebnisse, dass CCR9 notwendig ist, um pDC unter homöostatischen und inflammatorischen Bedingungen in den Dünndarm zu rekrutieren. Unklar ist, ob noch andere Adhäsionsmoleküle an diesem Prozess beteiligt sind. Die Daten in dieser Studie legen nahe, dass auch α4β7-Integrin oder P-Selectin dazu beitragen könnten (67).

2.2.3 pDC-abhängige Mobilisierung von myeloiden DC aus der *Lamina propria*

Wie bereits erläutert, ist das intestinale Immunsystem einer Vielzahl von harmlosen und pathogenen Antigenen ausgesetzt und reagiert auf diese Antigene unterschiedlich. Dendritische Zellen tasten das Darmlumen ab, transportieren Antigene und übermitteln wichtige Informationen, die für eine anschließende Regulation der adaptiven Immunantwort gebraucht werden. Die mikrobiologischen Reize, die die Wanderung und Reifung der mDC beeinflussen, werden dabei in der Regel über Toll-like-Rezeptoren (TLR) und/oder inflammatorische Zytokine übertragen. Wie diese Umgebungsinformationen von den intestinalen mDC genau verarbeitet werden, konnte bisher noch nicht entschlüsselt werden.

Vor kurzem konnte jedoch von der Arbeitsgruppe um Gordon MacPherson gezeigt werden, dass die orale Gabe des Toll-like-Rezeptor-Liganden Resiquimod (R848) eine Mobilisierung der *Lamina propria* mDC bewirkt, und dass diese Mobilisierung TNF-α-abhängig ist (68). Im Detail konnten die Autoren der genannten Studie beobachten, dass 4-8 Stunden nach der Fütterung des TLR7/8 Liganden, der Gesamtanteil der mDC in der Lymphe um das ca. hundertfache angestiegen ist. Als Quelle dieses Anstiegs konnte die *Lamina propria* ausgemacht werden. 12 Stunden nach der Choleratoxin-Applikation war die *Lamina propria* vollständig von mDC geleert, während im mesenterischen Lymphknoten eine Akkumulation von mDC zu beobachten war (68). Die Autoren konnten außerdem zeigen, dass TNF-α eine zentrale Rolle in der Regulation der Migration von intestinalen mDC einnimmt.

TNF-α stimuliert dendritische Zellen zur Wanderung aus dem peripheren Gewebe in die drainierenden Lymphknoten und zu ihrer Reifung zu hochgradig costimulatorischen antigenpräsentierenden Zellen.

MacPherson ist der Meinung, dass das TNF-α von pDC nach TLR7/8 vermittelter Stimulation freigesetzt wird.

Anders als mDC exprimieren pDC hauptsächlich TLR7 und 9, was es ihnen ermöglicht, auf einzelsträngige RNS und virale DNS zu reagieren (69). Die TLR sind Transmembranrezeptoren, die in der Evolution konserviert wurden und zu den

Mustererkennungsrezeptoren des angeborenen Immunsystems zählen. Sie erkennen pathogenassoziierte molekulare Muster, zu denen beispielsweise auch LPS zählt.

TLR7 und 8 erkennen zu großen Teilen die gleichen Liganden, nämlich einzelsträngige RNA. Synthetische Liganden für TLR7/8 sind die Imidazoquinoline Imiquimod und Resiquimod (R-848; ref. 68).

Die Untersuchungen in der vorliegenden Studie ergaben, dass die pDC des Dünndarms TNF-α produzieren, nachdem sie *in vitro* mit R848 stimuliert wurden. Des Weiteren konnte eine klare Abhängigkeit der Mobilisierung der *Lamina propria* mDC von der TNF-α Produktion der pDC des Dünndarms nachgewiesen werden.

Diese Ergebnisse legen den Schluss nahe, dass die CCR9-abhängige Migration von pDC in den Dünndarm mit der Ligation von TLR7/8 bei infektiösen Prozessen zusammenhängt.

MacPherson nimmt an, dass die pDC, die das TNF-α zur Mobilisierung der mDC produzieren, möglicherweise im mesenterischen Lymphknoten positioniert sind. Die vorliegende Studie lässt jedoch vermuten, dass es die pDC in der Mukosa des Dünndarms sind, die das nötige TNF-α sezernieren. Dies macht insofern Sinn, als dass die pDC im Darm in unmittelbarer Nachbarschaft zu den mDC liegen und diese daher schneller mobilisiert werden können.

Es ist bisher noch unklar, ob die beeinträchtigte Mobilisierung der mDC in den CCR9-defizienten Mäusen einen Einfluss auf die Immunität gegenüber Pathogenen hat. Es ist aber denkbar, dass die schnelle Mobilisierung der *Lamina propria* mDC eine rasche Induktion der adaptiven Immunantwort begünstigt.

Kelsall et al. konnten kürzlich zeigen, dass pDC in den Peyerschen Platten von Mäusen kaum IFN-α produzieren (70). Kelsall et al. nehmen an, dass die fehlende IFN-α Produktion der pDC in den Peyerschen Platten das immunologische Gleichgewicht zugunsten der kommensalen Bakterien verschiebt, indem potentiell gefährliche Immunantworten, die sich gegen diese Bakterien richten, verhindert werden. Denn antivirale Cytokine, wie IFN-α, können sowohl das angeborene als auch das adaptive Immunsystem aktivieren (71).

Dem entgegen stehen die bisherigen Untersuchungen zu pDC aus sekundären lymphatischen Organen, in denen dieser Zelltyp durch seine Eigenschaft, große Mengen IFN-α zu produzieren, charakterisiert wird (58). Zudem konnte in anderen Studien bereits gezeigt werden, dass auch die pDC der Peyerschen Platten zur IFN-α Abgabe befähigt sind (72, 73).

Untersuchungen, die im Rahmen dieser Studie durchgeführt wurden, ergaben, dass pDC der Dünndarmmukosa nach Induktion mit CpG 2216 in der Lage sind, IFN-α zu produzieren (unveröffentlichte Daten).

Eine IFN-α Abgabe der pDC im Darm macht im Falle einer viralen Darminfektion, wie sie beispielsweise von Rotaviren verursacht wird, durchaus Sinn. Die intestinalen pDC könnten helfen, die im Epithel ansässigen Lymphozyten im Falle einer viralen Infektion zu aktivieren.

Zusammenfassend lässt sich festhalten, dass mit den pDC des Darms eine weitere Population identifiziert wurde, deren gerichtete Migration in den Dünndarm von CCR9 abhängig ist (74). CCR9 ist ein Migrationsfaktor, der im Falle des Darms, die Zellen in die Peripherie führt. Um jedoch die Zellen in die Lymphknoten zu leiten, sind andere Migrationsfaktoren ,wie CCR7, notwendig.

2.2.4 Ausblick

Es wird angenommen, dass pDC während einer Virusinfektion die Hauptquelle der IFNα-Produktion sind. Es ist hinreichend bekannt, dass die meisten Zellpopulationen, dendritische Zellen eingeschlossen, in der Lage sind, bei einer Virusinfektion IFNα zu sezernieren (75, 76). Der Hauptunterschied zwischen pDC und den anderen Zellen besteht darin, dass die IFNα-Produktion bei den pDC durch TLR7 und TLR9-induziert wird, während in anderen Zellen, die diese Toll-like-Rezeptoren tragen, dies nicht geschieht (69).

So konnte in Mäusen mit Hilfe des Zytomegalievirus (77) und des Vesikulären Stomatitis Virus (78) gezeigt werden, dass die *in vivo* IFNα-Produktion tatsächlich von den pDC bestritten wird. Dies trifft jedoch nicht auf alle Virusinfektionen der Maus zu. Beim lymphozytären Choriomeningitisvirus und dem West-Nil Virus sind pDC nicht die Hauptproduzenten des INFα (71, 77). An dieser Stelle stellt sich die Frage: Wozu werden pDC benötigt, wenn sie nicht bei allen Virusinfektionen IFNα abgeben? Bis jetzt konnte die genaue Funktion der pDC noch nicht entschlüsselt werden. Klar ist nur, dass viele Viren Strategien entwickelt haben, um die IFN-Abgabe zu blockieren (79). Diese Mechanismen sind aber in den seltensten Fällen bei pDC wirksam, da sie entweder nicht infiziert werden oder da das Virus nicht in den Signalweg für die IFN-Induktion, der über TLR7 und TLR9 geht, eingreift (76).

Um einen Hinweis auf die Funktion der pDC im Darm zu bekommen, könnten Infektionsversuche an CCR9-defizienten Mäusen durchgeführt werden. Dazu bräuchte man einen Virus, der die Tiere über den Darm infiziert, wie beispielsweise Rotaviren dies tun. Da CCR9-defizienten Mäusen die pDC im Darm fehlen, müsste man untersuchen, ob sich durch diesen Defizit Unterschiede im Krankheitsverlauf ergeben.

In der vorliegenden Studie konnte CCR9 als darmspezifischer Migrationsfaktor für pDC identifiziert werden (74). Es ist jedoch unklar, ob noch andere Migrationsfaktoren, wie α4β7 und P-Selektin, daran beteiligt sind. Auch dies gilt es noch zu untersuchen.

2.3 Die Wanderung naiver T-Zellen ist CCR7/CCL21-abhängig

Wie bereits in Abschnitt 1.1.2 beschrieben, ist der Chemokinrezeptor CCR7 mit seinen Liganden, den Chemokinen CCL19 und CCL21, ein wichtiger Migrationsfaktor bei der gerichteten Einwanderung verschiedener Leukozytenpopulationen in lymphatische Organe.

2.3.1 Humanes CCR7 kann die Funktion des murinen CCR7 übernehmen

Im Rahmen dieser Studie ist es gelungen, eine Maus mit einem konditionellen *Knock-in* zu erzeugen. Durch den Austausch des murinen CCR7-Gens mit dem humanen CCR7 wurde unter anderem eine LoxP-flankierte PgK-NEO-Kassette als Selektionsmarker in das Genom der Maus eingefügt. Solange die PgK-NEO-Kassette im Genom integriert war, kam es nicht zur Expression des eingefügten humanen CCR7-Gens und die Maus zeigte einen für CCR7-defiziente Mäuse typischen Phänotyp (Mausbezeichnung: STOP-huCCR7). Wurde die modifizierte Maus jedoch mit einer Maus verpaart, die Cre-Rekombinase konstitutiv exprimierte, wurde der Selektionsmarker aus dem Genom entfernt und das humane CCR7 konnte exprimiert werden. Mäuse, die das humane CCR7 konstitutiv homozygot exprimierten, zeigten eine annährend normale Verteilung von T-, B- und dendritischen Zellen in den lymphatischen Organen.

Sowohl T-Zellen als auch aktivierte mDC zeigten in den mutierten huCCR7-Mäusen ein normales Migrationsverhalten in die peripheren Lymphknoten. Daraus lässt sich der Schluss ziehen, dass das humane CCR7 dem murinen CCR7 so stark ähnelt, dass es seine Funktion nahezu komplett kompensieren kann, um den Wildtyp-Zustand in der Maus wiederherzustellen.

Dies gab die Möglichkeit, die so mutierte Maus mit anderen Cre-Deleter-Mäusen zu verpaaren, die die Cre-Rekombinase nur in bestimmten Zellpopulationen freisetzten. Dadurch war es möglich, Tiere zu erzeugen, die selektiv nur auf den gewünschten Zellen CCR7 exprimierten, während alle anderen Zellen weiterhin CCR7-defizient blieben.

2.3.2 Generierung eines konditionalen *CCR7-Knock-ins* auf CCR7-defizientem Hintergrund

Um einen konditionalen *Knock-in* auf einem CCR7 Hintergrund zu erzeugen, wurden die mutierten Mäuse mit CD4-Cre-Deletern verpaart. CD4-Cre-Mäuse tragen ein transgenes Cre-Rekombinase-Gen unter der Kontrolle eines CD4-Promotors (80, 81). Alle T-Zellen exprimieren während ihrer Entwicklung im Thymus zeitweise CD4 (23). Dies ermöglichte die selektive Expression der Cre-Rekombinase durch den CD4-Promotor, was zu einer Deletion der PgK-NEO-Kassette auf allen T-Zellen führte. Die T-Zellen trugen den humanen Chemokinrezeptor CCR7 auf der Zelloberfläche, während alle anderen Zellen des Körpers, wie B-Zellen und mDC, nach wie vor CCR7-defizient waren. Dadurch waren die T-Zellen wieder in der Lage, *in vitro* und *in vivo* auf CCL21 zu migrieren. Mäuse, die diesen Genotyp tragen, werden im weiteren Verlauf als T-CCR7 *Knock-in* (T-CCR7ki) bezeichnet.

2.3.3 Eingeschränkte Migration von T-Zellen in T-CCR7-*Knock-in* Mäusen

Die Untersuchung der T-CCR7ki Mäuse lieferte vollkommen unerwartete Ergebnisse. Es wurde erwartet, dass die T-Zellen in den T-huCCR7ki Mäusen, die humanes CCR7 exprimierten, ein normales Migrationsverhalten aufweisen würden. Zwar waren die T-Zellen der T-huCCR7ki Mäuse in adoptiven Transfers wieder in der Lage, in die peripheren Lymphknoten einzuwandern (unveröffentlichte Daten), jedoch zeigten die Mäuse bezüglich der Zellzahl in den Lymphknoten eine starke Reduktion der T-Zellen, was einem CCR7-defizienten Phänotyp entspricht.

Das lässt darauf schließen, dass die Expression von CCR7 auf der Zelloberfläche der T-Zellen allein nicht ausreicht, um den Lymphknoten mit T-Zellen zu füllen. Vielmehr gibt es Grund zur Annahme, dass es durch das Fehlen CCR7 zu weiteren bisher unbekannten Defekten kommt.

2.3.4 Reduzierte Größe der Lymphknoten in T-huCCR7ki Mäusen

Untersuchungen der Organstruktur der T-CCR7ki Mäuse ergaben eine geringere Größe der Lymphknoten und eine reduzierte Länge der HEV im Vergleich zu Wildtyptieren. Doch das Verhältnis der Länge der HEV zur Größe des Lymphknotens ist in beiden Genotypen gleich.

Vor einiger Zeit konnten Mebius et al. in Mäusen beobachten, dass eine Unterbrechung des Zuflusses an afferenter Lymphe eine massive Verkleinerung des Lymphknotens bewirkt. Sie fand heraus, dass dabei die Anzahl der T-Zellen in der T-Zellzone stark reduziert ist. Mebius et al. kamen zu dem Schluss, dass es in der afferente Lymphe Zellen oder Faktoren geben muss, die maßgeblichen Einfluss auf die Anwesenheit von Zellpopulationen im Lymphknoten haben (82).

Es besteht die Möglichkeit, dass durch den CCR7-Defekt der T-CCR7ki Mäuse spezifische Zellen oder lösliche Faktoren nicht mehr in den Lymphknoten gelangen können, die normalerweise die Wanderung der T-Zellen regulieren. Dies könnte in den T-CCR7ki Mäusen zu der von Mebius et al. beobachteten reduzierten Größe des Lymphknotens führen.

Während einer akuten Immunantwort nehmen die Lymphknoten dagegen stark an Größe zu, was allgemein als Anschwellung wahrgenommen wird. Diese Vergrößerung wird von einem Wachstum des Gefäßsystems begleitet. Bisher ist aber noch nicht verstanden, wodurch dieses Wachstum bedingt wird. Kürzlich veröffentlichte Studien geben einen Hinweis darauf, dass dendritische Zellen, die bei Entzündung durch das afferente Lymphsystem in den Lymphknoten einwandern, dabei eine entscheidende Rolle spielen könnten (83). Webster et al. konnten zeigen, dass eine Injektion reifer Knochenmarks-DC in den Fuß der Maus zu einer Ansammlung der injizierten mDC im drainierenden Lymphknoten und zum Wachstum des Lymphknotens führt.

Die Autoren führen das Wachstum des Lymphknotens darauf zurück, dass die eingewanderten mDC eine Proliferation der Endothelzellen der HEV induzieren. Dies geschieht dadurch, dass die mDC die Einwanderung von Zellen fördern, die den VEGF (vascular endothelial groth factor)-Level im Lymphknoten erhöhen und so die Zellteilung der Endothelzellen stimulieren. Die Vermehrung der Endothelzellen bewirkt eine zunehmende Einwanderung von Zellen in den Lymphknoten. Zusätzlich fördert das erweiterte Gefäßsystem die Zufuhr von Sauerstoff und Nährstoffen, die für den Stoffwechsel des wachsenden Lymphknotens benötigt werden. Dies zeigt, dass mDC nicht nur die Aufgabe haben Antigen zu präsentieren, sondern weiterführend auch dafür zuständig sind, eine optimale Umgebung für die darauf folgende Immunantwort zu schaffen.

2.3.5 Die Zellzahl der Lymphknoten ist abhängig von der Einwanderung dendritischer Zellen

Auch in der vorliegenden Arbeit konnte beobachtet werden, dass nach der subkutanen Injektion von mDC die Anzahl der HEV im Lymphknoten und die Anzahl der eingewanderten T-Zellen in den Lymphknoten massiv angestiegen war. Wurden jedoch dendritische Zellen in CCR7$^{-/-}$ Mäuse transferiert und die Einwanderung von T-Zellen in den Lymphknoten untersucht, war die Anzahl der eingewanderten T-Zellen gegenüber der Kontrolle mit PBS nahezu gleich niedrig. Daraus lässt sich schließen, dass es nicht ausreicht, wenn mDC im Lymphknoten vorhanden sind, um eine Einwanderung von T-Zellen zu ermöglichen. Vielmehr ist die Expression von CCR7 auf den T-Zellen weiterhin notwendig, damit die Zellen in den Lymphknoten einwandern können.

Des Weiteren ist eine deutliche Abhängigkeit der Größe des Lymphknoten von der Anzahl der mDC in Lymphknoten zu erkennen, wie sie auch schon von Webster et al. beschrieben wurde (83). Je mehr mDC nach der Injektion in den Lymphknoten eingewanderten, desto höher war die Zellzahl des Lymphknotens. Daraus lässt sich ableiten, dass, wenn die Anzahl der mDC in den Lymphknoten durch das Fehlen des Chemokinrezeptors CCR7 auf den mDC reduziert ist, sich in direkter Korrelation dazu auch weniger T-Zellen im Lymphknoten finden, und er damit vergleichsweise kleiner ist.

Die Injektion von *in vitro* differenzierten mDC spiegelt jedoch nicht die *steady state* Situation im Körper wider.

Um die Abhängigkeit der T-Zellmigration von der Anwesenheit der mDC im Lymphknoten unter nichtentzündlichen Bedingungen zu untersuchen, wurden T-CCR7ki/Rag2$^{-/-}$ Chimären hergestellt, indem T-CCR7ki Mäusen, nach der Bestrahlung, zu gleichen Anteilen Knochenmarkszellen von T-CCR7ki Mäusen und Rag2$^{-/-}$ Mäusen injiziert wurde. In Rag-defizienten Mäusen kommt es aufgrund einer Störung bei der Umordnung der Antigenrezeptorgene zu einem Anhalten der Lymphozytenentwicklung, was zu einem Fehlen von B- und T- Lymphozyten führt (84). Die generierten Chimären konnten aufgrund der Rag2$^{-/-}$ Knochenmarkszellen wieder dendritische Zellen bilden, die CCR7 exprimieren. Durch das Knochenmark der T-CCR7ki Mäuse war weiterhin garantiert, dass ansonsten nur T-Zellen CCR7 exprimieren.

Die Analyse dieser Chimären ergab in den mikroskopischen und durchflusszytometrischen Analysen eine deutliche Füllung der T-Zellzone, verglichen mit unbehandelten T-CCR7ki Tieren. Dies zeigt deutlich, dass mDC auch unter nicht-inflammatorischen Bedingungen eine wichtige Rolle bei der Einwanderung von T-Zellen in den Lymphknoten haben.

2.3.6 Das Chemokin CCL21 hält T-Zellen im Lymphknoten zurück

In weiteren Untersuchungen dieser Studie galt es zu klären, in welchem Zusammenhang dendritischen Zellen im Lymphknoten mit dessen Füllung mit T-Zellen stehen.

Da bei einer Blockade der Einwanderung von T-Zellen in den Lymphknoten durch eine Behandlung mit Integrin-neutralisierenden Antikörper keine weiteren Zellen in den Lymphknoten einwandern können, ist es möglich, die Verweildauer der T-Zellen im Lymphknoten zu messen. Im Detail wurde bei behandelten und unbehandelten Wildtyp Mäusen nach dem Transfer von floureszenzmarkierten T-Zellen zu einem definierten

Zeitpunkt nach der Antikörperbehandlung die Anzahl der noch vorhandenen markierten T-Zellen gemessen. Es war kein Unterschied in der Anzahl der ansässigen T-Zellen zu erkennen. Anders war es in den Lymphknoten Antigen-behandelter T-huCCR7ki Mäuse. In ihnen hatte sich die Anzahl der T-Zellen in der gleichen Zeit massiv reduziert.

Gleichzeitig zeigte sich, dass in T-huCCR7ki Mäusen weniger CCL21 im Lymphknoten vorhanden war. Die niedrige CCL21-Konzentration im Lymphknoten würde erklären, warum die T-Zellen in T-huCCR7ki Mäusen nicht im Lymphknoten zurückgehalten werden können.

Eine mögliche Erklärung für die geringe CCL21-Konzentration in diesen Tieren liefert die Arbeit von Friedmann et al. Sie konnten zeigen, dass die mDC der T-Zellzone das dort in großen Mengen vorhandene CCL21 aufnehmen und präsentieren. Dies beeinflusst die Beweglichkeit und die Reaktivität der T-Zellen maßgeblich. Durch das von der dendritischen Zelle gebundenen CCL21 werden die T-Zellen für eine gewisse Zeitspanne von ihnen eingefangen. Dies ermöglicht den T-Zellen einerseits ein ausführliches Absuchen der näheren Umgebung. Andererseits erhöht sich die Wahrscheinlichkeit einer Antigen-abhängigen Interaktion der T-Zellen mit umgebenden mDC (85).

Durch die oben beschriebenen Untersuchungen lässt sich ein Bild davon zeichnen, welchen Einfluss der Chemokinrezeptor CCR7 auf das Migrationverhalten von T-Zellen nimmt.

Zum einen bestätigt sich durch diese und andere Studien, dass durch die CCR7-gesteuerte Einwanderung von mDC in den Lymphknoten eine vermehrte Proliferation der Endothelzellen der HEV ausgelöst wird. Befinden sich mehr HEV im Lymphknoten, können dadurch mehr T-Zellen einwandern, was den Lymphknoten füllt (83).

Zum anderen bedingt die An- oder Abwesenheit von dendritischen Zellen die Verschiebung des sensiblen Gleichgewichts von Ein- und Auswanderung der T-Zellen.

Lymphozyten wandern, getrieben durch die Expression des Cemokinrezeptors CCR7, in den Lymphknoten ein (26). Dort geben unter anderem die Interleukine IL-2 und IL-4 den Stimulus zur Proliferation der Zellen. Im Gegenzug stirbt ein Teil der eingewanderten Zellen durch Apoptose. Wie bereits in Abschnitt 1.2.2 beschrieben, wird das Chemokin CCL21 von den Stromazellen der T-Zellzone gebildet (22). Anschließend wird es von den dort ansässigen mDC gebunden und präsentiert und hält dadurch die T-Zellen im Lymphknoten zurück (46). $S1P_1$ dagegen induziert die Auswanderung der Zellen aus dem Lymphknoten heraus (86). Nach etwa vier Zellteilungszyklen verlieren die Zellen ihr CCR7 und regulieren stattdessen $S1P_1$ herauf. Dies stellt sicher, dass die neu generierten Effektor-T-Zellen nicht weiterhin den Lymphknoten nach Antigen absuchen, sondern ihn schnell verlassen, um zum Infektionsherd zu wandern.

Durch das Zusammenspiel dieser Faktoren kommt es im Lymphknoten zu einem Gleichgewichtszustand (Abb. 4). Lässt man die proliferierenden und sterbenden Zellen in diesem Zusammenhang außer Acht, wandern genau so viele Zellen in den Lymphknoten ein, wie ihn zur gleichen Zeit auch wieder verlassen. Das System ist ausgeglichen und der Lymphknoten stagniert in seiner Größe.

Durch das Fehlen des Chemokinrezeptors CCR7 auf den dendritischen Zellen wird dieser Gleichgewichtszustand jedoch verschoben. Die mDC können ihrerseits nicht in den Lymphknoten gelangen. Dadurch sind sie nicht in der Lage, das durch die dort ansässigen Stromazellen gebildete CCL21 zu binden. Dies hat zur Folge, dass das CCL21 mit der efferenten Lymphflüssigkeit aus dem Lymphknoten herausgespült wird, so dass die CCL21-Konzentration sinkt.

T-Zellen, die in den Lymphknoten eingewandert sind, werden dort nicht mehr durch das an mDC gekoppelte CCL21 zurückgehalten und verlassen ihn, bedingt durch $S1P_1$, schneller als neue T-Zellen einwandern können. Der Lymphknoten beginnt zu schrumpfen.

Durch die Applikation von dendritischen Zellen in dieses System, ist es möglich, den Gleichgewichtszustand wiederherzustellen. Die mDC gelangen in den Lymphknoten und können dort das empfindliche Zusammenspiel der Gegenspieler CCL21 und $S1P_1$ ausgleichen, indem die T-Zellen durch das an die mDC-gebundene CCL21 im Lymphknoten zurückgehalten werden. CCR7 steuert die Homöostase der T-Zellen nicht allein durch den direkten Effekt auf die T-Zellmigration, sondern auch indirekt über die homöostatische DC-Migration.

Zusammenfassend lässt sich sagen, dass durch die generierte T-huCCR7ki Maus eine Vielzahl neuer Einblicke in die CCR7-gesteuerte Homöostase von T-Lymphozyten ermöglicht wurde.

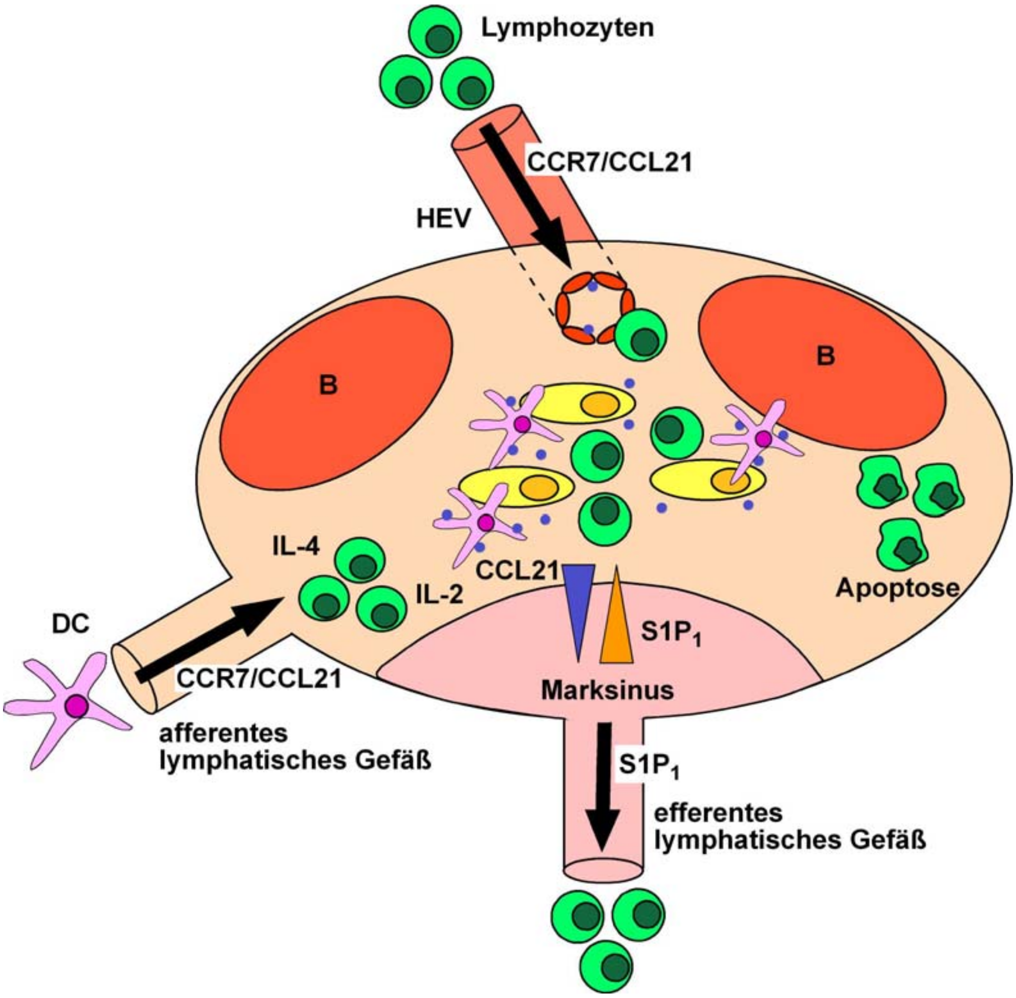
Lymphozyten
CCR7/CCL21
HEV
B
B
IL-4
IL-2
CCL21
S1P₁
Apoptose
DC
CCR7/CCL21
Marksinus
afferentes lymphatisches Gefäß
S1P₁
efferentes lymphatisches Gefäß

Abbildung 4: Schematische Darstellung der Faktoren, die die Immigration und Emigration der T-Zellen im Lymphknotens kontrollieren. Lymphozyten exprimieren CCR7 und gelangen über die HEV in den Lymphknoten. Dort beginnt ein Teil, bedingt durch Interleukine wie IL-2 und IL-4, zu proliferieren. Ein anderer Teil der Zellen geht in die Apoptose, da er beispielsweise körpereigene Antigene erkennt. Auch mDC wandern CCR7-abhängig über die afferente Lymphe in den Lymknoten ein. Dort binden sie das von den Stromazellen gebildete CC21. Das Chemokin CCL21 wirkt auf die Lymphozyten und hält sie im Lymphknoten zurück, während S1P$_1$ die Zellen zur Akkumulation im Marksinus anhält und ihre Auswanderung aus dem Lymphknoten einleitet. Sinkt die CCR7-Expression der Lymphozyten unter einen bestimmten Schwellenwert, überwiegt das Signal des S1P$_1$ und die Zellen verlassen den Lymphknoten.

2.3.7 Ausblick

Das Cre/LoxP-System der STOP-huCCR7 bietet vielfältige Möglichkeiten noch weitere konditionale *Knock-in* Mäuse herzustellen und zu untersuchen. Dabei kann auf unterschiedlichen Zelllinien die Funktion des Chemokinrezeptors CCR7 wieder hergestellt werden, während alle anderen Zellen des Organismus CCR7-defizient bleiben.

Für solche Experimente steht eine Vielzahl von unterschiedlichen Cre-Mäusen zur Verfügung. Dies bietet die Möglichkeit, die Funktion von CCR7 auf B-Zellen zu untersuchen. Für diese Anwendung können die STOP-huCCR7 Mäuse mit CD19-Cre Mäusen (87) oder mb1-Cre Mäusen (88) verpaart werden. In beiden Fällen wird die Cre-Rekombinase B-Zell-spezifisch exprimiert, so dass die Funktion von CCR7 auf B-Zellen wieder hergestellt wird.

Eine weitere Option ist die Verpaarung der STOP-huCCR7 Tiere mit DC-spezifischen Cre-Deleter-Mäusen. Dabei gibt es zum einen mx1-Cre Mäuse (89), die die Cre-Rekombinase nach Applikation von Interferon exprimieren, zum anderen bieten sich CD11c-Cre Mäuse (90) an. In beiden Fällen würde es nach einer Verpaarung mit STOP-huCCR7 Mäusen zu einer Expression von CCR7 auf dendritischen Zellen kommen.

3.1 Referenzen

1. MacDonald, T. T. 2003. The mucosal immune system. *Parasite Immunol* 25:235-246.
2. Ohl, L., G. Bernhardt, O. Pabst, and R. Forster. 2003. Chemokines as organizers of primary and secondary lymphoid organs. *Semin Immunol* 15:249-255.
3. Weninger, W., and U. H. von Andrian. 2003. Chemokine regulation of naive T cell traffic in health and disease. *Semin Immunol* 15:257-270.
4. Zlotnik, A., and O. Yoshie. 2000. Chemokines: a new classification system and their role in immunity. *Immunity* 12:121-127.
5. Stein, J. V., and C. Nombela-Arrieta. 2005. Chemokine control of lymphocyte trafficking: a general overview. *Immunology* 116:1-12.
6. Baggiolini, M. 2001. Chemokines in pathology and medicine. *J Intern Med* 250:91-104.
7. Rollins, B. J. 1997. Chemokines. *Blood* 90:909-928.
8. Sallusto, F., C. R. Mackay, and A. Lanzavecchia. 2000. The role of chemokine receptors in primary, effector, and memory immune responses. *Annu Rev Immunol* 18:593-620.
9. Butcher, E. C., and L. J. Picker. 1996. Lymphocyte homing and homeostasis. *Science* 272:60-66.
10. Zabel, B. A., W. W. Agace, J. J. Campbell, H. M. Heath, D. Parent, A. I. Roberts, E. C. Ebert, N. Kassam, S. Qin, M. Zovko, G. J. LaRosa, L. L. Yang, D. Soler, E. C. Butcher, P. D. Ponath, C. M. Parker, and D. P. Andrew. 1999. Human G protein-coupled receptor GPR-9-6/CC chemokine receptor 9 is selectively expressed on intestinal homing T lymphocytes, mucosal lymphocytes, and thymocytes and is required for thymus-expressed chemokine-mediated chemotaxis. *J Exp Med* 190:1241-1256.
11. Vicari, A. P., D. J. Figueroa, J. A. Hedrick, J. S. Foster, K. P. Singh, S. Menon, N. G. Copeland, D. J. Gilbert, N. A. Jenkins, K. B. Bacon, and A. Zlotnik. 1997. TECK: a novel CC chemokine specifically expressed by thymic dendritic cells and potentially involved in T cell development. *Immunity* 7:291-301.
12. Wurbel, M. A., J. M. Philippe, C. Nguyen, G. Victorero, T. Freeman, P. Wooding, A. Miazek, M. G. Mattei, M. Malissen, B. R. Jordan, B. Malissen, A. Carrier, and P. Naquet. 2000. The chemokine TECK is expressed by thymic and intestinal epithelial cells and attracts double- and single-positive thymocytes expressing the TECK receptor CCR9. *Eur J Immunol* 30:262-271.
13. Johansson-Lindbom, B., M. Svensson, M. A. Wurbel, B. Malissen, G. Marquez, and W. Agace. 2003. Selective generation of gut tropic T cells in gut-associated lymphoid tissue (GALT): requirement for GALT dendritic cells and adjuvant. *J Exp Med* 198:963-969.
14. Kunkel, E. J., J. J. Campbell, G. Haraldsen, J. Pan, J. Boisvert, A. I. Roberts, E. C. Ebert, M. A. Vierra, S. B. Goodman, M. C. Genovese, A. J. Wardlaw, H. B. Greenberg, C. M. Parker, E. C. Butcher, D. P. Andrew, and W. W. Agace. 2000. Lymphocyte CC chemokine receptor 9 and epithelial thymus-expressed chemokine (TECK) expression distinguish the small intestinal immune compartment: Epithelial expression of tissue-specific chemokines as an organizing principle in regional immunity. *J Exp Med* 192:761-768.
15. Bowman, E. P., N. A. Kuklin, K. R. Youngman, N. H. Lazarus, E. J. Kunkel, J. Pan, H. B. Greenberg, and E. C. Butcher. 2002. The intestinal chemokine thymus-expressed chemokine (CCL25) attracts IgA antibody-secreting cells. *J Exp Med* 195:269-275.

16. Svensson, M., J. Marsal, A. Ericsson, L. Carramolino, T. Broden, G. Marquez, and W. W. Agace. 2002. CCL25 mediates the localization of recently activated CD8alphabeta(+) lymphocytes to the small-intestinal mucosa. *J Clin Invest* 110:1113-1121.
17. Marsal, J., M. Svensson, A. Ericsson, A. H. Iranpour, L. Carramolino, G. Marquez, and W. W. Agace. 2002. Involvement of CCL25 (TECK) in the generation of the murine small-intestinal CD8alpha alpha+CD3+ intraepithelial lymphocyte compartment. *Eur J Immunol* 32:3488-3497.
18. Crabbe, P. A., and J. F. Heremans. 1966. The distribution of immunoglobulin-containing cells along the human gastrointestinal tract. *Gastroenterology* 51:305-316.
19. Selby, W. S., L. W. Poulter, S. Hobbs, D. P. Jewell, and G. Janossy. 1983. Heterogeneity of HLA-DR-positive histiocytes in human intestinal lamina propria: a combined histochemical and immunohistological analysis. *J Clin Pathol* 36:379-384.
20. Rescigno, M., M. Urbano, B. Valzasina, M. Francolini, G. Rotta, R. Bonasio, F. Granucci, J. P. Kraehenbuhl, and P. Ricciardi-Castagnoli. 2001. Dendritic cells express tight junction proteins and penetrate gut epithelial monolayers to sample bacteria. *Nat Immunol* 2:361-367.
21. Rot, A., and U. H. von Andrian. 2004. Chemokines in innate and adaptive host defense: basic chemokinese grammar for immune cells. *Annu Rev Immunol* 22:891-928.
22. Luther, S. A., H. L. Tang, P. L. Hyman, A. G. Farr, and J. G. Cyster. 2000. Coexpression of the chemokines ELC and SLC by T zone stromal cells and deletion of the ELC gene in the plt/plt mouse. *Proc Natl Acad Sci U S A* 97:12694-12699.
23. Misslitz, A., O. Pabst, G. Hintzen, L. Ohl, E. Kremmer, H. T. Petrie, and R. Forster. 2004. Thymic T cell development and progenitor localization depend on CCR7. *J Exp Med* 200:481-491.
24. Reif, K., E. H. Ekland, L. Ohl, H. Nakano, M. Lipp, R. Forster, and J. G. Cyster. 2002. Balanced responsiveness to chemoattractants from adjacent zones determines B-cell position. *Nature* 416:94-99.
25. Sallusto, F., D. Lenig, R. Forster, M. Lipp, and A. Lanzavecchia. 1999. Two subsets of memory T lymphocytes with distinct homing potentials and effector functions. *Nature* 401:708-712.
26. Forster, R., A. Schubel, D. Breitfeld, E. Kremmer, I. Renner-Muller, E. Wolf, and M. Lipp. 1999. CCR7 coordinates the primary immune response by establishing functional microenvironments in secondary lymphoid organs. *Cell* 99:23-33.
27. von Andrian, U. H., and T. R. Mempel. 2003. Homing and cellular traffic in lymph nodes. *Nat Rev Immunol* 3:867-878.
28. Sackstein, R. 2005. The lymphocyte homing receptors: gatekeepers of the multistep paradigm. *Curr Opin Hematol* 12:444-450.
29. Girard, J. P., and T. A. Springer. 1995. High endothelial venules (HEVs): specialized endothelium for lymphocyte migration. *Immunol Today* 16:449-457.
30. von Andrian, U. H., and C. R. Mackay. 2000. T-cell function and migration. Two sides of the same coin. *N Engl J Med* 343:1020-1034.
31. Kansas, G. S. 1996. Selectins and their ligands: current concepts and controversies. *Blood* 88:3259-3287.
32. Vestweber, D., and J. E. Blanks. 1999. Mechanisms that regulate the function of the selectins and their ligands. *Physiol Rev* 79:181-213.
33. Lawrence, M. B., and T. A. Springer. 1991. Leukocytes roll on a selectin at physiologic flow rates: distinction from and prerequisite for adhesion through integrins. *Cell* 65:859-873.
34. von Andrian, U. H., J. D. Chambers, L. M. McEvoy, R. F. Bargatze, K. E. Arfors, and E. C. Butcher. 1991. Two-step model of leukocyte-endothelial cell interaction in

inflammation: distinct roles for LECAM-1 and the leukocyte beta 2 integrins in vivo. *Proc Natl Acad Sci U S A* 88:7538-7542.

35. Cyster, J. G. 1999. Chemokines and cell migration in secondary lymphoid organs. *Science* 286:2098-2102.
36. Carlson, H., A. S. Zhang, W. H. Fleming, and C. A. Enns. 2005. The hereditary hemochromatosis protein, HFE, lowers intracellular iron levels independently of transferrin receptor 1 in TRVb cells. *Blood* 105:2564-2570.
37. Pribila, J. T., A. C. Quale, K. L. Mueller, and Y. Shimizu. 2004. Integrins and T cell-mediated immunity. *Annu Rev Immunol* 22:157-180.
38. Worbs, T., T. R. Mempel, J. Bolter, U. H. von Andrian, and R. Forster. 2007. CCR7 ligands stimulate the intranodal motility of T lymphocytes in vivo. *J Exp Med* 204:489-495.
39. Okada, T., and J. G. Cyster. 2007. CC chemokine receptor 7 contributes to Gi-dependent T cell motility in the lymph node. *J Immunol* 178:2973-2978.
40. Cyster, J. G. 2005. Chemokines, sphingosine-1-phosphate, and cell migration in secondary lymphoid organs. *Annu Rev Immunol* 23:127-159.
41. Sanna, M. G., S. K. Wang, P. J. Gonzalez-Cabrera, A. Don, D. Marsolais, M. P. Matheu, S. H. Wei, I. Parker, E. Jo, W. C. Cheng, M. D. Cahalan, C. H. Wong, and H. Rosen. 2006. Enhancement of capillary leakage and restoration of lymphocyte egress by a chiral S1P1 antagonist in vivo. *Nat Chem Biol* 2:434-441.
42. Wei, S. H., H. Rosen, M. P. Matheu, M. G. Sanna, S. K. Wang, E. Jo, C. H. Wong, I. Parker, and M. D. Cahalan. 2005. Sphingosine 1-phosphate type 1 receptor agonism inhibits transendothelial migration of medullary T cells to lymphatic sinuses. *Nat Immunol* 6:1228-1235.
43. Allende, M. L., J. L. Dreier, S. Mandala, and R. L. Proia. 2004. Expression of the sphingosine 1-phosphate receptor, S1P1, on T-cells controls thymic emigration. *J Biol Chem* 279:15396-15401.
44. Matloubian, M., C. G. Lo, G. Cinamon, M. J. Lesneski, Y. Xu, V. Brinkmann, M. L. Allende, R. L. Proia, and J. G. Cyster. 2004. Lymphocyte egress from thymus and peripheral lymphoid organs is dependent on S1P receptor 1. *Nature* 427:355-360.
45. Rosen, H., M. G. Sanna, S. M. Cahalan, and P. J. Gonzalez-Cabrera. 2007. Tipping the gatekeeper: S1P regulation of endothelial barrier function. *Trends Immunol* 28:102-107.
46. Pham, T. H., T. Okada, M. Matloubian, C. G. Lo, and J. G. Cyster. 2008. S1P1 receptor signaling overrides retention mediated by G alpha i-coupled receptors to promote T cell egress. *Immunity* 28:122-133.
47. Gunn, M. D., S. Kyuwa, C. Tam, T. Kakiuchi, A. Matsuzawa, L. T. Williams, and H. Nakano. 1999. Mice lacking expression of secondary lymphoid organ chemokine have defects in lymphocyte homing and dendritic cell localization. *J Exp Med* 189:451-460.
48. Banchereau, J., and R. M. Steinman. 1998. Dendritic cells and the control of immunity. *Nature* 392:245-252.
49. Yao, V., C. Platell, and J. C. Hall. 2002. Dendritic cells. *ANZ J Surg* 72:501-506.
50. Yanagihara, S., E. Komura, J. Nagafune, H. Watarai, and Y. Yamaguchi. 1998. EBI1/CCR7 is a new member of dendritic cell chemokine receptor that is up-regulated upon maturation. *J Immunol* 161:3096-3102.
51. Lennert, K., and W. Remmele. 1958. [Karyometric research on lymph node cells in man. I. Germinoblasts, lymphoblasts & lymphocytes.]. *Acta Haematol* 19:99-113.
52. Lennert, K., E. Kaiserling, and H. K. Muller-Hermelink. 1975. Letter: T-associated plasma-cells. *Lancet* 1:1031-1032.
53. Muller-Hermelink, H. K., H. Stein, G. Steinmann, and K. Lennert. 1983. Malignant lymphoma of plasmacytoid T-cells. Morphologic and immunologic studies characterizing a special type of T-cell. *Am J Surg Pathol* 7:849-862.

54. Facchetti, F., C. De Wolf-Peeters, J. J. van den Oord, R. De vos, and V. J. Desmet. 1988. Plasmacytoid T cells: a cell population normally present in the reactive lymph node. An immunohistochemical and electronmicroscopic study. *Hum Pathol* 19:1085-1092.
55. Facchetti, F., W. Vermi, D. Mason, and M. Colonna. 2003. The plasmacytoid monocyte/interferon producing cells. *Virchows Arch* 443:703-717.
56. Siegal, F. P., N. Kadowaki, M. Shodell, P. A. Fitzgerald-Bocarsly, K. Shah, S. Ho, S. Antonenko, and Y. J. Liu. 1999. The nature of the principal type 1 interferon-producing cells in human blood. *Science* 284:1835-1837.
57. Nakano, H., M. Yanagita, and M. D. Gunn. 2001. CD11c(+)B220(+)Gr-1(+) cells in mouse lymph nodes and spleen display characteristics of plasmacytoid dendritic cells. *J Exp Med* 194:1171-1178.
58. Asselin-Paturel, C., A. Boonstra, M. Dalod, I. Durand, N. Yessaad, C. Dezutter-Dambuyant, A. Vicari, A. O'Garra, C. Biron, F. Briere, and G. Trinchieri. 2001. Mouse type I IFN-producing cells are immature APCs with plasmacytoid morphology. *Nat Immunol* 2:1144-1150.
59. Liu, Y. J. 2005. IPC: professional type 1 interferon-producing cells and plasmacytoid dendritic cell precursors. *Annu Rev Immunol* 23:275-306.
60. Grouard, G., M. C. Rissoan, L. Filgueira, I. Durand, J. Banchereau, and Y. J. Liu. 1997. The enigmatic plasmacytoid T cells develop into dendritic cells with interleukin (IL)-3 and CD40-ligand. *J Exp Med* 185:1101-1111.
61. Pabst, O., L. Ohl, M. Wendland, M. A. Wurbel, E. Kremmer, B. Malissen, and R. Forster. 2004. Chemokine receptor CCR9 contributes to the localization of plasma cells to the small intestine. *J Exp Med* 199:411-416.
62. Iwata, M., A. Hirakiyama, Y. Eshima, H. Kagechika, C. Kato, and S. Y. Song. 2004. Retinoic acid imprints gut-homing specificity on T cells. *Immunity* 21:527-538.
63. Yoneyama, H., K. Matsuno, Y. Zhang, T. Nishiwaki, M. Kitabatake, S. Ueha, S. Narumi, S. Morikawa, T. Ezaki, B. Lu, C. Gerard, S. Ishikawa, and K. Matsushima. 2004. Evidence for recruitment of plasmacytoid dendritic cell precursors to inflamed lymph nodes through high endothelial venules. *Int Immunol* 16:915-928.
64. Kohrgruber, N., M. Groger, P. Meraner, E. Kriehuber, P. Petzelbauer, S. Brandt, G. Stingl, A. Rot, and D. Maurer. 2004. Plasmacytoid dendritic cell recruitment by immobilized CXCR3 ligands. *J Immunol* 173:6592-6602.
65. Cella, M., D. Jarrossay, F. Facchetti, O. Alebardi, H. Nakajima, A. Lanzavecchia, and M. Colonna. 1999. Plasmacytoid monocytes migrate to inflamed lymph nodes and produce large amounts of type I interferon. *Nat Med* 5:919-923.
66. Anjuere, F., C. Luci, M. Lebens, D. Rousseau, C. Hervouet, G. Milon, J. Holmgren, C. Ardavin, and C. Czerkinsky. 2004. In vivo adjuvant-induced mobilization and maturation of gut dendritic cells after oral administration of cholera toxin. *J Immunol* 173:5103-5111.
67. Berlin, C., E. L. Berg, M. J. Briskin, D. P. Andrew, P. J. Kilshaw, B. Holzmann, I. L. Weissman, A. Hamann, and E. C. Butcher. 1993. Alpha 4 beta 7 integrin mediates lymphocyte binding to the mucosal vascular addressin MAdCAM-1. *Cell* 74:185-195.
68. Yrlid, U., S. W. Milling, J. L. Miller, S. Cartland, C. D. Jenkins, and G. G. MacPherson. 2006. Regulation of intestinal dendritic cell migration and activation by plasmacytoid dendritic cells, TNF-alpha and type 1 IFNs after feeding a TLR7/8 ligand. *J Immunol* 176:5205-5212.
69. Asselin-Paturel, C., and G. Trinchieri. 2005. Production of type I interferons: plasmacytoid dendritic cells and beyond. *J Exp Med* 202:461-465.
70. Contractor, N., J. Louten, L. Kim, C. A. Biron, and B. L. Kelsall. 2007. Cutting edge: Peyer's patch plasmacytoid dendritic cells (pDCs) produce low levels of type I

interferons: possible role for IL-10, TGFbeta, and prostaglandin E2 in conditioning a unique mucosal pDC phenotype. *J Immunol* 179:2690-2694.

71. Colonna, M., G. Trinchieri, and Y. J. Liu. 2004. Plasmacytoid dendritic cells in immunity. *Nat Immunol* 5:1219-1226.

72. Bilsborough, J., T. C. George, A. Norment, and J. L. Viney. 2003. Mucosal CD8alpha+ DC, with a plasmacytoid phenotype, induce differentiation and support function of T cells with regulatory properties. *Immunology* 108:481-492.

73. Castellaneta, A., M. Abe, A. E. Morelli, and A. W. Thomson. 2004. Identification and characterization of intestinal Peyer's patch interferon-alpha producing (plasmacytoid) dendritic cells. *Hum Immunol* 65:104-113.

74. Wendland, M., N. Czeloth, N. Mach, B. Malissen, E. Kremmer, O. Pabst, and R. Forster. 2007. CCR9 is a homing receptor for plasmacytoid dendritic cells to the small intestine. *Proc Natl Acad Sci U S A* 104:6347-6352.

75. Lopez, C. B., A. Garcia-Sastre, B. R. Williams, and T. M. Moran. 2003. Type I interferon induction pathway, but not released interferon, participates in the maturation of dendritic cells induced by negative-strand RNA viruses. *J Infect Dis* 187:1126-1136.

76. Diebold, S. S., M. Montoya, H. Unger, L. Alexopoulou, P. Roy, L. E. Haswell, A. Al-Shamkhani, R. Flavell, P. Borrow, and C. Reis e Sousa. 2003. Viral infection switches non-plasmacytoid dendritic cells into high interferon producers. *Nature* 424:324-328.

77. Dalod, M., T. P. Salazar-Mather, L. Malmgaard, C. Lewis, C. Asselin-Paturel, F. Briere, G. Trinchieri, and C. A. Biron. 2002. Interferon alpha/beta and interleukin 12 responses to viral infections: pathways regulating dendritic cell cytokine expression in vivo. *J Exp Med* 195:517-528.

78. Barchet, W., M. Cella, B. Odermatt, C. Asselin-Paturel, M. Colonna, and U. Kalinke. 2002. Virus-induced interferon alpha production by a dendritic cell subset in the absence of feedback signaling in vivo. *J Exp Med* 195:507-516.

79. Hengel, H., U. H. Koszinowski, and K. K. Conzelmann. 2005. Viruses know it all: new insights into IFN networks. *Trends Immunol* 26:396-401.

80. Lee, P. P., D. R. Fitzpatrick, C. Beard, H. K. Jessup, S. Lehar, K. W. Makar, M. Perez-Melgosa, M. T. Sweetser, M. S. Schlissel, S. Nguyen, S. R. Cherry, J. H. Tsai, S. M. Tucker, W. M. Weaver, A. Kelso, R. Jaenisch, and C. B. Wilson. 2001. A critical role for Dnmt1 and DNA methylation in T cell development, function, and survival. *Immunity* 15:763-774.

81. Sawada, S., J. D. Scarborough, N. Killeen, and D. R. Littman. 1994. A lineage-specific transcriptional silencer regulates CD4 gene expression during T lymphocyte development. *Cell* 77:917-929.

82. Mebius, R. E., P. R. Streeter, J. Breve, A. M. Duijvestijn, and G. Kraal. 1991. The influence of afferent lymphatic vessel interruption on vascular addressin expression. *J Cell Biol* 115:85-95.

83. Webster, B., E. H. Ekland, L. M. Agle, S. Chyou, R. Ruggieri, and T. T. Lu. 2006. Regulation of lymph node vascular growth by dendritic cells. *J Exp Med* 203:1903-1913.

84. Chen, J., Y. Shinkai, F. Young, and F. W. Alt. 1994. Probing immune functions in RAG-deficient mice. *Curr Opin Immunol* 6:313-319.

85. Friedman, R. S., J. Jacobelli, and M. F. Krummel. 2006. Surface-bound chemokines capture and prime T cells for synapse formation. *Nat Immunol* 7:1101-1108.

86. Pappu, R., S. R. Schwab, I. Cornelissen, J. P. Pereira, J. B. Regard, Y. Xu, E. Camerer, Y. W. Zheng, Y. Huang, J. G. Cyster, and S. R. Coughlin. 2007. Promotion of lymphocyte egress into blood and lymph by distinct sources of sphingosine-1-phosphate. *Science* 316:295-298.

87. Rickert, R. C., J. Roes, and K. Rajewsky. 1997. B lymphocyte-specific, Cre-mediated mutagenesis in mice. *Nucleic Acids Res* 25:1317-1318.
88. Hobeika, E., S. Thiemann, B. Storch, H. Jumaa, P. J. Nielsen, R. Pelanda, and M. Reth. 2006. Testing gene function early in the B cell lineage in mb1-cre mice. *Proc Natl Acad Sci U S A* 103:13789-13794.
89. Kuhn, R., F. Schwenk, M. Aguet, and K. Rajewsky. 1995. Inducible gene targeting in mice. *Science* 269:1427-1429.
90. Caton, M. L., M. R. Smith-Raska, and B. Reizis. 2007. Notch-RBP-J signaling controls the homeostasis of CD8- dendritic cells in the spleen. *J Exp Med* 204:1653-1664.

3.2 Danksagung

Zuerst möchte ich mich bei Prof. Dr. Reinhold Förster bedanken, der mir die Möglichkeit gegeben hat an dieser Doktorarbeit zu arbeiten. Ohne seine stetige Hilfe und Unterstützung wäre vieles nicht möglich gewesen. Des weiteren möchte ich mich bei Prof. Dr. Reinhard Schwinzer für die Übernahme des Korreferats bedanken.

Mein besonderer Dank gilt PD Dr. Oliver Pabst, der mich schon seit sieben Jahren bei meiner Arbeit betreut. Oliver hat mir immer bei Probleme geholfen und ohne seine guten Ideen wäre ich hoffnungslos verloren gewesen.

Dankbar bin ich auch meinen Kollegen aus dem Labor 1450. Insbesondere Simon Berberich und Michaela Friedrichsen, die mir immer geholfen haben, wenn es mal etwas holprig wurde. Sie haben den Laboralltag mit Spaß und Abwechslung verschönert und mir meinen „leichten“ Hang zur Unordentlichkeit hoffentlich nachgesehen. Besonders genossen habe ich die regen Diskussion mit Simon, die nicht immer fachlicher Art waren. Bedanken möchte ich mich auch bei unsere chaotischen Austauschspanierin María-Luisa del Rio-González (Malu), Sarvari Velaga, Sabrina Daehne, Swantje Hammerschmidt und all den anderen, die ich hier nicht alle aufzählen werden, da es inzwischen recht viele geworden sind.

Bedanken möchte ich mich bei den Mädels vom Mittagessen, Jasmin Bölter, Heike Danzer und Michaela Friedrichsen. Ich habe die anregenden Unterhaltungen während des Essens sehr genossen. Außerden haben die drei mir oft bei Versuchen geholfen, die alleine kaum zu bewältigen gewesen wären (schütteln!!).

Ich möchte nicht versäumen, mich bei Steffi Willenzon zu bedanken, die seit meiner Elternzeit an meinem Projekt weitergearbeitet hat und deswegen lange Tage und Abende im Labor verbracht hat. Ohne ihren Einsatz wäre das letzte Manuskript niemals fertig geworden.

Mein ganz spezieller Dank gilt natürlich meinen Eltern, Geschwistern und meiner Oma, die mich immer unterstütz haben und einfach für mich da waren.

Fast zuletzt möchte ich mich bei meinem Mann Stefan bedanken. Ohne ihn wäre dies alles nicht möglich gewesen. Er hat mich immer wieder aufgebaut, wenn es mal nicht so gut lief,

und sich über Erfolge mit mir gefreut. Mein letzter Dank geht an meine süße Tochter Matilda, die dies noch gar nicht lesen kann. Sie hat mein Leben so sehr bereichert und mich auf liebevolle Weise davon abgehalten, diese Arbeit zügig zu Ende zu schreiben. Aber ich bin ihr überhaupt nicht böse.

3.3 Eigenen Publikationen

1. Oliver Pabst, Lars Ohl, Meike Wendland, Marc-André Wurbel, Elisabeth Kremmer, Bernard Malissen, and Reinhold Förster
Chemokine Receptor CCR9 Contributes to the Localization of Plasma Cells to the Small Intestine.
J. Exp. Med. 2004 Feb 2;199(3):411-6.
Ausführung und Analyse der Histologie der Peyerschen Platten mit fluoreszierenden Beads.

2. Wendland M, Czeloth N, Mach N, Malissen B, Kremmer E, Pabst O, Förster R.
CCR9 is a homing receptor for plasmacytoid dendritic cells to the small intestine.
Proc. Natl. Acad. Sci. U S A. 2007 Apr 10;104(15):6347-52.

3. Meike Wendland, Stephanie Willenzon, Jessica Kocks, Ana Clara Davalos-Misslitz, Svantje Hammerschmidt, Elisabeth Kremmer, Angelika Hoffmeyer, Oliver Pabst, Reinhold Förster
A CCR7-dependent steady state homing of dendritic cells essentially required for lymph node T cell homeostasis
Ausführung und Analyse der Experimente aus Abb. 7-10 wurden größtenteils von Stefanie Willenzon, Dr. Ana Clara Davalos-Misslitz und Prof. Dr. Reinhold Förster durchgeführt.

Brief Definitive Report

The Journal of Experimental Medicine

Chemokine Receptor CCR9 Contributes to the Localization of Plasma Cells to the Small Intestine

Oliver Pabst,[1] Lars Ohl,[1] Meike Wendland,[1] Marc-André Wurbel,[2]
Elisabeth Kremmer,[3] Bernard Malissen,[2] and Reinhold Förster[1]

[1] *Institute of Immunology, Hannover Medical School, 30625 Hannover, Germany*
[2] *Centre d'Immunologie de Marseille-Luminy, Institut National de la Santé et de la Recherche Medicale-Centre National de la Recherche Scientifique-Université de la Méditerranée, Parc Scientifique de Luminy, 13288 Marseille Cedex 9, France*
[3] *Institute of Molecular Immunology, GSF, 81377 München, Germany*

Abstract

Humoral immunity in the gut-associated lymphoid tissue is characterized by the production of immunoglobulin A (IgA) by antibody-secreting plasma cells (PCs) in the lamina propria. The chemokine CCL25 is expressed by intestinal epithelial cells and is capable of inducing chemotaxis of IgA$^+$ PCs in vitro. Using a newly generated monoclonal antibody against murine CCR9, we show that IgA$^+$ PCs express high levels of CCR9 in the mesenteric lymph node (MLN) and Peyer's patches (PPs), but down-regulate CCR9 once they are located in the small intestine. In CCR9-deficient mice, IgA$^+$ PCs are substantially reduced in number in the lamina propria of the small intestine. In adoptive transfer experiments, CCR9-deficient IgA$^+$ PCs show reduced migration into the small intestine compared with wild-type controls. Furthermore, CCR9 mutants fail to mount a regular IgA response to an orally administered antigen, although the architecture and cell type composition of PPs and MLN are unaffected and are functional for the generation of IgA PCs. These findings provide profound in vivo evidence that CCL25/CCR9 guides PCs into the small intestine.

Key words: gut • IgA • lamina propria • CCL25 • cell trafficking

Introduction

The gut acts as the port of entry for a vast array of foreign antigens, including food components, but also potentially harmful pathogens. A first line of defense against these antigens is built by neutralizing immunoglobulins directed against pathogens or toxins (1). For this purpose, antibody-secreting plasma cells (PCs) of the lamina propria produce dimeric IgA that is transported into the gut lumen by transcytosis and bound to the mucus overlying the intestinal epithelium.

In the intestine, antigens are sampled by DCs located in the epithelium or by specialized epithelia overlying Peyer's patches (PPs). In these follicle-associated epithelia, microfold cells nonspecifically sample antigens from the gut lumen and transport them to professional antigen-presenting cells located in the subepithelial dome (SED; reference 2). To elicit an immune response, these cells migrate into either the adjacent interfollicular T cell zone, the B cell–rich follicles of PPs, or even into the draining mesenteric lymph node (MLN) to activate lymphocytes (3, 4). Some of the activated B cells start to proliferate and generate germinal centers within PPs or MLN, which have been identified as the places where affinity maturation and probably isotype switch from IgM to IgA occurs. However, more recently it has been shown that isotype switch of B220$^+$ IgM$^+$ cells at least in part occurs in the lamina propria under the influence of local stimuli (5). Most of the fully differentiated B cells leave PPs and MLN and migrate via the lymphatics and the thoracic duct into the blood and from there to the lamina propria of the small intestine.

It has been proposed that signaling through the chemokine receptor CCR9 might be an important factor that targets cells to the intestine (6, 7). The CCR9 ligand CCL25/TECK is expressed by epithelial cells of the small, but not the large, intestine. CCR9 is expressed on virtually all small intestinal T cells, and murine IgA-producing PCs from the spleen, PPs, and MLN have been shown to migrate toward CCL25 and CXCL12, a ligand for CXCR4 in vitro (8–10). Notably, PCs of IgG or IgM isotype do not respond to

---

Address correspondence to Reinhold Förster, Institute of Immunology, Hannover Medical School, Feodor-Lynen-Str. 21, 30625 Hannover, Germany. Phone: 49-511-5329721; Fax: 49-511-5329722; email: foerster.reinhold@mh-hannover.de

J. Exp. Med. © The Rockefeller University Press • 0022-1007/2004/02/411/6 $8.00
Volume 199, Number 3, February 2, 2004 411–416
http://www.jem.org/cgi/doi/10.1084/jem.20030996

CCL25 but migrate toward CXCL12 and CXCL9 (9, 11, 12), suggesting that the differential expression of chemokine receptors targets PCs to their final destination depending on the isotype of immunoglobulins they produce. Furthermore, during the course of a memory response, CXCR3 and CXCR4 have been implicated in guiding plasma blasts to inflamed tissues or to the bone marrow, respectively (13). In this report, we provide in vivo evidence that CCR9 is crucial for the positioning of PCs to the small intestine.

Materials and Methods

Isolation of Lamina Propria Cells (LPCs) and Flow Cytometry. Animals were bred at the animal facility of Hannover Medical School under specific pathogen-free conditions. CCR9-deficient mice have been described previously (14). In this analysis, CCR9-deficient mice and littermates of a mixed genetic background were used. 8–10-wk-old animals were killed, and LPCs were isolated using standard procedures.

Cells were stained using the following antibodies: anti-CD3-PE (Caltag), IgA-biotin, CD19-biotin (Biosource International), CD138-PE, B220-PerCP, IgM, and IgD (BD Biosciences). To stain cytoplasmatic IgA, cells were fixed for 20 min in 2% PFA in PBS on ice, washed, and resuspended for 20 min in 0.1% saponin in PBS.

Generation of Monoclonal CCR9 Antibody. A peptide comprising amino acids 3–22 of mouse CCR9 was synthesized and coupled to KLH or OVA. Rats were immunized subcutaneously and intraperitoneally with a mixture of 50 μg peptide-KLH, 5 nmol CPG oligonucleotide (Tib Molbiol), 500 μl PBS and 500 μl IFA as described previously (15). Supernatants were tested by a differential ELISA and analyzed by flow cytometry using thymocytes derived from wild-type and CCR9-deficient mice.

Immunofluorescence. Immunohistological analysis of adult PPs and MLN was done on cryosections as described previously (16). For detection of CXCR4 (clone 2B11) and CCR9 (clone 7E7, IgG2b), sections were blocked with mouse serum, incubated with hybridoma supernatants, and detected using mouse anti–rat Cy3 antibodies (Jackson ImmunoResearch Laboratories).

In Vivo Migration of BrdU-labeled Cells. To label proliferating cells in vivo, wild-type and CCR9-deficient animals were injected intraperitoneally with 120 mg/kg BrdU (Sigma-Aldrich) in PBS 1 h before killing. Cells were isolated from MLN and PPs, and a total of 10^8 cells was injected intravenously into wild-type recipients. After 16 h, mice were killed, and the small intestine was embedded in paraffin using standard procedures. Sections were dewaxed, and BrdU-incorporated cells were detected using the BrdU staining kit (Oncogene Research Products) and Cy3-tyramid (NEN Life Science Products). IgA^+ cells were identified using anti-IgA FITC antibody (Caltag).

Oral OVA Immunizations and Serum Ig Analysis. ELISA assays for total serum Ig levels were performed as described previously (16). Biotinylated anti-Ig antibodies were purchased from BD Biosciences (anti-IgM, anti-IgG1, anti-IgG2a, anti-IgG2b, and anti-IgG3) and Biosource International (anti-IgA).

10 mice per genotype were gavaged with 2.5 mg OVA and 10 μg cholera toxin (CT) six times at 10-d intervals. For detection of OVA-specific IgA and IgM antibodies, plates were coated overnight with 5 μg/ml OVA, and appropriate dilutions of serum samples were added (1:100–1:6,400). Anti–IgA-biotin and anti–IgM-biotin followed by streptavidin-peroxidase and 5-thio-2-nitrobenzoic acid were used for detection.

Results and Discussion

IgA^+ PCs Express CCR9 Abundantly in Secondary Lymphoid Organs but Not the Small Intestine. It has been suggested that the interaction of CCL25 with CCR9 might play an important role in the establishment of an IgA^+ PC pool in the small intestine. Therefore, we characterized the expression of CCR9 on PCs in different organs with a newly generated monoclonal antibody against CCR9. The antibody displayed high levels of CCR9 on wild-type thymocytes but not on thymocytes derived from CCR9-deficient mice (Fig. 1 A).

In cell preparations isolated from the LPCs of wild-type mice, two distinct populations of cells can be distinguished based on size and granularity. Small LPCs are predominantly $CD3^+$ lamina propria lymphocytes, whereas large LPCs heavily stain with anti-IgA mAb after permeabilization (unpublished data). Additionally, the majority these cells show a $CD138^+$, IgD^-, IgM^-, and $CD19^-$ surface phenotype and, thus, can be defined as lamina propria PCs (unpublished data). CCR9 could be detected on most lamina propria lymphocytes (Fig. 1 B), but more importantly, only ~5% of all lamina propria PCs are $CCR9^+$ (Fig. 1 C).

These observations were confirmed applying the CCR9 mAb in immunohistology. In contrast to IgA^+ cells of MLN and PPs, which showed high levels of CCR9 (Fig. 1 D and not depicted), the majority of IgA^+ PCs of the small intestine showed weak or undetectable staining with the anti-CCR9 mAb (Fig. 1 E; compare with staining intensity shown in Fig. 1 D). In addition, cells staining positive for CCR9 seem to represent T cells (Fig. 1 E). Interestingly, another chemokine receptor, CXCR4, was readily detectable on all IgA^+ PCs of all lymphoid organs examined, including PPs, MLN, and the small intestine (Fig. 1 F and not depicted). Because IgA^+ PCs are known to readily leave the place where they have been generated (i.e., the secondary lymphoid organs), high expression of CCR9 appears to be specific for newly generated PCs, whereas this receptor becomes down-regulated once these cells reached their final destination. These data suggest that high levels of CCR9 are required for the homing of newly generated IgA^+ PCs to the intestine, whereas this receptor seems to be dispensable for retaining PCs within this compartment. Because CXCR4 remains expressed on resident IgA^+ PCs within the intestine, it seems possible that CXCR4 participates in this process. Indeed, data derived from CXCR4-deficient mice suggest a role for this chemokine receptor in retaining PCs within lymphoid organs such as bone marrow (11).

Reduced Numbers of PCs in the Intestinal Lamina Propria of CCR9 Mutant Mice. Based on these findings, we compared the PC populations of wild-type and CCR9 mutant mice by counting the number of IgA^+ PCs on cryosections of the small intestine (Fig. 2, A and B). In this paper, only villi were counted that were cut (judged on the analysis of serial sections) through the core of the villus. In wild-type animals, an average of 20.6 ± 1.2 (mean ± SEM) IgA^+ cells per villus section was found. In contrast,

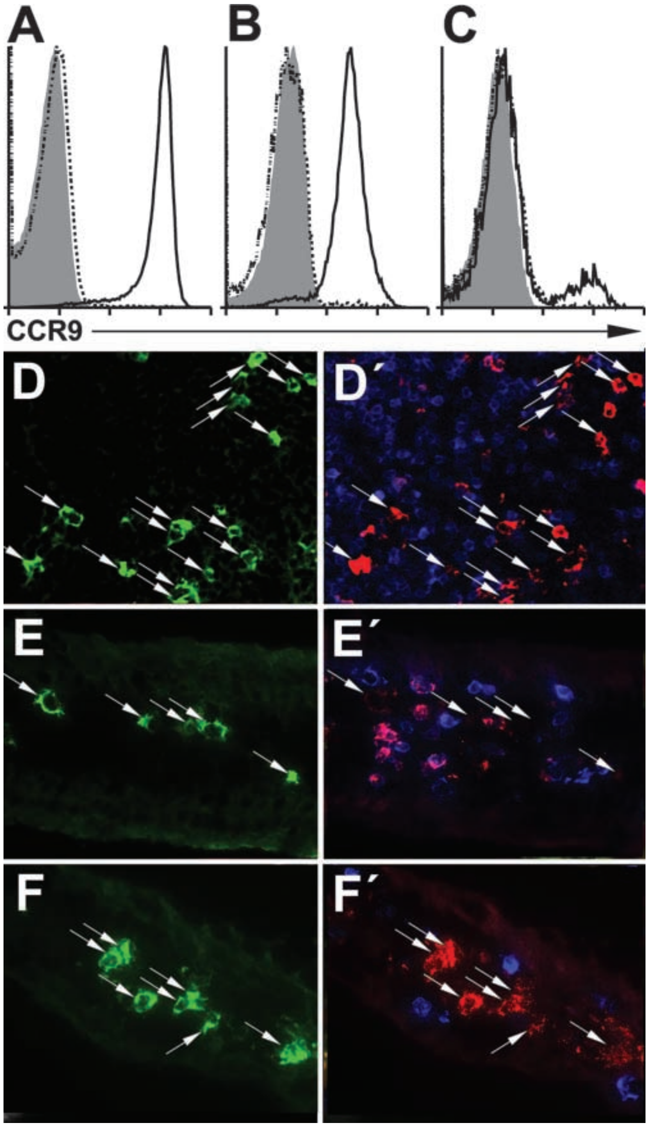

Figure 1. CCR9 is expressed on all IgA$^+$ PCs in MLN but on few lamina propria PCs. (A–C) Cells isolated from thymus (A) and small intestinal lamina propria (B and C) of wild-type mice (solid line) and CCR9-deficient animals (dashed line) were stained using a CCR9-specific monoclonal antibody or an isotype control (shaded area). The histograms shown in B were obtained by gating on small LPCs, whereas data shown in C were obtained from large LPCs. (D–F) Three color immunohistology. Sections of MLN (D) and small intestine (E and F) from wild-type mice were stained with anti-CCR9 (D′ and E′, red) or anti-CXCR4 (F′, red). Sections were further stained with anti-IgA (D–F, green) and anti-CD3 (D′–F′, blue). The three colors obtained from single sections have been separated as depicted. Arrows indicate the position of IgA$^+$ PCs.

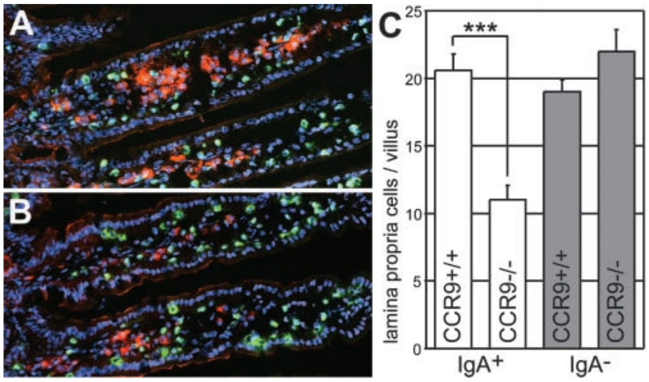

Figure 2. CCR9 mutant intestines harbor reduced numbers of IgA$^+$ PC. Cryosections through the small intestine of wild-type (A) and CCR9-targeted mice (B) were stained for IgA (red), CD3 (green), and nuclei (blue). Unaltered numbers of IgA$^-$ cells were present in the lamina propria of wild-type and CCR9 mutant animals, whereas numbers of IgA$^+$ cells were reduced in CCR9 mutants (C, ***, $P < 0.001$; data were derived from five wild type and five mutants analyzing 60 villi each).

in CCR9 mutant mice, the number of PCs per villus section was severely reduced to 11 ± 1.1 (mean ± SEM) cells per villus section (Fig. 2 C). As an internal control, the number of IgA$^-$ DAPI$^+$ LPCs was determined on the same sections, revealing that CCR9 deficiency does not affect cell types other than IgA$^+$ PCs in this compartment (Fig. 2 C, 19 ± 0.9 cells vs. 22 ± 1.6 cells). These results could also be confirmed by flow cytometry on permeabilized LPCs using an anti-IgA mAb that revealed a reduction of IgA$^+$ PC numbers by ~50% in CCR9 mutants (unpublished data).

Because it has been suggested that isotype switch can take place in the lamina propria (5), we also used antibodies specific for other immunoglobulin isotypes to detect differences between wild-type and CCR9 mutant mice. However, immunohistology for IgM and IgG did not reveal any significant differences between both strains (unpublished data), rendering it unlikely that impaired local isotype switching accounts for the reduced number of IgA-positive cells in CCR9 mutants. Furthermore, the phenotype of the residual PC population in CCR9 mutants as determined by expression of surface antigens (CD138, CD19, B220, IgA, IgM, and IgD) was indistinguishable from that of wild-type PCs, suggesting that loss of CCR9 does not affect the differentiation of PCs.

Interestingly, in wild-type mice, most of the PCs locate to the lower half of the villus (Fig. 2 C), which is the region where peak levels of CCL25 expression by the abutting epithelial cells have been described previously (8), further supporting the hypothesis that CCL25 signaling via CCR9 contributes considerably to the efficient homing to the small intestine. Most notably, no differences in the number of IgA$^+$ PCs were identified in the large intestine of CCR9 mutants (wild type: 1 PC/4699 ± 255 μm^2; CCR9 deficient: 1 PC/4832 ± 331 μm^2; $n = 5$ animals for each group). This observation is also in line with the reported absence of CCL25 in the large intestine (8).

Reduced Homing Capacity of CCR9-deficient IgA$^+$ PCs. More than two decades ago, McDermott et al. identified proliferating cells in MLN and PPs, but not in peripheral LN, that were able to migrate into mucosal tissues and give rise to IgA-secreting cells (17). To directly address the function of CCR9 in this process, we labeled proliferating cells using BrdU and isolated them from MLN and PPs of wild-type and CCR9-deficient mice. 10^8 cells were injected i.v. into wild-type recipients, and after 16 h, the

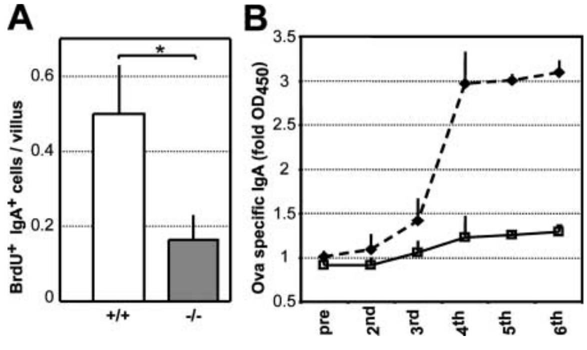

Figure 3. CCR9 mutant PCs show an impaired migration into the small intestine. (A) 16 h after adoptive transfer of BrdU-labeled cells isolated from MLN and PP of wild-type and CCR9 mutant mice, the number of $BrdU^+$ IgA^+ cells per villus was determined (*, $P < 0.05$; data were derived from three recipients of each group analyzing 60 villi each). CCR9 mutant mice show a reduced humoral IgA response. (B) Groups of 10 CCR9 mutants (solid line) and control animals (dashed line) were each gavaged with OVA and CT at 10-d intervals, and serum levels of OVA-specific IgA were measured. In contrast to wild-type animals showing a robust increase of OVA-specific IgA levels, CCR9 mutants barely produced OVA-specific IgAs.

numbers of $BrdU^+$ IgA^+ PCs in the small intestine had been determined. Interestingly, PCs from wild-type mice were threefold more efficient in migrating into the small intestine compared with cells derived from CCR9-deficient mice (Fig. 3 A). These results contributed further weight to the idea that CCR9 is required for efficient migration of newly formed PCs into the small intestine.

CCR9-deficient Mice Do Not Mount a Proper Immune Response to Oral Antigens. To test whether the reduced number of IgA-secreting PCs observed in the intestine of CCR9 mutants and the reduced migration efficiency of IgA^+ PCs are paralleled by reduced serum IgA levels, we analyzed the amount of serum Ig in wild-type and CCR9 mutant mice. CCR9-deficient and wild-type mice were not found to differ significantly with regard to normal serum levels of any immunoglobulin isotypes tested (IgG1, IgG2a, IgG2b, IgG3, IgM, and IgA), indicating that CCR9 is dispensable for systemic immunoglobulin production (unpublished data).

Although the total amount of serum IgA was found to be unchanged between wild-type and mutant mice, we were interested to know whether differences exist between CCR9 mutants and wild-type mice in the induction of antigen-specific IgA response after oral immunization with a T cell–dependent antigen. To this end, wild-type mice and CCR9 mutants were gavaged with 2.5 mg OVA and 10 μg CT at 10-d intervals. Serum levels of OVA-specific IgA were determined 9 d after each single OVA application. In wild-type animals, significant OVA-specific IgA levels were detectable after three OVA applications that further increased after subsequent applications of the antigen (Fig. 3 B). Interestingly, in CCR9 mutants, a barely detectable increase in OVA-specific IgA titers could be determined within the period of time analyzed, suggesting a severe impairment in the production of OVA-specific IgA in these animals (Fig. 3 B).

Unaltered Architecture and Cell Composition of MLN and PPs in CCR9-deficient Mice. Because it is assumed that the induction of an IgA-specific antibody response after oral application of antigen plus CT requires antigen presentation within morphologically intact PPs and MLN, we further analyzed both organs. We used immunohistology and flow cytometry to identify possible alterations in cellular composition or architecture of both organs in CCR9 mutants that contained normal numbers of B and T cells, and both cell types were located in their appropriate microenvironments. In addition, PPs contained normal numbers of $CD11c^+$, $CD11b^-$, and $CD11c^+CD11b^+$ DCs (unpublished data). Recently, it has been described that DCs of the SED can be labeled and their path subsequently followed using fluorescent latex beads (4). Because we found CCR9-expressing cells, including DC within the SED (unpublished data), we tested whether the mobilization of DCs of the SED is affected in CCR9 mutants. Wild-type and CCR9-deficient mice were deprived of water and food for 4 h and subsequently gavaged with 10^{12} fluorescent latex beads (200 nm diameter; Polysciences) per animal. After 24 h, the mice were gavaged with 50 μg of CT. After another 24 h, PPs and MLN were sectioned and stained for CD11c and CD3 (Fig. 4, A–D, PPs only). In wild type and CCR9 mutants, application of CT lead to reduced numbers of $CD11c^+$ cells (red) present in the SED (Fig. 4, A–D). To quantify this effect, the absolute number of fluorescent beads in the SED was counted in 20 PPs derived from four wild type and four CCR9 mutants. In both wild type and CCR9 mutants, CT administration triggers an identical fivefold decrease of bead-labeled DCs localized to the SED, suggesting that no differences in DC mobilization exist and that the activation of naive B cells should proceed normally in these $CCR9^{-/-}$ organs (unpublished data). Indeed, analysis of cryosections from MLN of wild-type and mutant mice that were immunized five times with OVA and CT revealed comparable numbers of IgA^+ PCs in both strains (Fig. 4, E and F). Furthermore, in wild type and mutants likewise, the total numbers of IgA^+ PCs strongly increased after immunization in comparison to nonimmunized mice (unpublished data) strongly supporting the idea that the generation of IgA PCs is not affected by CCR9 deficiency.

The data provided in the present work demonstrate that CCR9-deficient mice possess reduced numbers of IgA-secreting PCs within the lamina propria, an observation that correlates well with the reduced migration efficiency of CCR9-deficient PCs into the small intestine and the inability of these animals to mount a T-dependent antigen-specific IgA response after oral application of antigen.

One hypothesis accounting for these defects would postulate the existence of a rather uniform PC population inside the small intestine. In this scenario, freshly generated plasma blasts that express high levels of CCR9 gain efficient entry into the intestinal lamina propria by CCL25-mediated signaling, whereas the residual PC population in CCR9-deficient mice would enter the lamina propria in-

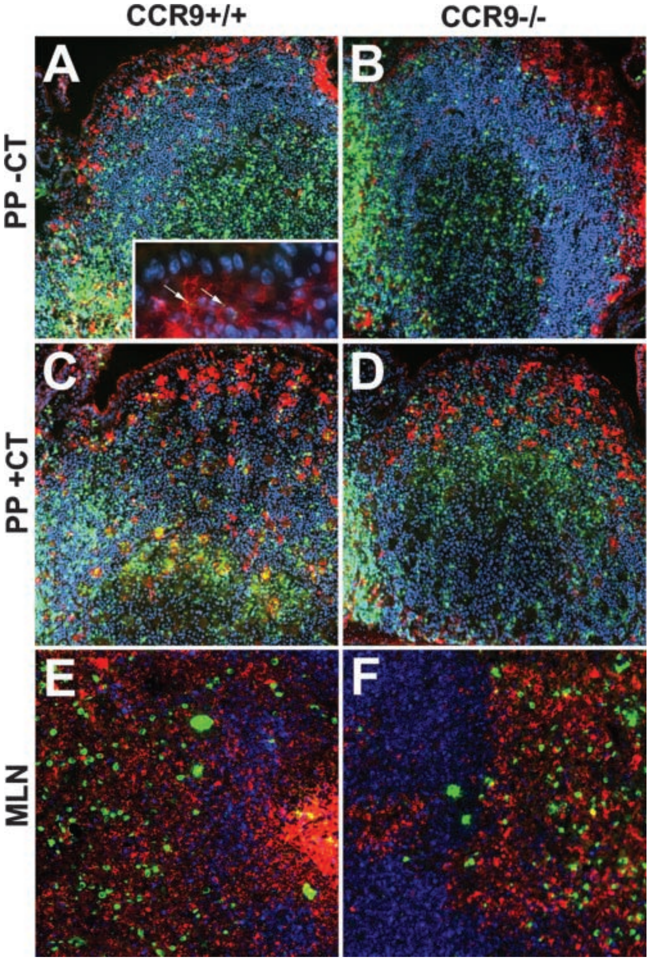

Figure 4. Regular generation of IgA$^+$ PCs in CCR9-deficient animals. Wild-type (A and C) and CCR9-deficient mice (B and D) were gavaged with fluorescent latex beads and treated after 24 h with PBS alone (A and B) or CT in PBS (C and D). After 24 h, PP were removed, sectioned, and stained for CD11c (red), CD3 (green), and nuclei (blue). Wild-type and CCR9-deficient mice showed no differences in architecture, nor mobilization of CD11c$^+$ cells or mobilization of bead-loaded cells. (A, inset) Arrows point to bead-loaded CD11c$^+$ cells. Sections of MLN of wild type (E) and CCR9 mutants (F) that had been immunized with OVA and CT five times at 10-d intervals were stained with anti-IgA (green), anti-IgM (red), and anti-CD3 (blue). Similar numbers of IgA$^+$ PCs are present in wild type and CCR9 MLN, demonstrating that the generation of IgA PCs is not grossly altered in CCR9-deficient mice.

dependent of CCR9, probably by a time-consuming and inefficient bypass mechanism.

Alternatively, dependence on CCR9 signaling might reflect the different developmental fate and origin of PCs populating the small intestine. It has been suggested that besides conventional B2 cells, B1 cells from the peritoneal cavity can give rise to lamina propria IgA$^+$ PCs (18). However, this issue remains discussed controversially because intestinal IgA production in conventionally reared animals (as performed in this work) has been shown to be the source of almost exclusively B2, but not B1, cells (19). Unfortunately, available immunological tools would not allow dissection of B1 and B2 cell–derived PCs once they settled the lamina propria. Interestingly, intraperitoneal immunization with T cell–independent antigen results in a normal antigen-specific IgM response in CCR9 mutants, suggesting that B1 cell function per se is not affected in these animals (unpublished data). Thus, a more likely explanation for the decrease of IgA$^+$ PCs in CCR9 mutants is the less efficient recruitment of B2 cell–derived PCs into the lamina propria in the absence of CCR9 signaling. This idea is consistent with a strongly reduced IgA response in orally immunized mice assuming that antigen-specific PCs are generated in CCR9 mutants but fail to reach a compartment that supports secretion and long-term survival of these cells.

In any case, CCR9-independent chemokine receptor signaling would be required to guide the remaining PCs into the lamina propria in CCR9-deficient mice, resulting in serum and fecal IgA levels that do not significantly differ from those present in wild-type animals (unpublished data). Indeed, surface expression of CXCR4 can be detected on IgA$^+$ PCs (Fig. 1 F) consistent with the responsiveness of these cells to CXCL12 in in vitro migration assays (9). Furthermore, in humans, CCR10 has been documented in PCs, including intestinal IgA$^+$-secreting PCs (20), and we were able to detect CCR10 expression in mouse PCs using a CCL27-IgG$_1$ fusion protein (unpublished data) suggesting that CCR9 and CCR10 might cooperate in directing PCs into the small intestine in mice. In conclusion, our findings represent the first in vivo evidence that CCR9 is critical for the homing of IgA-secreting PCs to the small intestine.

We thank G. Bernhardt for critical reading of the manuscript and M. Friedrichsen and S. Wilkening for excellent technical work.

This work was supported by a Deutsche Forschungsgemeinschaft grants (SFB621-A1 and Fo334/1-1) to R. Förster and by institutional grants from the Institut National de la Santé et de la Recherche Medicale, the Centre National de la Recherche Scientifique, and a specific grant from the European Community (QLG1-CT1999-00202).

Submitted: 19 June 2003
Accepted: 26 November 2003

References

1. Kato, H., R. Kato, K. Fujihashi, and J.R. McGhee. 2001. Role of mucosal antibodies in viral infections. *Curr. Top. Microbiol. Immunol.* 260:201–228.
2. Neutra, M.R., N.J. Mantis, and J.P. Kraehenbuhl. 2001. Collaboration of epithelial cells with organized mucosal lymphoid tissues. *Nat. Immunol.* 2:1004–1009.
3. Pron, B., C. Boumaila, F. Jaubert, P. Berche, G. Milon, F. Geissmann, and J.L. Gaillard. 2001. Dendritic cells are early cellular targets of Listeria monocytogenes after intestinal delivery and are involved in bacterial spread in the host. *Cell. Microbiol.* 3:331–340.
4. Shreedhar, V.K., B.L. Kelsall, and M.R. Neutra. 2003. Cholera toxin induces migration of dendritic cells from the subepithelial dome region to T- and B-cell areas of Peyer's patches. *Infect. Immun.* 71:504–509.
5. Fagarasan, S., K. Kinoshita, M. Muramatsu, K. Ikuta, and T. Honjo. 2001. In situ class switching and differentiation to

IgA-producing cells in the gut lamina propria. *Nature*. 413: 639–643.

6. Zabel, B.A., W.W. Agace, J.J. Campbell, H.M. Heath, D. Parent, A.I. Roberts, E.C. Ebert, N. Kassam, S. Qin, M. Zovko, et al. 1999. Human G protein–coupled receptor GPR-9-6/CC chemokine receptor 9 is selectively expressed on intestinal homing T lymphocytes, mucosal lymphocytes, and thymocytes and is required for thymus-expressed chemokine-mediated chemotaxis. *J. Exp. Med.* 190:1241–1256.
7. Johansson-Lindbom, B., M. Svensson, M.A. Wurbel, B. Malissen, G. Marquez, and W. Agace. 2003. Selective generation of gut tropic T cells in gut-associated lymphoid tissue (GALT): requirement for GALT dendritic cells and adjuvant. *J. Exp. Med.* 198:963–969.
8. Kunkel, E.J., J.J. Campbell, G. Haraldsen, J. Pan, J. Boisvert, A.I. Roberts, E.C. Ebert, M.A. Vierra, S.B. Goodman, M.C. Genovese, et al. 2000. Lymphocyte CC chemokine receptor 9 and epithelial thymus-expressed chemokine (TECK) expression distinguish the small intestinal immune compartment: epithelial expression of tissue-specific chemokines as an organizing principle in regional immunity. *J. Exp. Med.* 192: 761–768.
9. Bowman, E.P., N.A. Kuklin, K.R. Youngman, N.H. Lazarus, E.J. Kunkel, J. Pan, H.B. Greenberg, and E.C. Butcher. 2002. The intestinal chemokine thymus-expressed chemokine (CCL25) attracts IgA antibody-secreting cells. *J. Exp. Med.* 195:269–275.
10. Papadakis, K.A., J. Prehn, V. Nelson, L. Cheng, S.W. Binder, P.D. Ponath, D.P. Andrew, and S.R. Targan. 2000. The role of thymus-expressed chemokine and its receptor CCR9 on lymphocytes in the regional specialization of the mucosal immune system. *J. Immunol.* 165:5069–5076.
11. Hargreaves, D.C., P.L. Hyman, T.T. Lu, V.N. Ngo, A. Bidgol, G. Suzuki, Y.R. Zou, D.R. Littman, and J.G. Cyster. 2001. A coordinated change in chemokine responsiveness guides plasma cell movements. *J. Exp. Med.* 194:45–56.
12. Wehrli, N., D.F. Legler, D. Finke, K.M. Toellner, P. Loetscher, M. Baggiolini, I.C. MacLennan, and H. Acha-Orbea. 2001. Changing responsiveness to chemokines allows medullary plasmablasts to leave lymph nodes. *Eur. J. Immunol.* 31:609–616.
13. Hauser, A.E., G.F. Debes, S. Arce, G. Cassese, A. Hamann, A. Radbruch, and R.A. Manz. 2002. Chemotactic responsiveness toward ligands for CXCR3 and CXCR4 is regulated on plasma blasts during the time course of a memory immune response. *J. Immunol.* 169:1277–1282.
14. Wurbel, M.A., M. Malissen, D. Guy-Grand, E. Meffre, M.C. Nussenzweig, M. Richelme, A. Carrier, and B. Malissen. 2001. Mice lacking the CCR9 CC-chemokine receptor show a mild impairment of early T- and B-cell development and a reduction in T-cell receptor gamma/delta(+) gut intraepithelial lymphocytes. *Blood*. 98:2626–2632.
15. Forster, R., T. Emrich, E. Kremmer, and M. Lipp. 1994. Expression of the G-protein–coupled receptor BLR1 defines mature, recirculating B cells and a subset of T-helper memory cells. *Blood*. 84:830–840.
16. Forster, R., A. Schubel, D. Breitfeld, E. Kremmer, I. Renner-Muller, E. Wolf, and M. Lipp. 1999. CCR7 coordinates the primary immune response by establishing functional microenvironments in secondary lymphoid organs. *Cell*. 99:23–33.
17. McDermott, M.R., and J. Bienenstock. 1979. Evidence for a common mucosal immunologic system. I. Migration of B immunoblasts into intestinal, respiratory, and genital tissues. *J. Immunol.* 122:1892–1898.
18. Kroese, F.G., R. de Waard, and N.A. Bos. 1996. B-1 cells and their reactivity with the murine intestinal microflora. *Semin. Immunol.* 8:11–18.
19. Thurnheer, M.C., A.W. Zuercher, J.J. Cebra, and N.A. Bos. 2003. B1 cells contribute to serum IgM, but not to intestinal IgA, production in gnotobiotic Ig allotype chimeric mice. *J. Immunol.* 170:4564–4571.
20. Kunkel, E.J., C.H. Kim, N.H. Lazarus, M.A. Vierra, D. Soler, E.P. Bowman, and E.C. Butcher. 2003. CCR10 expression is a common feature of circulating and mucosal epithelial tissue IgA Ab-secreting cells. *J. Clin. Invest.* 111:1001–1010.

CCR9 is a homing receptor for plasmacytoid dendritic cells to the small intestine

Meike Wendland*, Niklas Czeloth*, Nicolas Mach†, Bernard Malissen‡, Elisabeth Kremmer§, Oliver Pabst*, and Reinhold Förster*¶

*Institute of Immunology, Hannover Medical School, 30625 Hannover, Germany; †Oncology Division, Geneva University Hospital, 1211 Geneva, Switzerland; ‡Centre d'Immunologie de Marseille-Luminy, Institut National de la Santé et de la Recherche Médicale, U631, Centre National de la Recherche Scientifique, UMR6102, 13288 Marseille Cedex 9, France; and §GSF National Research Center for Environment and Health, Institute of Molecular Immunology, 81377 Munich, Germany

Edited by Dan R. Littman, New York University Medical Center, New York, NY, and approved February 23, 2007 (received for review October 17, 2006)

Small intestine plasmacytoid dendritic cells (pDC) are poorly characterized. Here, we demonstrate that intestinal pDC show the characteristic plasma cell-like morphology, and are recognized by antibodies against B220, Ly6c, 120G8, and PDCA-1, markers that are typically expressed by pDC. Furthermore, intestinal pDC carry high levels of CCR9 and are largely absent in the intestine, but not in lung, liver, or secondary lymphoid organs of CCR9-deficient animals. Competitive adoptive transfers reveal that CCR9-deficient pDC are impaired in homing to the small intestine after i.v. transfer. In a model of cholera toxin-induced gut inflammation, pDC are recruited to the intestine in WT but not CCR9-deficient animals. Furthermore, after oral application of a Toll-like receptor (TLR) 7/8 ligand, myeloid DC of the lamina propria are rapidly mobilized in WT but not in CCR9-deficient animals. Mobilization of myeloid DC can be completely rescued by adoptively transferred WT pDC to CCR9-deficient mice before oral challenge. Together, our data reveal an essential role for CCR9 in the homing of pDC to the intestine under homeostatic and inflammatory conditions and demonstrate an important role for intestinal pDC for the rapid mobilization of lamina propria DC.

chemokine receptor | gut | dendritic cell migration | Toll-like receptor 7 | cell mobilization

Among the different dendritic cell (DC) subsets described, a population of cells has been identified possessing a distinct morphology and secreting large amounts of type I IFN after viral infection (1) or triggering through Toll-like receptors (TLR) 7 or 9. This subpopulation has gained much attention recently, because it is believed that these cells link innate and adaptive immunity (2). Based on their morphology, some have termed these cells plasmacytoid DC (pDC; ref. 3), whereas others have referred to them as natural IFN-producing cells (IPC; ref. 4). In mice, pDC are $CD11c^{int}B220^{+}Ly6C^{+}$ (3) and, after activation, up-regulate MHC class II and costimulatory molecules (4). pDC are continuously produced in the bone marrow (BM), and fms-like tyrosine kinase3 ligand (Flt3L) has been identified as an important growth and differentiation factor for these cells (5, 6). Some have suggested that pDC, like naive B and T cells, may constitutively migrate from blood to noninflamed lymphoid organs via high endothelial venules (3, 7), whereas others have proposed that circulating pDC are preferentially recruited to inflamed lymph nodes (8, 9). In this model, L- and E-selectin mediate rolling of pDC on inflamed endothelium whereas firm attachment of pDC to the vessel wall is mediated by $\beta1$ and $\beta2$ integrins. pDC express both inflammatory and homeostatic chemokine receptors: CXCR3, CCR2, and CCR5, which all bind inflammatory chemokines, and CXCR4 and CCR7, which bind the constitutive chemokines CXCL12 and CCL19/CCL21, respectively. Although each of these chemokine receptors is capable of mediating chemotactic response of pDC *in vitro*, there is evidence that only CXCR3 (8–10) or CCR5 (7) is able to fulfill this task at the inflamed lymph node (LN) vessel *in vivo*. In contrast to the scenario described for inflamed LN there is currently virtually no information available regarding the role of chemokines in homing of pDC to nonlymphoid tissues such as mucosal tissues.

In the present study, we reveal a role for intestinal pDC in the rapid mobilization of lamina propria (LP) myeloid DC and show that the chemokine receptor CCR9 controls the migration of pDC to the small intestine under both steady-state and inflammatory conditions.

Results

Characterization of Plasmacytoid Dendritic Cells of the Small Intestine. We applied standard procedures to isolate immune cells located in the epithelium (intraepithelial, IE) and the LP from the intestine. In both cell preparations we found a distinct population of $CD11c^{+}B220^{+}Ly6C^{+}$ cells that accounted for up to 1% of all cells. In contrast to pDC, myeloid (m)DC ($CD11c^{+}MHCII^{+}CD3^{-}B220^{-}Ly6C^{-}$) were present only at very low numbers in the IE preparation (Fig. 1*A*). Both pDC of the LP and IE preparation showed low levels of surface MHC class II expression (Fig. 1*A*). Further analysis revealed that $CD11c^{+}B220^{+}Ly6C^{+}$ cells of both preparations uniformly express the pDC markers PDCA1 as well as 120G8 (Fig. 1*B*). Cytospins from sorted pDC ($CD11c^{+}B220^{+}Ly6C^{+}$) and myeloid DC (mDC) of the IE preparation revealed a round and smooth, plasma cell-like morphology of pDC, whereas mDC showed the characteristic dendrites (Fig. 1*C*). To further characterize the localization of pDC within the intestine we applied anti-B220, anti-120G8, and anti-CD3 mAb in immunohistology. Micrographs were randomly taken from sections and, as depicted in Fig. 1*D*, the positioning of $120G8^{+}B220^{+}CD3^{-}$ cells was determined relative to epithelial cells by using image analysis (analySIS; Olympus, Hamburg, Germany). Evaluating the positioning of $\approx$150 pDC we observed that 4.9% of these cells were clearly located within the epithelial cell layer whereas another 6.7% were situated within a distance of 5–10 μm from the apical tip of the epithelial cells (Fig. 1*D*). These data demonstrate that a certain amount of the pDC locate within or close to the

---

Author contributions: O.P. and R.F. contributed equally to this work; O.P. and R.F. designed research; M.W. and N.C. performed research; N.M., B.M., and E.K. contributed new reagents/analytic tools; M.W. and N.C. analyzed data; and R.F. wrote the paper.

The authors declare no conflict of interest.

This article is a PNAS Direct Submission.

Abbreviations: DC, dendritic cell; mDC, myeloid DC; pDC, plasmacytoid DC; TLR, Toll-like receptor; Flt3L, fms-like tyrosine kinase3 ligand; LN, lymph node; LP, lamina propria; IE, intraepithelial; PP, Peyer's patches; BM, bone marrow; CFSE, carboxyfluorescein diacetate-succinimidyl ester; TAMRA, carboxytetramethylrhodamine; CT, cholera toxin.

¶To whom correspondence should be addressed at: Institute of Immunology, Hannover Medical School, Carl Neuberg Strasse 1, 30625 Hannover, Germany. E-mail: foerster.reinhold@mh-hannover.de.

This article contains supporting information online at www.pnas.org/cgi/content/full/0609180104/DC1.

© 2007 by The National Academy of Sciences of the USA

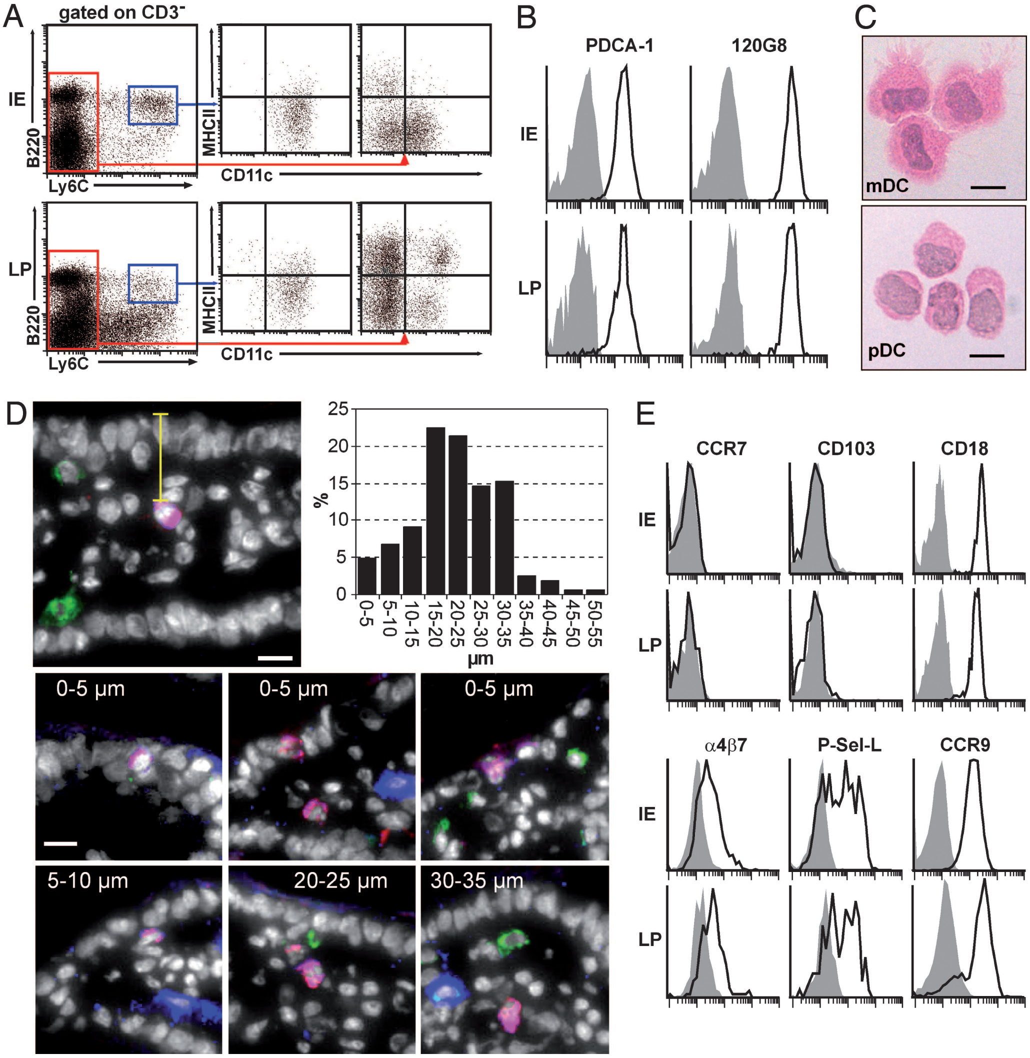

Fig. 1. Phenotype of plasmacytoid DC in the small intestine of mice. (*A*) Cells of the IE and LP preparation of the small intestine were stained with antibodies specific for CD3, CD11c, B220, MHCII, and Ly6C. $CD3^-$ cells were analyzed for the expression of B220 and Ly6C (*Left*). The expression of MHCII and CD11c is shown for $Ly6C^+$ $B220^+$ (blue box, *Center*) and $Ly6C^-$ cells (red box, *Right*). (*B*) Expression pDC-marker. pDC ($CD11c^+$, $B220^+$, and $Ly6C^+$) of the IE and LP preparation were stained for PDCA-1 or 120G8 (solid lines) or isotype controls (shaded area) as indicated. (*C*) Cytospins of flow sorted IE mDC and pDC were stained with H&E (pDC: $CD3^-CD11c^+B220^+Ly6C^+$; mDC: $CD3^-CD11c^+B220^-Ly6C^-$). (Scale bars: 10 μm.) Representative data from one of two experiments are shown. (*D*) Cryostat sections of the small intestinal villi were stained for nuclei (DAPI, white), B220 (blue), CD3 (green), and 120G8 (red). The yellow bar in the upper left micrograph indicates how the positioning of pDC ($120G8^+B220^+$) relative to the epithelial layer was determined. (*Top Right*) Distance distribution of 150 pDC analyzed relative to the epithelium. (*Middle* and *Bottom*) Examples of the positioning of individual pDC with distances as indicated. (Scale bars: 10 μm.) (*E*) Flow cytometric analysis of pDC of the IE and LP preparation. Cells were stained with antibodies as indicated (solid lines) or isotype controls (shaded area) and gated on pDC ($CD11c^+$, $B220^+$, and $Ly6C^+$). Shown are representative data from four independent experiments with cells pooled from two to six mice each.

intestinal epithelium, whereas >80% of the cells analyzed were positioned at distances >15 μm, which renders them as LP cells (Fig. 1*D*). Because similar numbers of pDC were present in the IE and LP preparation following standard isolation procedures, it is currently unclear whether pDC of the LP contaminate the IE preparation or whether pDC locating to the epithelium are more efficiently isolated. Because we hardly find any mDC within the IE preparation we favor the latter possibility. Yet it remains to be determined whether both populations serve different functions or belong to a common cell population. Because pDC of the IE preparation, in contrast to pDC of the LP preparation, can be isolated by rather gentle procedures, exclusively pDC of the IE preparation were used for functional assays in this study.

CCR9 Expression on Intestinal pDC. To identify the molecular mechanisms that allow the migration of pDC to the intestine, we analyzed the expression of homing molecules. Although it is well established that the integrin α_E (CD103) mediates lymphocyte adhesion to epithelial cells in the intestine, we failed to identify expression of this integrin on intestinal pDC. Similarly, CCR7 (Fig. 1*E*), essentially involved in homing of lymphocytes into peripheral lymphoid organs is not expressed by pDC of the intestine. In contrast, we observed high levels of CD18 (β2-integrin) and intermediate levels of $\alpha4\beta7$ whereas ≈50% of pDC express P-selectin ligands (Fig. 1*E*). Of interest, the vast majority of intestinal pDC expressed high amounts of the chemokine receptor CCR9 (Fig. 1*E*), whereas mDC of the LP expressed no, or low levels of CCR9 [supporting information (SI) Fig. 6*A*].

CCR9 Expression of pDC Isolated from Different Lymphoid Organs. Considering the uniform expression of CCR9 on intestinal pDC, we analyzed expression of CCR9 on pDC isolated from second-

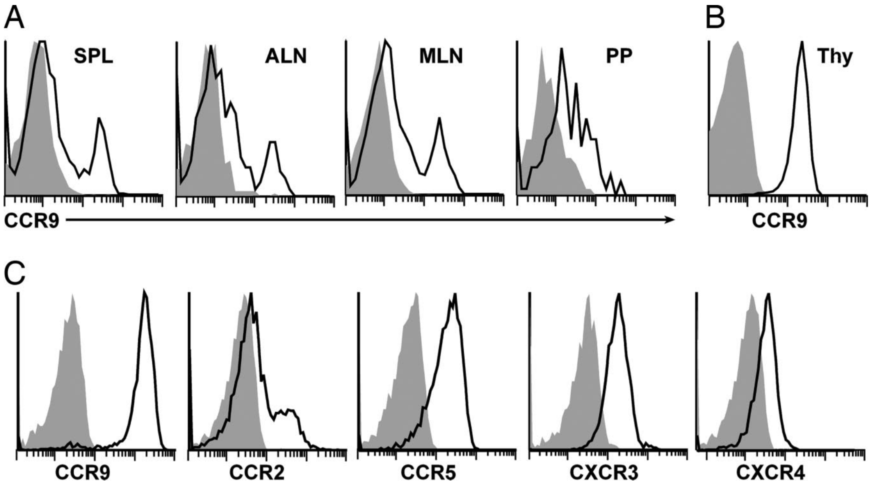

Fig. 2. Expression of CCR9 on pDC. (*A*) Cells were isolated from different lymphoid organs as indicated. pDC were addressed as CD11c$^+$B220$^+$Ly6C$^+$ and analyzed for the expression of CCR9 (solid line). (*B*) CD4$^+$CD8$^+$ thymocytes served as a positive control. (*C*) Expression of chemokine receptors (solid lines) on pDC isolated from the BM (shaded area: isotype control). SPL, spleen; ALN, axillary LN; MLN, mesenteric LN; PP, Peyer's patches; Thy, thymus). Representative data from four independent experiments with cells pooled from two to six mice each (*A* and *B*) or from three mice (*C*).

ary lymphoid organs including spleen, skin-draining LN, mesenteric LN, and Peyer's patches (PP; Fig. 2*A*) and used CD4$^+$CD8$^+$ thymocytes, known to express high levels of CCR9, as a positive control (11); Fig. 2*B*). Interestingly, only a fraction of pDC present in any of these organs expressed CCR9 (Fig. 2*A*), whereas ≈95% of pDC isolated from the BM carried this receptor (Fig. 2*C*). Most BM pDC also express CCR5 and CXCR3 whereas CCR2 is present on only roughly 25% of the cells. CXCR4, known to retain cells to the BM, is only very weakly expressed (Fig. 2*C*). Together, these data demonstrate that pDC are equipped with various chemokine receptors before being released from the BM. This feature presumably allows homing not only to places of inflammation but also to the noninflamed intestine.

Chemotaxis Analysis of Flt3L-Expanded pDC. Based on the strong expression of CCR9 on BM and intestinal pDC, we compared the migration capacity of pDC and mDC toward the chemokine CCL25/TECK, which is the sole known ligand for this receptor (12). The frequency of pDC varies between different mouse strains and it is well known that, for example, C57BL/6 (B6) mice harbor much less pDC than 129SV mice (13). However, irrespective of the genetic background the number of pDC that can be isolated from mouse tissues is insufficient to conduct standard *in vitro* chemotaxis assays. To overcome this limitation we expanded the DC population *in vivo* by implanting a Flt3-L-secreting tumor cell line (B16-FL) in B6 mice for 14 days (14).

During this time period, the percentage of CD11c$^+$ cells present in the spleen increased from 3% to 30–35% (data not shown). Eighty percent of the *in vivo* expanded pDC expressed CCR9, with levels very similar to those present on BM pDC (Figs. 2*C* and Fig. 4*C*) whereas *in vivo* expanded mDC expressed only small amounts of this receptor (SI Fig. 6*B*). Spleen pDC were enriched by CD11c$^+$ MACS-sorting, resulting in 95% purity for CD11c$^+$ cells that contained ≈15% Ly6C$^+$B220$^+$ pDC. *In vitro* transwell migration assays revealed strong chemotactic response of pDC to CCL25, as well as to CXCL9, a ligand for CXCR3 and to CXCL12, which is a ligand for CXCR4. Only a weak response was observed toward CCL19, which serves as a ligand for CCR7. mDC showed little chemotactic response toward CCL25 and CXCL9 and moderate response toward CXCL12 and CCL19 (Fig. 3*A*).

Reduced Numbers of pDC in the Small Intestine of CCR9-Deficient Mice. Based on these observations, we characterized the distribution of pDC in CCR9-deficient mice. We found similar percentages of pDC in lung and liver (SI Fig. 7) as well as in inguinal and mesenteric lymph nodes whereas the number of splenic pDC was slightly increased in CCR9$^{-/-}$ mice. In contrast, we observed a >90% decrease of intestinal and a 50% reduction of PP pDC (Fig. 3*B*).

pDC Preferentially Migrate to the Small Intestine. Based on the findings described so far, it seemed likely that pDC require CCR9 for homing to the small intestine. To prove this hypothesis, we adoptively transferred cells from B6 and CCR9$^{-/-}$ donors that carried a Flt3-L-secreting tumor for 14 days. Under the influence of Flt3L pDC expanded to a similar extent in B6 and CCR9$^{-/-}$ mice (Fig. 4*A* and SI Fig. 8) and were indistinguishable regarding the expression of CCR2, CCR5, and CXCR3 whereas CCR9 was only detected on pDC derived from B6 but not CCR9-deficient donors (Fig. 4*C*). Without further purification, splenocytes of these donors were labeled with 5(6)-carboxyfluorescein diacetate *N*-succinimidyl ester (CFSE) and 5(6)-carboxytetramethylrhodamine *N*-succinimidyl ester (TAMRA) respectively. A mixture of WT and CCR9-deficient cells, adjusted to contain equal numbers of pDC, was i.v. transferred in B6 recipients. After 18 h of transfer, we first analyzed the composition of adoptively transferred WT cells present in the IE as well as LP preparation and noticed that 54% and 25% of all cells recovered from the IE and LP fraction respectively were pDC (Fig. 4*B*). These findings demonstrate that among the diverse cell populations transferred pDC home most efficiently to the intestine. These competitive transfers also revealed that CCR9-deficient pDC are largely impaired in their capacity to home to the intestine as reflected by the low migration ratio of CCR9-deficient vs. WT pDC found in the IE and LP preparation (Fig. 4*D*). In contrast, CCR9-deficient and B6 pDC migrated with similar efficiency to peripheral and mesenteric lymph nodes (Fig. 4*D*). The nature of the cell labeling had no impact on these experiments because interchanging the dyes between B6 and CCR9$^{-/-}$ cells yielded identical results (data not shown). Although these data clearly demonstrate that pDC require CCR9 for efficient homing to the gut, it should be mentioned that the trafficking properties of pDC from Flt3-

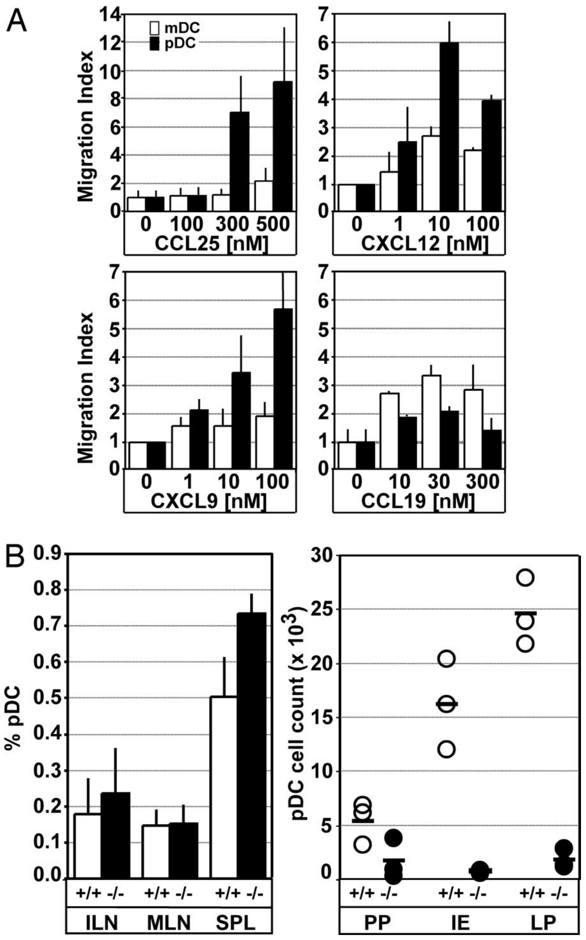

Fig. 3. Chemotactic response of pDC toward the CCR9 ligand CCL25. (*A*) DC were expanded *in vivo* by treating B6 mice with Flt3L-secreting tumor cells for 14 days. Chemotactic activity of splenic pDC and mDC toward different concentrations of CCL25, CXCL9, CXCL12, and CCL19 was analyzed (open columns, mDC; black columns, pDC; mean + SD; $n = 4$ independent experiments with pooled cells from two or three mice each). (*B*) Lack of intestinal pDC in CCR9-deficient mice. Shown are the percentage (*Left*) and number (*Right*) of pDC isolated from the inguinal LN (ILN), mesenteric LN (MLN), spleen (SPL), PP, and the IE and the LP preparation of the small intestine from B6 and CCR9-deficient mice. Circles represent data of individual mice ($n = 3$); bars show mean values. Similar results were obtained in four additional experiments using mice on a mixed genetic background (BALB/c 129SV; $n = 20$ mice per genotype).

ligand treated mice might be different from those present under physiologic situations.

pDC Are Recruited to the Inflamed Intestine. Because it is known that pDC play an important role in anti viral immunity (4, 10) we speculated that pDC might be recruited to the intestine during inflammatory processes to strengthen first line defense. Cholera toxin (CT) is known to induce intestinal inflammation when administered orally and it has been reported that within 2 h after oral application the number of mDC transiently recruited to the intestine increases 4-fold (15). We observed that, in addition to mDC, pDC numbers also increased 3-fold when feeding B6 mice with 10 μg of CT (Fig. 4*E*). Of interest, the identical experimental setup never resulted in any increase of pDC neither in the IE nor the LP preparation of CCR9-deficient mice after 1, 2, or 3 h of CT-treatment (Fig. 4*E* and data not shown). The specific requirement for CCR9 on pDC for their recruitment to the intestine during inflammatory processes was

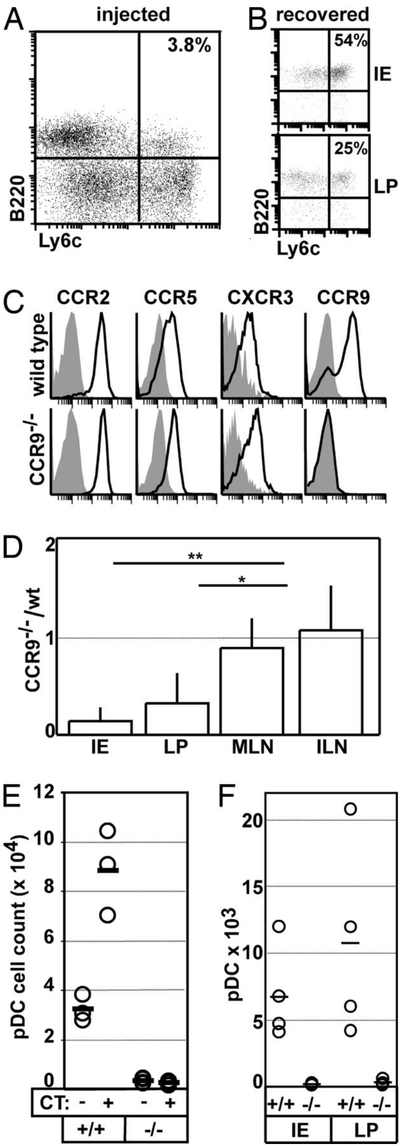

Fig. 4. CCR9-dependent homing of pDC to the small intestine. (*A–D* and *F*) DC were expanded *in vivo* by treating B6 and CCR9-deficient mice with Flt3L-secreting tumor cells. (*A*) Splenocytes of B6 donors were analyzed for the presence of pDC (B220$^+$Ly6C$^+$). (*B*) Nonpurified WT Flt3L-expanded splenocytes were labeled with CFSE and i.v. injected into recipients. The occurrence of donor pDC in the recipient's IE (*Upper*) and LP (*Lower*) preparation was analyzed 18 h later (gate on CFSE$^+$ cells). (*A* and *B*) Data shown are representative for five animals of two independent experiments. (*C*) CD11$^+$B220$^+$Ly6C$^+$ pDC in Flt3L-expanded splenocytes of B6 (*Upper*) and CCR9-deficient mice (*Lower*) were stained for the expression of different chemokine receptors as indicated. (*D*) Splenocytes isolated from Flt3L-treated B6 or CCR9-deficient mice were labeled with CFSE and TAMRA, respectively. Cells were adjusted to equal numbers of pDC and injected at a ratio of 1:1 in B6 recipients. After 18 h, recipients were killed, and the ratio of donor B6 and CCR9-deficient pDC was analyzed in the recipient's IE and LP preparation of the intestine and the inguinal (ILN) and mesenteric (MLN) lymph node (mean + SD; $n = 5–9$ recipients). (*E*) WT (+/+) and CCR9-deficient (−/−) mice received 10 μg of CT or saline orally. After 1 h, animals were killed, and the number of pDC present in the small intestine IE preparation was determined. Circles represent individual mice; bars are mean values. Similar results were obtained in two additional experiments. (*F*) CFSE-labeled splenocytes isolated from Flt3L-treated B6 and TAMRA-labeled splenocytes isolated from Flt3L-treated CCR9-deficient mice were adoptively transferred to CCR9-deficient mice at a ratio of 1:1. After 18 h, recipients were gavaged orally with 10 μg of CT. One hour later, mice were killed, and the number of labeled WT (+/+) and CCR9$^{-/-}$ (−/−) pDC isolated from the IE and LP preparation was analyzed. Circles represent individual mice; bars are mean values.

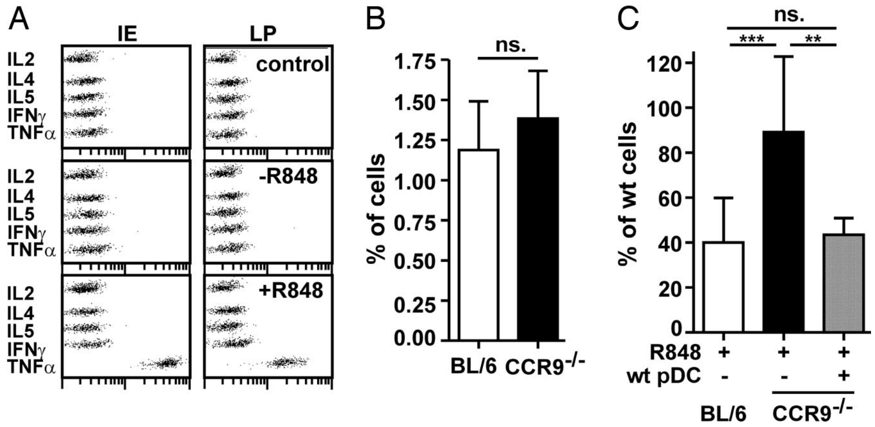

Fig. 5. Rapid mobilization of LP mDC relies on the intestinal pDC. (*A*) Cytokine bead array profile from the supernatant of sorted pDC of IE (*Left*) and LP (*Right*) preparation after 16 h *in vitro* stimulation in the absence (−R848) or presence (+R848) of R848. Control, cell culture medium. (*B*) Percentage of LP mDC ($CD45^+CD11c^+MHCII^{high}$) of untreated mice (mean +SD, $n = 6$ per group). (*C*) WT (open column) or $CCR9^{-/-}$ mice (black column) were orally gavaged with 10 μg of R848. After 2 h, the number of mDC ($CD45^+CD11c^+MHCII^{high}$) present in the LP of the small intestine was determined and expressed as percentage of untreated WT control. Gray column, $CCR9^{-/-}$ mice that i.v. received MACS-purified B6 pDC 16 h prior R848 treatment (mean + SD; $n = 6$–11 mice per group; ns, not significant; **, $P < 0.01$; ***, $P < 0.001$).

confirmed by adoptive transfer of WT and CCR9-deficient pDC to CCR9-deficient recipients followed by application of CT as described above. Whereas adoptively transferred WT pDC were amply present in the IE and LP preparation, CCR9-deficient pDC were almost completely excluded from these compartments (Fig. 4*F*). Together, these results show that during inflammatory events pDC can be recruited to the intestinal mucosa and that this mechanism relies to a large extend on CCR9.

A Role for Intestinal pDC for the Rapid Mobilization of LP Myeloid DC. It has been shown recently that oral application of the TLR7/8 ligand resiquimod (R848) results in the rapid mobilization of LP DC and that TNFα, possibly released by pDC, is involved in this process (16). We thus speculated that intestinal pDC might be the source of TNFα that potentially triggers the mobilization of neighboring mDC. To test this hypothesis, we *in vitro* stimulated B6 pDC of the IE and LP preparation for 16 h with R848. Indeed, pDC secreted considerable amounts of TNFα but failed to produce any detectable quantities of IL-2, IL-4, IL-5, or IFNγ (Fig. 5*A*). We then analyzed the mobilization of LP mDC *in vivo* after oral application of R848. Whereas untreated B6 and $CCR9^{-/-}$ mice did not differ regarding the presence of intestinal mDC (Fig. 5*B*), within 2 h oral R848 induced the mobilization of ≈60% of mDC in WT but only 10.8% in $CCR9^{-/-}$ mice. Importantly, once CCR9-deficient mice i.v. received splenic pDC of Flt3L-treated WT donors 16 h prior oral application of R848, this deficiency in intestinal mDC mobilization could be completely rescued (Fig. 5*C*). These experiments show that a CCR9-dependent homing of pDC to the intestine is involved in the rapid mobilization of intestinal mDC after oral application of a TLR7/8 ligand. Because it has been shown by others in the rat model that application of LPS also induces mobilization of LP mDC (17), we applied 50 μg of LPS i.p. to WT and CCR9-deficient animals. Of interest, under these experimental conditions we failed to observe any difference between WT and CCR9-deficient animals regarding the mobilization of LP mDC (SI Fig. 9).

Discussion

The CCR9 ligand, CCL25, is expressed by epithelial cells of the small intestine and has been suggested to target immune cells to the intestinal epithelium (18). The present study supports the idea that this chemokine attracts defined populations of immune cells to the small intestine. Agace and colleagues (19) further demonstrated that $CD8\alpha\beta^+$ T cells, activated within the mesenteric LN, selectively home to the small intestinal mucosa and that this homing depends on CCR9. Data from our group suggest a similar mechanism for plasma cells (11). Results provided here demonstrate that CCR9-deficient mice possess reduced numbers of pDC in the small intestine under steady-state conditions, an observation that correlates well with the impaired recruitment of CCR9-deficient pDC to this organ under inflammatory conditions. In accordance with the hypothesis that CCR9 is required for pDC gut homing is our finding that pDC derived from CCR9-deficient donors are impaired in homing to the intestine once adoptively transferred to WT recipients.

In addition to targeting immune cells to the epithelium, CCL25 also mediates T cell entrance into the LP across intestinal venules (20). A similar mechanism might allow homing of pDC to the small intestine. Therefore, it seems possible that CCR9 recruits pDC into the LP and, in addition, targets a fraction of these cells to the epithelium. Apart from CCR9, it is currently unclear, which adhesion molecules are involved in pDC homing to the intestine. Our data would suggest that $\alpha4\beta7$ integrin, as well as P-selectin, might also be involved in this process.

This study also reveals a previously undescribed function for intestinal pDC. We show that after oral application of a TLR7/8 ligand, intestinal pDC are required for the rapid mobilization of LP mDC, a mechanism that might involve the release of TNFα from this cell population. Although it is currently unclear how impaired mobilization might affect immunity to pathogens, it seems conceivable that the rapid mobilization of LP DC to the mesenteric LN favors the fast onset of adaptive immunity. Interestingly, pDC mediated mobilization of mDC seems restricted to distinct TLR ligands because LPS-activity bypasses the need of pDC for successful emigration of mDC from the small intestine. This finding corroborates the concept that pathogens may bias immune responses already at the early stage of their entry into the body because it is known that immature DC primed under distinct cytokine environment such as TNFα cause a shift to the subsequent $T_{helper}1/T_{helper}2$ answer. Furthermore, it is also tempting to speculate that pDC might help to enforce the armed battery of IE lymphocytes residing at the frontline of mucosal immune defense. In particular intestinal pDC might supplement mucosal protection against viral attack. However, these scenarios still await experimental approval encompassing animal models for inflammatory bowel disease and viral infections.

Materials and Methods

Mice. Animals were bred under specific pathogen-free conditions. CCR9-deficient mice, either on a mixed genetic (BALB/c × 129SV) or a C57BL/6 background (backcrosses for 5 or 9 generations) have been described elsewhere (21). Most of the experiments described in this manuscript were performed on both genetic backgrounds yielding identical results. Data depicted derive from experiments performed with mice on a C57BL/6 background except those depicted in Fig. 4*E*. All animal experiments were conducted in accordance with local and institutional guidelines.

Flow Cytometry. Immune cells of the intestine were isolated from 6- to 8-week-old mice as recently described in detail (22). Cells were stained with the following antibodies: Ly6C-FITC, $\alpha4\beta7$-biotin, CD103-biotin, B220-PerCP, CD11c-PE (all from BD Bioscience), CD4-PE, CD62L-PE, CD45-APC, CD18-FITC (Caltag), P-selectin-ligand (R & D Systems), CCR7-biotin (eBioscience), 120G8, (Vector Laboratories), PDCA-1-APC (Dianova). Anti CD3-Cy5 (clone 17A2) and anti CD8 (clone CD8.2) were grown in our laboratories. Anti CCR2 and CCR5 mAb were kindly provided by Matthias Mack (University of Regensburg, Regensburg, Germany) (23). The rat anti-mouse CCR9 mAb (clone 7E7) was produced in our lab and has been described (11).

Immunohistology and Cytospins. Immunhistological analysis of the small intestine of mice was done on 8-μm cryosections as described (11, 22). pDC ($CD3^-CD11c^+B220^+Ly6C^+$) and mDC ($CD3^-CD11c^+B220^-Ly6C^-$) of the IE preparation were sorted by flow cytometry (FACSAria, BD Biosciences). Acetone-fixed cytospins were prepared from sorted cells.

***In Vivo* Generation of pDC and *in Vitro* Migration Assay.** B6 and CCR9-deficient mice received s.c. 5×10^5 to 1×10^6 B16-FL cells, a murine melanoma tumor cell line engineered to stably produce murine Flt3-L (14). After 14 days, animals were killed. Flt3L-expanded, $CD11c^+$ MACS-sorted splenocytes (1×10^6), containing ≈15% pDC, were resuspended in 100 μl of RPMI medium 1640 and loaded into collagen-coated transwells (Corning BV; 5 μm pore size) that were placed in 24-well plates containing 400 μl medium or medium supplemented with various concentrations of CCL25, CXCL9, CCL19, or CXCL12 (R & D systems). After 3 h of incubation at 37°C, the migrated cells were collected, counted, and stained with mAb to determine by flow cytometry the number of migrated pDC and mDC. The ratio of the number of pDC that migrated in the presence of chemokine vs. the number of cells that migrated to PBS control was calculated and is given as the migration index.

Adoptive Transfer of Labeled Cells. Splenocytes from B16-FL tumor-carrying B6 or CCR9-deficient mice were labeled with TAMRA (red fluorescent) or CFSE (green fluorescent) or vice versa. Cell populations were adjusted to contain equal numbers of pDC. For adoptive transfers, 10^6 pDC for both colors were i.v. injected into the tail vein of recipients. After 18 h, recipients were killed and cells were isolated from the intestine as well as from mesenteric and peripheral lymph nodes.

MACS-Purification of pDC. Splenocytes from B16-FL tumor-bearing mice were negative sorted for CD3 and CD19. In a subsequent step $B220^+$ cells were enriched.

***In Vivo* Mobilization of Cells.** Ten micrograms of CT (Sigma) in 300 μl of carbonic buffer (0.1 M $NaHCO_3$) or 10 μg of R848 in 300 μl of PBS were orally administered by gavage. Fifty micrograms of LPS were i.p. injected in 150 μl of PBS. One hour to 3 h after the application of CT, mice were killed, and the number of intestinal pDC was determined. Mice that received R848 were killed 2 h after the application of this drug, and the number of mDC of the LP was determined. Mice that received LPS were killed 12 h later, and the number of LP mDC was determined. Some of the R848-treated $CCR9^{-/-}$ mice received 2–4 × 10^6 MACS-purified WT pDC i.v. 16 h prior R848 application.

***In Vitro* Stimulation of pDC.** 10^6 MACS-purified pDC were cultured in 200 μl of RPMI medium 1640/10% FCS for 14 h in the absence or presence of CpG2216 (16.5 μg/ml) or R848 (2 μg/ml). mDC ($CD11c^+MHCII^+$) of the LP preparation were sorted by flow cytometry (MoFlo, Dako-Cytomation) and activated with CpG2216 as describe above. Supernatants were collected and the amount of IFN-α determined by ELISA (Hycult). Interleukins and TNFα were detected by cytokine bead arrays (BD).

We thank Matthias Mack for providing CCR2 and CCR5 mAb and Günter Bernhardt for valuable suggestions on the manuscript. The generation and characterization of CCR9-deficient mice was supported by the Association pour la Recherche sur le Cancer and MUGEN. This work was supported by Deutsche Forschungsgemeinschaft Grant SFB621-A1 (to R.F.).

1. Siegal FP, Kadowaki N, Shodell M, Fitzgerald-Bocarsly PA, Shah K, Ho S, Antonenko S, Liu YJ (1999) *Science* 284:1835–1837.
2. Iwasaki A, Medzhitov R (2004) *Nat Immunol* 5:987–995.
3. Nakano H, Yanagita M, Gunn MD (2001) *J Exp Med* 194:1171–1178.
4. Asselin-Paturel C, Boonstra A, Dalod M, Durand I, Yessaad N, Dezutter-Dambuyant C, Vicari A, O'Garra A, Biron C, Briere F, Trinchieri G (2001) *Nat Immunol* 2:1144–1150.
5. Maraskovsky E, Brasel K, Teepe M, Roux ER, Lyman SD, Shortman K, McKenna HJ (1996) *J Exp Med* 184:1953–1962.
6. Gilliet M, Boonstra A, Paturel C, Antonenko S, Xu XL, Trinchieri G, O'Garra A, Liu YJ (2002) *J Exp Med* 195:953–958.
7. Diacovo TG, Blasius AL, Mak TW, Cella M, Colonna M (2005) *J Exp Med* 202:687–696.
8. Yoneyama H, Matsuno K, Zhang Y, Nishiwaki T, Kitabatake M, Ueha S, Narumi S, Morikawa S, Ezaki T, Lu B, *et al.* (2004) *Int Immunol* 16:915–928.
9. Kohrgruber N, Groger M, Meraner P, Kriehuber E, Petzelbauer P, Brandt S, Stingl G, Rot A, Maurer D (2004) *J Immunol* 173:6592–6602.
10. Cella M, Jarrossay D, Facchetti F, Alebardi O, Nakajima H, Lanzavecchia A, Colonna M (1999) *Nat Med* 5:919–923.
11. Pabst O, Ohl L, Wendland M, Wurbel MA, Kremmer E, Malissen B, Forster R (2004) *J Exp Med* 199:411–416.
12. Zabel BA, Agace WW, Campbell JJ, Heath HM, Parent D, Roberts AI, Ebert EC, Kassam N, Qin S, Zovko M, *et al.* (1999) *J Exp Med* 190:1241–1256.
13. Asselin-Paturel C, Brizard G, Pin JJ, Briere F, Trinchieri G (2003) *J Immunol* 171:6466–6477.
14. Mach N, Gillessen S, Wilson SB, Sheehan C, Mihm M, Dranoff G (2000) *Cancer Res* 60:3239–3246.
15. Anjuere F, Luci C, Lebens M, Rousseau D, Hervouet C, Milon G, Holmgren J, Ardavin C, Czerkinsky C (2004) *J Immunol* 173:5103–5111.
16. Yrlid U, Milling SW, Miller JL, Cartland S, Jenkins CD, MacPherson GG (2006) *J Immunol* 176:5205–5212.
17. Turnbull EL, Yrlid U, Jenkins CD, Macpherson GG (2005) *J Immunol* 174:1374–1384.
18. Kunkel EJ, Campbell JJ, Haraldsen G, Pan J, Boisvert J, Roberts AI, Ebert EC, Vierra MA, Goodman SB, Genovese MC, *et al.* (2000) *J Exp Med* 192:761–768.
19. Svensson M, Marsal J, Ericsson A, Carramolino L, Broden T, Marquez G, Agace WW (2002) *J Clin Invest* 110:1113–1121.
20. Hosoe N, Miura S, Watanabe C, Tsuzuki Y, Hokari R, Oyama T, Fujiyama Y, Nagata H, Ishii H (2004) *Am J Physiol Gastrointest Liver Physiol* 286:G458–G466.
21. Wurbel MA, Malissen M, Guy-Grand D, Meffre E, Nussenzweig MC, Richelme M, Carrier A, Malissen B (2001) *Blood* 98:2626–2632.
22. Pabst O, Herbrand H, Worbs T, Friedrichsen M, Yan S, Hoffmann MW, Korner H, Bernhardt G, Pabst R, Forster R (2005) *Eur J Immunol* 35:98–107.
23. Mack M, Cihak J, Simonis C, Luckow B, Proudfoot AE, Plachy J, Bruhl H, Frink M, Anders HJ, Vielhauer V, *et al.* (2001) *J Immunol* 166:4697–4704.

A CCR7-dependent steady state homing of dendritic cells essentially required for lymph node T cell homeostasis

Meike Wendland[1]
Stephanie Willenzon[1]
Jessica Kocks[1]
Ana Clara Davalos-Misslitz[1]
Svantje Hammerschmidt[1]
Elisabeth Kremmer[2]
Angelika Hoffmeyer[3]
Oliver Pabst[1]
Reinhold Förster[1]

[1] Institute of Immunology, Hannover Medical School, D-30625 Hannover, Germany
[2] Helmholtz-Zentrum München, Institute of Molecular Immunology, D-81377 Munich, Germany
[3] Nycomed GmbH, D-78467 Konstanz, Germany

Running title: dendritic cells and T cell homeostasis

Send correspondence to:
Prof. Dr. Reinhold Forster,
Institute of Immunology,
Hannover Medical School,
30625 Hannover, Germany;
phone:+49-511-5329721
Fax: +49-511-5329722;
email: forester.reinhold@mh-hannover.de

Summary

Although several molecular mechanisms have been elucidated that mediate homing of lymphocytes from the blood to lymphoid organs, little is known about factors that determine the dwell time of homed lymphocytes within lymph nodes. Applying a novel conditional CCR7 knock-in mouse model we now show that mice expressing CCR7 in T cells only (T-CCR7ki), are unexpectedly devoid of lymph node T cells although T cells of these mice readily home to lymph nodes of wild type recipients following intravenous adoptive transfer. We show that lymph nodes of T-CCR7ki mice have reduced numbers of high endothelial venules resulting in impaired homing of T cells to lymph nodes. Furthermore those T cells that homed to lymph nodes are not retained and rapidly leave lymph nodes. Applying different complementation approaches we found that impaired homing of dendritic cells from the periphery into the draining lymph nodes causes both defects. We provide evidence that steady state migrating dendritic cells provide vascular endothelial growth factor to support HEV formation. Furthermore, CCL21 produced by T zone stromal cells bind through its heparin-binding domain to dendritic cells allowing T cells to stay in an ICAM-1 dependent way for prolonged periods of time within lymph nodes. Thus our data reveal an essential role of dendritic cells in lymph node T cell homeostasis.

Introduction

Secondary lymphoid organs, such as lymph nodes, play an important role for the initiation and maintenance of adaptive immune responses. They provide the environment that allows efficient interaction of different subsets of immune cells with each other or with non hematopoietic stromal cells. The contact of naïve T cells with dendritic cells (DC) presenting antigen in secondary lymphoid organs can serve as a paradigmatic example for the need for controlled spatio-temporal interaction of cells of the immune system. T cells enter lymph nodes from the blood via specialized high endothelial venules (HEV) applying a program of sequential adhesion stages including the interaction of T cell-expressed selectins, integrins and chemokine receptors with their corresponding ligands which are expressed at the luminal side of HEV (for recent reviews see ref. (1; 2)).

While T cells continuously re-circulate between secondary lymphoid organs immature DC reside as sentinels in the skin and mucosal surfaces (3). Therefore, DC have to be mobilized from peripheral sides and migrate via afferent lymphatics into the draining lymph node to present antigen to those T cells carrying a cognate antigen receptor. Depending on the nature of the antigen, the maturation status and the subset of the dendritic cell, this initial interaction either leads to the induction of tolerance or protective immunity. Immunity is induced by DC that present antigens derived from pathogens (4) while DC presenting self-antigen or innocuous environmental antigens under non-inflammatory situations to T cells induce tolerance (5). Data obtained from CCR7-deficient mice revealed that this chemokine receptor is essential for DC mobilization as well as T cell homing. In CCR7-deficient mice lymph nodes and Peyer's patches are devoid of T cells and mature DC and upon adoptive transfer into wild type recipients, CCR7-deficient T cells fail to home to lymph nodes (6).

Along the same line, DC differentiated from bone marrow of CCR7-deficient mice do not migrate to the draining lymph node following subcutaneous injection or intra-tracheal instillation (7-9). Furthermore , applying *in vivo* mobilization assays such as fluorescein-isithiocyanate (FITC) skin-painting, CCR7-deficient DC entirely fail to migrate to the draining lymph node (6). Taken together these data identify CCR7 as a key regulator that control entry of T cells and DC to lymph node. Of interest the sphingolipid sphingosine-1-phosphate (S1P) and sphingosin-1-phosphate receptor1 (S1P1) have been identified as the key molecules that regulate egress of lymphocytes from lymphoid organs. Adoptively transferred S1P1-deficient T cells accumulate in lymphoid organs and mice deficient for sphingosine kinase (SphK), an enzyme that is involved in S1P synthesis, have enlarged lymph nodes (10). The idea that S1P and its receptors control lymphocyte egress have been fuelled by the observation that the oral application of FTY720 which induced internalization and thus functional inactivation of S1P1 lead to peripheral blood lymphopenia but lymph node lymphocytosis (11). Recently, it has been suggested that the balanced expression of CCR7 and S1P1 on T cells as well as the spatial distribution of their cognate ligands contribute to the dwell time T cells stay within lymph nodes and thus to lymph node homeostasis (12). Here we demonstrate that DC essentially contribute to T cell homeostasis at least at two checkpoints. First they produce vascular endothelial growth factor (VEGF) thus contribute to HEV growth and lymphocyte homing. In addition, by binding CCL21 via its heparin-binding domain they provide cues that allow T cells to stay for prolonged periods of time within lymph nodes.

Results

Generating humanized CCR7 knock-in mice

To further study the biology of CCR7 we generated a mouse which expressed the human CCR7 instead of the mouse homologue. To this end a targeting vector has been constructed that consists of a neomycin resistance gene flanked by two loxP sides, an internal ribosomal entry side (IRES), the entire coding cDNA of *huCCR7* followed by the 3'-UTR. Following homologous recombination the entire construct was knocked into the locus of the third exon of *muccr7* leaving all potentially regulatory elements for *CCR7* gene expression untouched (Fig 1A). Homologously recombined ES cells were identified using Southern blot analysis applying 5'- as well as 3' specific probes (Fig 1B). Gene-targeted ES cells were injected into Balb/c blastocysts to generate chimeric mice which were then bred to Balb/c mice. Offspring carrying the targeted allele was crossed to germline Cre-deleter mice and the offspring carrying both the *huCCR7* allele as well as the Cre allele were then again inter-crossed. PCR analyses of the resulting litters carrying various combinations of *neo muccr7* and *huCCR7* are shown in Fig 1C.

Expression of human CCR7 in mice

Applying mAb either specific for huCCR7 or muCCR7 analysis of CD4+ cells from peripheral blood revealed that these mice express this chemokine receptor as anticipated. While anti-muCCR7 bound to wild type mice and mice carrying one allele of both human and *muccr7* it failed to bind to cells derived from mice carrying *huCCR7* on both alleles (Fig 1D). Conversely, the anti-huCCR7 mAb did not bind to cells of wild type mice nor to cells isolated from mice still carrying the neomycin resistance gene. However, mice carrying at least one huCCR7 allele and lacking the *neo* resistance cassette bound anti-huCCR7 mAb (Fig 1D). Mice carrying both human and mouse CCR7 were further subjected to flow cytometric analysis revealing that all cell expressing mouse CCR7 also expressed huCCR7 and that human CCR7 was not expressed on cells that lacked expression of muCCR7 (data not shown). Together, these results indicate that the CCR7 knock-in (ki) mice described here express human CCR7 instead of the mouse homologue once the neo cassette has been deleted. As long as the neo cassette is present on both alleles, mice do neither express mouse nor human CCR7. For reasons of convenience, mice with two *huCCR7* alleles not carrying any *neo* due to deletion at the germ line (GL) level will be referred to as GL-huCCR7ki mice throughout the manuscript. Mice carrying *huCCR7* as well as *neo* on both alleles will be referred to as STOP-huCCR7, while mice generated by inter crossing STOP-huCCR7 mice with mice expressing Cre under control of the CD4 promoter, thus expressing human CCR7 in T cell only (see below) will be referred to as T-CCR7ki mice.

Humanized CCR7 mice show a wild type phenotype

Analyzing the phenotype of wild type, STOP-huCCR7, as well as GL-huCCR7ki mice revealed that GL-huCCR7ki mice were virtually indistinguishable from wild type mice while STOP-huCCR7 mice showed the phenotype of the earlier described CCR7-deficient mice (Fig. 2). Lymph nodes from wild type as well as GL-huCCR7ki mice contained similar numbers of T lymphocytes while lymph nodes of STOP-huCCR7 mice were devoid of both $CD4^+$ and $CD8^+$ T cells (Fig. 2A). Furthermore, a high percentage of T cells present in SLO of wild type and GL-huCCR7ki mice expressed L-selectin, thus showing the characteristic phenotype of naïve cells, while most of peripheral blood T cells in these mice were negative for L-selectin. In contrast, the few T cells present in lymph nodes of STOP-huCCR7 mice contained a higher proportion of L-selectin-negative cells, while the majority of peripheral blood T cell expressed this homing molecule in this strain, indicating that the homing of naïve T cells to LN is impaired in STOP-huCCR7 mice (Fig. 2B). Furthermore immunohistology revealed prominent T cell areas as well as prominent splenic peri-arteriolar lymphoid sheaths (PALS) filled with T cells in both wild type as well as GL-huCCR7ki mice. In contrast in STOP-huCCR7 mice the paracortex of LN as well as the splenic PALS were largely devoid of T cells. In addition, as described for CCR7-deficient mice, T cells in STOP-huCCR7 mice were distributed throughout the red pulp (Fig. 2C). Together these data strongly suggest that the human homologue of muCCR7 is fully functional in mice, and that STOP-huCCR7 mice show the same phenotype as CCR7-deficient mice.

Human CCR7 is fully functional in mice

A more detailed analysis of the humanized CCR7 mice confirmed full functionality of human CCR7 in these animals. Applying transwell migration assays, T cells from GL-huCCR7ki and wild type mice showed a comparable chemotactic response towards CCL21 while T cells from STOP-huCCR7 mice did not migrate towards this chemokine (Fig. 3A). Furthermore, following intravenous injection wild type and GL-huCCR7ki T cells home to the same extent to SLO of wild type recipient mice under competitive *in vivo* situations (Fig. 3B). In addition, subcutaneous injection of bone marrow-derived DC revealed a similar result with regard to homing efficacy. In these experiments wild type and GL-huCCR7ki DC migrate to the same extent to the draining LN while DC derived from the bone marrow of STOP-huCCR7 mice complete failed to migrate to skin-draining LN in this experimental setup (Fig. 3C).

T cell restricted expression of CCR7

To specifically address the role of CCR7 in T cell function STOP-huCCR7 mice were inter crossed to mice expressing Cre recombinase under control of the CD4 promotor to finally derive T-CCR7ki mice. These animals express huCCR7 in T cells but not in B cells or DC (Fig. 4A). *In vitro* migration assays revealed that T cells isolated from SLO of wild type as well as T-CCR7ki mice migrate towards CCL21 when tested in vitro transwell migration assay (Fig. 4B). The T cell specificity of the CCR7 knock-in could also be demonstrated functionally, since BM-derived DC of these animals neither migrated *in vitro* towards CCL21 nor *in vivo* into skin-draining LN following s.c. application (Fig. 4B +4C). Since these data strongly indicated that CCR7 is fully functional in T cells (but no other cells) of T-huCCR7ki mice, we were rather surprised to find a massive T cell lymphopenia in all LN of these mice which was similar to the one found in STOP-huCCR7 mice (Fig. 5A). Therefore we tested the ability of wild type T cells to home to SLO of wild type and T-CCR7ki mice and compared this in competitive homing assays to the homing capacity of T cells from STOP-huCCR7 mice. While T cells from wild type and STOP-huCCR7 mice home with comparable numbers to the spleens of wild type and T-huCCR7ki mice, wild type T cells homed considerably less efficient to brachial and inguinal LN of T-CCR7ki mice compared to wild type recipients being nearly as inefficient as T cells from STOP-huCCR7ki donor (Fig. 5B). These observations suggest that LN of T-huCCR7ki mice might not provide the environment required for efficient T cell homing to LN or the retention of T cells in these organs.

Reduced numbers but fully functional HEV in lymph nodes of T-huCCR7ki mice

In order to identify factors that might account for reduced homing of T cells in LN of T-huCCR7ki mice we analyzed HEV in wild type and T-CCR7ki mice. To that end iLN cryosections were stained with DAPI, anti-CD31 and MECA79 mAb and the largest sections of each lymph node were analyzed. Based on the DAPI staining the section area was determined morphometrically and found to be reduced by 30%-40% in T-huCCR7ki mice (Fig 6A). We next determined the length of all CD31$^+$MECA79$^+$ HEV present on the entire LN section and again found an approximately 30% reduction in T-huCCR7ki mice (Fig. 6A). However, once we calculated HEV length per mm^2 section area, we could not see any difference between wild type and T-huCCR7ki, showing that LN of T-huCCR7ki LN are smaller and in absolute (but not relative) numbers contain less HEV. We next compared the capacity of wild type and T-huCCR7ki HEV to allow homing of wild type cells. Following adoptive transfer of red-fluorescent, TAMRA-labeled T cells wild type as well as T-huCCR7ki recipients were sacrificed 30 min later. Cyrosection of iLN were stained with MECA79 mAb and the number and position of adoptively transferred cells was determined. With regard to the location of the adoptively transferred cells five differentiated 5 positions were determined: i) with the lumen of a HEV; ii) attached to the luminal site of the HEV, iii) within HEV iv) at the abluminal site of the HEV, v) within tissue (Fig. 6B). With the exception of cell located within the HEV lumen, we found significantly more adoptively transferred cells per entire LN section in wild type recipients at all sites analyzed (Fig. 6C). However, we could not find any significant difference between wild type and T-huCCR7ki recipients once numbers of homed cells were calculated per section area unit. Together these data show that T-huCCR7ki mice have less HEV and suggest that these HEV are fully functional.

DC migration and lymph node T cell homeostasis

Since both CCR7-deficient mice as well as T-huCCR7ki mice do not express CCR7 on DC we hypothesized that impaired DC trafficking might contribute to LN lymphopenia observed in both strains. To test this idea, we subcutaneously injected TAMRA-labeled immature wild type bone marrow DC into the left foot pad and PBS into the right foot pad of CCR7$^{-/-}$ mice. After 5 days mice were sacrificed and popLN were analyzed by flow cytometry. Compared to PBS-draining LN, DC-draining LN showed a strong increase of HEV endothelial cells (CD45$^-$CD31$^+$PNAd$^+$; Fig. 7A) indicating that continuous trafficking of DC from the periphery to LN might influence its number of HEV. To test whether the induced HEV are fully functional wild type and CCR7$^{-/-}$ mice that received PBS or immature DC sc. into the footpad 4 days earlier, intravenously received a mixture of green and red fluorescently labeled wild type and CCR7-deficient lymphocytes respectively. 30 min later mice were sacrificed and the number of adoptively transferred wild type and CCR7-deficient T cells present in the popLN were determined. As shown in Fig. 7B wild type T cells homed approx 5 times more frequent into the LN that drained the s.c. applied DC compared to those that drained the injected PBS. Interestingly, CCR7-deficient T cells also homed more efficiently to the DC- rather than the PBS-draining LN. However, compared to wild type cells, CCR7$^{-/-}$ T cells were severely impaired with regard to LN homing (Fig. 7B). Along the same line, the sc. application of immature DC to T-huCCR7ki mice induced a profound increase in LN size (Fig. 7C and 7D). The lymph node that drained the transferred DC, but not LN that drained the applied PBS also showed a regularly developed paracortex full of T cells (Fig. 7C). Further analysis revealed a very good correlation between LN cellularity and the number of adoptively transferred DC reaching the popLN (Fig. 7E). Together these data suggest that the migration of DC to LN contribute to HEV formation and efficient homing of T cells.

Rag2$^{-/-}$ bone marrow chimeras rescue the phenotype of T-huCCR7ki mice

To further address the role of steady state DC migration on LN T cell homeostasis, we generated Rag2$^{-/-}$T-huCCR7 bone marrow chimeras. To this end T-huCCR7ki mice were lethally eradiated and reconstituted with either T-huCCR7ki bone marrow (T-huCCR7ki chimeras) or a mixture of 30% T-huCCR7ki and 70% Rag2$^{-/-}$ bone marrow (T-huCCR7ki/Rag2$^{-/-}$). All lymphocytes present in the latter mice are of T-huCCR7ki origin while a considerable part of the non lymphoid hematopoietic cells, including DC, are derived from Rag2$^{-/-}$ progenitors thus carrying the wild type *ccr7* alleles.

Analyzing bone marrow chimeras 8 weeks after reconstitution, we found that LN of T-huCCR7ki/Rag2 chimeras contained significantly increased numbers of CD11c+MHCII high cells compared to mice reconstituted with T-huCCR7 bone marrow solely. Interestingly, in contrast the T-huCCRki chimeras the vast majority of DC present in the T-huCCRki/Rag2 chimeras expressed muCCR7 (Fig. 8A). Furthermore, immunohistology revealed that LN paracortices in T-huCCR7ki/Rag2$^{-/-}$ chimeras are filled with T cells while this area in LN of mice that were reconstituted with bone marrow from T-huCCR7ki solely are still devoid of T cells (Fig. 8B). A flow cytometry based analysis confirmed strongly increased T cell counts in ThuCCR7ki/Rag2$^{-/-}$ chimeras (Fig. 8C) and revealed a regular T/B cells ratio of 2.7/1 which is close to the one found in B6 mice (Fig. 8D).

Based on the observation that the paracortex of LN from T-huCCR7ki/Rag2$^{-/-}$ bone marrow chimeras was filled with T cells, we speculated that the continuous homing of DC to LN not only might affect T cell homing but also the LN dwell time of T cells. To test this hypothesis we analyzed how fast T cells leave skin-draining LN of wild type and T-huCCR7ki mice. To that end, pooled lymphocytes from wild type spleen and LN, containing approximately equal numbers of B and T cells, were TAMRA-labeled and adoptively transferred to wild type and T-huCCR7ki recipients. After 20 hrs half of the animals of each group were sacrificed while the remaining recipients received i.v. anti-L-selectin antibodies for 14 h to prevent further homing of re-circulating lymphocytes before they were analyzed. Analyzing the number and type of adoptively transferred T and B cells that homed to wild type LN before applying the anti-L-selctin mAb, we found that T and B cells were present at a ratio of 3.75:1 indicating that the adoptively transferred cells reached a steady state situation in wt LN since this ratio of T/B cells was rather similar to the one observed for endogenous cells (data not shown). In contrast, in LN of T-huCCR7ki mice the ratio of T/B cells was approximately 2:1 indicating that the environment that accounts for LN T cells homeostasis differs considerably between the two mouse strains. Analyzing the distribution of T and B cells in LN of mice that were treated for 14 h with the MEL-14 mAb we found that the ratio T/B cells dropped from 3.75:1 to 3.14:1 in wild type recipients while the ratio of T/B cells decreased from 2:1 to 0.6:1 in T-huCCR7ki mice (Figure 8E). Comparing the absolute cell count of adoptively transferred T cells in untreated or Mel-14 treated mice, we found a 55% reduction in wild type recipient following antibody treatment while a 75% reduction was observed in T-huCCR7ki. In both recipients, B cell count dropped by 16% following Mel-14 treatment (data not shown). Together these data indicate that T cells are less efficiently retained in the LN of T-huCCR7ki mice compared to wild type mice. To test whether ICAM-1 is involved in retaining T cells within LN wild type mice were treated as described above with the modification that one group received in addition to the MEL-14 mAb also an neutralizing anti-ICAM-1 mAb. Of interest, flow cytometry revealed that the T/B ratio was lowest in the anti-ICAM-1 treated group indicating that ICAM-1 indeed provided signals that retain T cells in LN (Fig. 8E).

DC bind stromal cell-derived CCL21.

Based on the above described results and due to the observation that T-huCCR7ki T cells accumulate in the T zone of T-huCCR7ki/Rag2$^{-/-}$ chimeras we speculated that non T cell factors might be responsible for the reduced dwell time observed in T-huCCR7ki mice. Since CCR7 expression on T cells has recently be described to affect retention in T cells we analyzed the expression of CCL21 in the above described T-huCCR7ki/Rag2$^{-/-}$ and T-huCCR7ki chimeras. Applying anti-CCL21 antibodies and immunohistology our quantitative morphometric expression analysis over the entire LN section revealed a two fold increase of CCL21 expression per pixel in T-huCCR7ki/Rag2$^{-/-}$ compared to T-huCCR7ki chimeras (Fig. 9B). While in both groups CCL21 was amply expressed on HEV, LN stromal cells of T-huCCR7ki/Rag2$^{-/-}$ chimeras showed considerably higher staining with the anti CCL21 Ab compared to the T-huCCR7ki chimeras (Fig. 9A). Since LN of T-huCCR7ki/Rag2$^{-/-}$ harbor skin-derived DC we hypothesized that skin derived DC might induce increased CCL21 expression in LN. We therefore assessed the expression of CCL21 in draining LN of T-huCCR7ki mice that s.c. received immature DC or PBS 4 days earlier and found an more than two-fold increase per LN in the group that received the DC (Fig. 9C). Since LN DC do not express CCL21 (13) these results strongly indicate that a steady state trafficking of DC from the periphery to the draining LN is required to maintain CCL21 expression on stromal cells which in turn strongly affects the dwell time of T cells within LN. To further substantiate this hypothesis, we took advantage of transgenic mice that express under the control of the CD11c Promoter the diphtheria toxin receptor (CD11c-DTRtg). Following the application of diphtheria toxin (DT) DC get depleted in these animals (14). Of interest, treatment of these mice with DT also leads to reduced numbers of T cells in the LN as reflected by a 50% reduction of the T/B ratio in the DT-treated group compared to the control group (Fig 9D). We next tested whether the increased expression of CCL21 in the Rag2 bone marrow is due to increased transcription. However, applying qRT-PCR we failed to find increased expression of CCL21 when compared to the expression of the stromal cell-specific expression of gp38 or pdgra mRNA (Fig 10A). Since we did not observe increased numbers of stromal cells in the LN of the Rag2 chimeras compared to the control group (data not shown) these data indicate that increased levels of CCL21 are most likely not due to transcriptional chances. Of interest, immunohistology on B6 LN sections revealed co-staining of CD11c and CCL21 (Fig 10B) suggesting that DC bind CCL21. In order to test this experimentally, we stained bone marrow-derived DC from wild type and CCR7-deficient mice with different concentrations of recombinant CCL21. Applying anti-CCL21 Ab flow cytometry revealed that DC indeed bind CCL21 and that this binding to a large degree does not occur via binding specifically to its receptor since it is also observed in CCR7-deficient DC (Fig 10C). Since mouse DC do not express CCL21 (13) these data collectively indicate that DC bind CCL21 produced by stromal cells thus increasing the amount of CCL21 present within LN.

Discussion

Data derived from CCR7-deficient mice as well as plt mice, which lack the CCR7 ligands CCL19 and CCL21 in lymphoid organs, helped to elucidate the role of this chemokine receptor and its ligands, in promoting immune cell homing, compartmentalization of lymphoid organs as well as cell motility within these structure (2, 6, 15). Furthermore, recent evidence suggests that CCR7 delivers retention signals which keep T cells within the T cell area thus counteracting sphingosin-1-phospate receptor-mediated signals that promote lymphocyte egress from lymph nodes towards afferent lymphatics (12). Using a newly established conditional CCR7 knock-in mouse data obtained in the present study puts another layer of complexity to the biological function of CCR7 for T cell homeostasis. Surprisingly, CCR7 affects T cell homeostasis not only through its direct effect on T cell migration, but also indirectly in controlling homeostatic DC migration. The above results indicate that a CCR7-dependent steady state migration of DC into peripheral lymph nodes is a key event for the maintenance of unperturbed lymph node T cell homeostasis. We provide evidence that steady state trafficking DC are involved at least at two different steps both essentially contributing to lymph node homeostasis. Steady state trafficking DC i) produce VGEF which acts as a growth and differentiation factor for HEV (16), thus allowing the efficient homing of T cells to LN, and ii) DC bind CCL21 produced by T zone stromal cells which, by binding to CCR7, provides retention signals for T cells to stay for prolonged periods of time within lymph nodes.

Secondary lymphoid organs, such as lymph nodes, are essentially involved in initiating immune responses since they provide a highly organized microenvironment that allows the efficient presentation of peptide antigen presented in the context of MHC by DC and their recognition by T cells carrying a cognate T cell receptor. While the majority of DC is believed not to re-circulated after entering LN via afferent lymphatics, it is well established that naïve T cell leave LN within the order of 8-12 hrs if they are not stimulated. In the steady state the number of T cells entering a given LN plus the number of cells generated through cell division within there by definition equals the number of T cells dying within or leaving this organ. Since neither proliferation nor apoptosis are observed to a large extent in naïve T cells in mice kept under specific pathogen-free conditions the number of cells entering a given LN should be rather similar to the ones leaving it. While it has been well established that different classes of adhesion molecules such as selectins and integrin as well as chemokines and their receptors are essentially involved in LN homing (2, 17) little is known about factors that control lymphocyte egress. Based on gene-targeting in mice and on studies using the immunomodulatory drug FTY720 sphingosin-1-phosphate receptor 1 ($S1P_1$) has been identified a key regulator of lymphocyte egress (18, 19). In vivo, FTY720 is phosphorylated by sphingosin kinase 2 and phosphorylated FTY720 acts as a potent agonist for four of the five sphingosin-1-phosphate receptors including $S1P_1$. $S1P_1$ is abundantly expressed on naïve T cells and has been shown to be vitally required for steady state T cell egress from thymus, spleen and LN (10, 20-23). Furthermore it has been suggested that, on activated T cells, $S1P_1$ is internalized by interacting with CD69 thus allowing for an efficient retention of activated T cells within inflamed LN (24). As a mode of action it seems that LN egress might reflect a $S1P_1$-mediated chemotactic response of T cells towards high levels of S1P present in the efferent lymph fluid within medullary regions or so-called cortical sinusoids present in the T cell area. Interestingly, a recent study showed that CCR7-deficient T cells egress more efficiently from LN than wt T cells, whereas CCR7 over expressing T cells are retained for prolonged periods within LN suggesting that the S1P-egress-promoting signals are counteracted by CCL21 expressed by fibroblastic reticular cells (FRC) present in the T cell zone (12). Data from the present study supports and extents this model since we show that LN of a conditional T-CCR7 knock in strain are lymphopenic which to a large extent is seemingly caused by reduced levels of CCL21 present in the T cell zone which is owed to impaired steady state migrating DC *“presenting”* CCL21 to T cells.

Although we can not formally exclude the possibility that human CCR7 might not work exactly as murine CCR7 in mice, data obtained from the GL-huCCR7 mice strongly indicate that human CCR7 can fully substitute for muCCR7-deficiency. These animals exhibit the same phenotype as their wild type littermates, LN contain normal CD4 and CD8 T cell counts, and T cell zone in LN and spleen are regularly developed (Fig. 2). Both *in vivo* and *in vitro* T cell as well as DC from wild type and GL-huCCR7 mice migrate towards CCR7 ligands with similar efficiency (Fig. 3). Furthermore, in T-huCCR7 mice where expression of CCR7 is restricted to T cells we observed a robust chemotactic response of T towards CCL21 while DC neither migrated *in vitro* nor *in vivo* following FITC skin painting showing that the T-huCCR7 mice express functional CCR7 in T cells but not in DC. Therefore, it was unexpected to see that the T-huCCR7 mice have strongly reduced LN T cell counts (Fig. 5A). Adoptive transfers revealed that considerably less wild type donor cells were present in T-huCCR7 recipients than in wild type recipients 3 hrs after transfer indicating that non T-cell factors might cause LN T lymhopenia in T-huCCR7 mice (Fig 5B). Indeed short term adoptive transfers of wild type donor cells in wild type and T-huCCR7 mice suggest that the latter animals have approximately 30 to 40% less HEV, while those that are present seem to be fully functional (Fig. 6). Under inflammatory conditions, DC have been recently identified as a source for VGEF that triggers vascular growth including proliferation HEV endothelial cells which is associated with increased lymphocyte entry into the LN (16). Data from the present study indicates that also in the steady state DC contribute to HEV endothelial growth. Following subcutaneous injection of immature BM-DC, which produce VEGF to considerable amounts into T-huCCR7 recipients we observed increased numbers of HEV endothelial cells, increased homing of T cells as well as increased expression of VGEF in the draining LN (Fig. 7).

In addition to their effect on HEV, several lines of evidence from the present study support the idea that steady state migrating DC seemingly also effect the dwell time naïve T cells stay within a LN. i) In contrast to T-huCCR7 mice T-huCCR7/Rag2$^{-/-}$ chimeras not only possess a regular frequency LN DC but also a threefold increase of T cells resulting in a strongly increase in the T/B ratio in all peripheral LN. ii) adoptively transferred T cells egress much faster from LN of T-huCCR7 than from wild type recipients, and iii) injection of DT in CD11c-DTRtg mice not only results in the depletion of DC within LN but also in a reduced cellularity within the T cell area resulting in a strongly reduced T/B ratio in these organs. It is still not entirely clear how DC affect the dwell time of T cells but data provided here suggest that the CCL21/CCR7 axis is involved. A recent study failed to demonstrate CCL21 mRNA in LN DC in mice rendering the possibility unlikely that DC serve as a direct source for CCL21 (13). However, since we could show that CCL21 can bind to the surface of DC independent of the presence of CCR7 our data would support a model in which DC ‘present’ CCL21 expressed by stromal cells on their cell surface. We and others could recently reveal that CCL21 provides strong haptokinetic stimuli to T cells (25). Thus decreased levels of CCL21 could therefore influence the migration behavior in particular of such T cells moving during random walk towards cortical or medullary sinusoids where they would be exposed to an egress-promoting S1P gradient.

In this model promigratory CCR7 signals would keep T cells on the FRC network or increase their scanning behavior of dendritic cells thus making them less susceptible to react to the $S1P_1$-mediated egress signal. However, once CCR7 is less efficiently triggered due to reduced availability of CCL21 in the T cell area, T cells are less efficiently retained and, consequently, have a higher chance to leave the LN via efferent lymphatics. This model is supported by Cyster and colleagues showing that CCR7-deficient T lymphocytes egress faster from LN than wt T cells (12).

In a recent in vitro study T cells were reported to exhibit random walk migration on immobilized CCL21 irrespective of the presence or absence of co-immobilized ICAM-1 or VCAM-1. These results would suggest that integrins such as LFA-1 and VLA-4 which have the capacity to bind these adhesion molecules are kept in a non-adhesive state and are thus not involved in random walk migration of T cells in a shear-free environment such as LN parenchyma. However, 2 Photon microscopy revealed that T lymphocytes deficient for LFA-1 or VLA-4 migrate with reduced velocity as well as directionality putting forward the idea that low levels of integrin-mediated adhesion forces might help T cells to stay in contact with FRC and DC to continuously receive haptotactic stimuli. This model is supported by the present study since the application of a neutralizing anti-ICAM mAb results in a considerably reduced dwell time of T cells in LN most likely by preventing the interaction of ICAM-1 with LFA-1.

It is currently unclear whether CCR7 signals are involved in generating such possible low level integrin adhesion forces. Since CCR7 signals together with shear forces induce conformational changes in LFA-1 resulting in high affinity binding to ICAM-1, it theoretically seems possible that the chemokine receptor-intergrin pathway indeed might be involved. Alternatively, T cell receptor-mediated signals could be involved in this process since it is well established that TCR signals modulate integrin function in processes such as the formation of immunological synapses between T cells and DC following cognate interaction. Furthermore, recent evidence suggest that constant TCR signalling provided by endogenous self-peptide/MHC class II contacts are required to preserve the proliferative capacity and the basal motility of CD4 T cells and to keep activity of the small GTPases Rac and Rap1 (26).

Materials and Methods

Construction of humanized CCR7 mice

The targeting construct was generated according to established methods (27) using standard PCR and recombinant DNA technology. A genomic mouse library was screened. As a targeting vector a modified pBlueskript KS was used that already contained a loxP site-flanked neomycin-resistance gene (neo) that is under the control of the phosphoglycerate promotor (pGK). Following the neo-resistance cassette the EMCV-IRES (internal ribosomal entry site; (28) was cloned from the pMT7-REMCVIF into the targeting vector. The cDNA of the human CCR7 gene was positioned downstream of the IRES element separated only by a CC sequence. Upstream of the neo-resistance cassette 2.7 kilobases of genomic DNA containing also the first and the second exon of the murine CCR7 flanked the construct for homologous recombination. This 5'-recombination site ends directly in front of the third exon. For 3'-recombination 2.8 kilobases of genomic DNA beginning at the translation stop codon in the 3rd exon and containing the 3'-UTR region of the endogenous CCR7 gene was inserted into the targeting vector downstream of the human CCR7 gene. The targeting vector was introduced into E14 (genetic strain 129P2Ola/Hsd) embryonic stem (ES) cells by electroporation, and G418 resistant ES cell-clones were selected after standard protocol as described (Torres, R.M. & Kühn, R. Laboratory protocols for conditional gene targeting (OxfordUniversity Press, Oxford, 1997). In short, homologous recombinants were screened by digestion of the genomic ES cell DNA with the restriction enzyme BamHI (New England BioLabs) followed by a southern blot using a external 5'-probe. An external 3'-probe was used in a second southern blot after digestion with EcoRI (New England BioLabs).

Chimeric mice were generated by injecting homologously recombinated ES cells into Balb/C blastocyst. Chimeric males were crossed to Balb/C mice. Germline transmission was detected by scoring of coat colour. Mice carrying the homologous recombinated construct homocygously were crossed to a deleter strain (C57BL/6-rosa26(SA-CrepA) expressing Cre ubiquitously. Furthermore, mice carrying the targeted allele were back-crossed to C57BL/6 and then crossed to a deleter strain expressing Cre under the control of a CD4 Promotor (CD4Cre; (29, 30). Mice were genotyped by PCR for the presence or absence of neo, IRES, and Cre (Fig. 1D). In experiments described in figures 1 to 3 littermates were used on a mixed 129SV x

C57BL/6 x Balb/c background or 129SV x Balb/C, respectively. All other experiments were performed with mice on a C57BL/6 background. All animals were bred under standard conditions in specific pathogen-free mouse facilities. All mice homocygous for the integrated construct or after crossing to the Cre-deleter strain were healthy and bred well.

Antibodies

The following antibodies and conjugates were used in this study: rat anti-human CCR7 mAb (clone 3D12), rat anti-mouse CCR7 (clone 4B12), anti-CD4-PerCp, anti-MHCII(I-A^b), anti-CD11c-biotin, anti-Meca79 (BD Biosciences), anti-CD19-FITC (Southern Biotechnologies), anti-CD62L-PE (Caltag), anti-CD31-PE (Pharmingen), anti-CD3 (clone 17A2), anti-B220-Cy3 (clone TIB 146) anti-IgD (clone HB250) and anti-CD8-FITC (clone RM CD8) antibodies were provided by Elisabeth Kremmer (GSF München, Germany). Biotinylated antibodies were recognized by streptavidin coupled to Alexa°488 (Molecular Probes). Unconjugated anti-human and anti-mouse CCR7 antibodies were revealed by mouse anti-rat-Cy5 (Jackson Laboratories). FITC-, Cy3- and Cy5-conjugates of anti-IgD, anti-CD3 and anti-CD8b antibodies were prepared as recommended by the manufacturer (Amersham).

Flow cytometry

To obtain single-cell suspensions of lymph nodes and spleen, organs were minced through a nylon mesh and washed with PBS supplemented with 3% FCS. Erythrocytes of blood and spleen were lysed by using a buffer containing ammonium chloride (1.7M), potassium hydrogen carbonate (100mM) and EDTA (1mM). For LN preparation containing endothelial cells of the HEV, LN were treated with 564 U/ml collagenase type 2 (Worthington Biochemical) + 40µg/ml DNase I (Sigma-Aldrich) for 30 min at 37°C. The cell suspension was resuspended 40 times using a Pasteur pipette. EDTA was added to a final concentration of 10 mM EDTA and cells were incubated for additional 5 min at 37°C. After passing cell suspension through a 70-µm filter, cells were stained with antibodies as described above and analyzed by using a FACSCalibur or LSRII (BD Biosciences).

Immunohistology and measurement of high endothelial venules length

Organs were embedded in OCT and 8 µm cryosection were made. Section were air dried and fixed in ice-cold acetone for 10 min and stained with indicated antibodies as described earlier (31). Slides were analyzed with an Axiovert 200M microscope and Axiovision software (Carl Zeiss) or an IX81 microscope and analySIS^D software (Olympus). HEV length and LN section area calculated using ImageJ software.

in vitro differentiation and transfer of DC

2 x 10^6 bone marrow cells from tibia and femur of C57/BL6, Rag2$^{-/-}$ and T-huCCR7ki mice were cultured in RPMI 1640, 10% FCS, β-ME, glutamine, and penicillin/streptomycin supplemented with 100–200 ng/ml GM-CSF produced by a recombinant cell line for 8 days. Cells were matured for 2 additional days with 1 µg/ml PGE_2 (Sigma-Aldrich) and 30 ng/ml TNF-α (PeproTech). For DC transfer immature BMDC were gathered at day 8, labeled with 5µM CFSE and 1-3x10^6 BMDC were injected s.c. in the femoral leg, the flank of the mice, and the footpad. 5 days after injection mice were sacrificed and the popliteal, axilary and inguinal lymph nodes were analyzed by flowcytometry and immunohistolgy.

Chemotaxis assay and *in vitro* inhibition

1x10^6 Splenic cells or *in vitro* differentiated BMDC were resuspended in 100µl RPMI and loaded in collagen-coated transwells (Corning BV, 5 µm pore size) that were placed in 24-well plates containing 400µl medium or medium supplemented with 100nM to 300 mM CCL21. After incubation for 3h at 37°C, cells migrated were collected, counted, and stained with mAb to determine the number of migrated T cells by flow cytometry.

Skin painting

The skin of the ears was painted two times with 0.1% Fluoresceinisothiocyanate (FITC) in acetone/dibutylphthalate (1:1). 24 h later the mice were sacrificed, the facial lymph nodes were isolated, and single cell suspensions were prepared. The frequency of cells positive for CD11c, MHC II and FITC were analyzed by flow cytometry.

in vivo migration

Splenic lymphocytes from wild type, STOP-huCCR7, huCCR7ki and T-huCCR7ki mice were isolated as described above. $2x10^6$ cells/ml were pre-incubated at 37°C for 30 min in RPMI 1640 containing 5% FCS, subsequently incubated with 5 µM CFSE or TAMRA for 10 min at 37°C and washed in ice-cold PBS with 3% FCS. $5x10^6$ cells of each color were mixed and i.v. transferred into the tail vein of recipients. 3 h later, mice were sacrificed and lymphocytes were isolated from different LN and spleen. The ratio or total number of recovered CFSE- and TAMRA-labeled T cells was determined by flow cytometry. Ratios obtained were corrected for the ratio present in the injected mixtures.

For analyzing the location of T cells in relation to HEV position T cells of C57BL/6 donors were enriched by MACS-sorting using biotinylated anti-B220 mAb and streptavidin-beads (Miltenyi). $1x10^6$ Tamar-labeled T cells were i.v. transferred in C57BL/6 wild type and T-huCCR7ki recipients. 30min later, mice were sacrificed, the LN isolated and frozen in OCT. 8 µm sections were anaylzed by immunohistology.

Stable bone marrow chimeras.

Bone marrow was prepared from femurs and tibiae of T-huCCR7ki and $Rag2^{-/-}$ mice followed by separation on Lympholyte M. Recipients for bone marrow transplantation were 6–8 wk-old sex-matched T-huCCR7ki mice. Before transplantation, adult recipient mice were lethally irradiated (5 Gy) twice at an interval of 4 h. Approximately 1.5×10^7 bone marrow cells were transferred to irradiated recipients. For chimeras, 80% $Rag2^{-/-}$ and 20% T-huCCR7ki bone marrow were mixed before transplantation. Control animals received 100% T-huCCR7ki bone marrow cells. 3-4 wk later later, chimeras were shaved and UV-irradiated for 30 min mobilizes dendritic cells of the skin and their progenitors to allow for replacement of these cells. 11–12 wk after transplantation chimeric mice were killed, and lymph nodes were harvested and analyzed.

Treatment with blocking antibody.

Some mice received the blocking antibody anti-L-selectin (clone MEL-14) 26 hours after the i.v. transfer of TAMRA labeled lymphocytes. 125 µg anti-L-selectin were injected i.v. and 125 µg anti-L-selectin were injected i.p. in these mice. 16 hours later mice were killed, and lymph nodes were harvested and analyzed. In some experiments mice also i.v. received 125µg of an neutralizing anti-ICAM mAb.

Figure 1

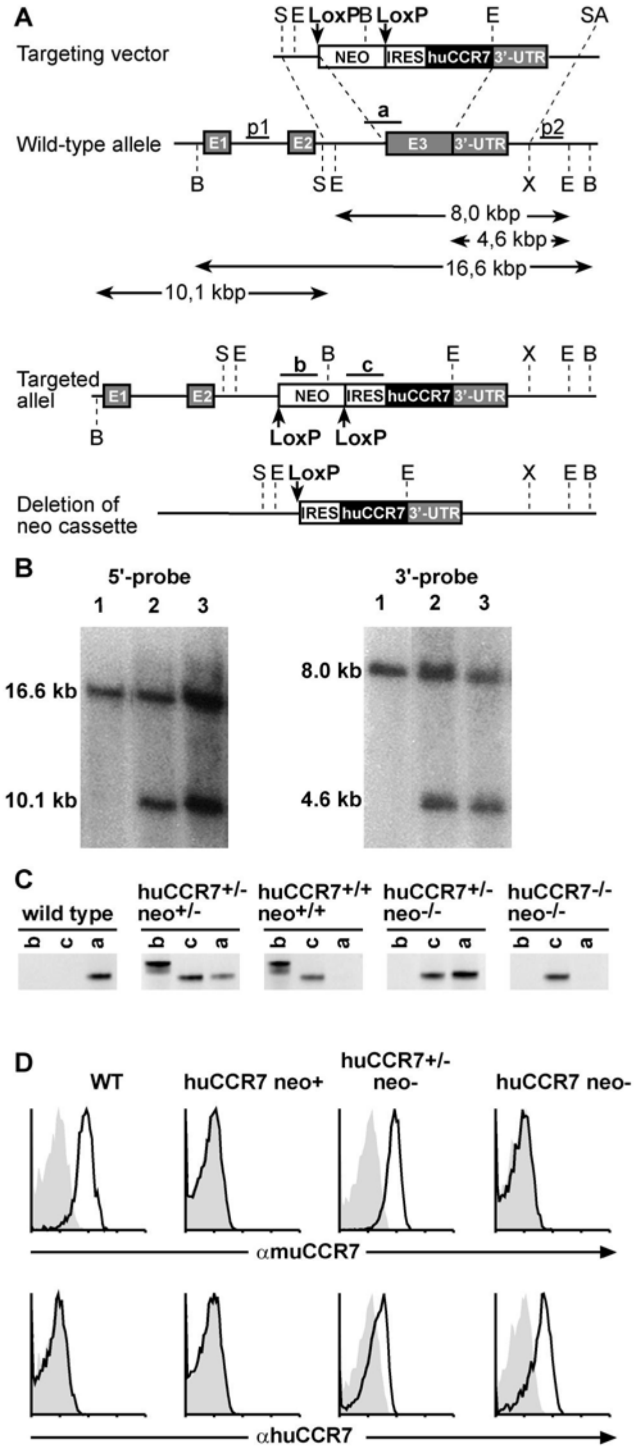
A
S E LoxP B LoxP E SA
Targeting vector
NEO
IRES
huCCR7
3'-UTR
a
p1
p2
Wild-type allele
E1
E2
E3
3'-UTR
B
S E
X E B
8,0 kbp
4,6 kbp
16,6 kbp
10,1 kbp
S E
b
B
c
E
X E B
Targeted allel
E1
E2
NEO
IRES
huCCR7
3'-UTR
B
LoxP LoxP
S E LoxP
E
X E B
Deletion of neo cassette
IRES
huCCR7
3'-UTR
B
5'-probe
1 2 3
16.6 kb
10.1 kb
3'-probe
1 2 3
8.0 kb
4.6 kb
C
wild type
huCCR7+/- neo+/-
huCCR7+/+ neo+/+
huCCR7+/- neo-/-
huCCR7-/- neo-/-
b c a
b c a
b c a
b c a
b c a
D
WT
huCCR7 neo+
huCCR7+/- neo-
huCCR7 neo-
αmuCCR7
αhuCCR7

Figure 2

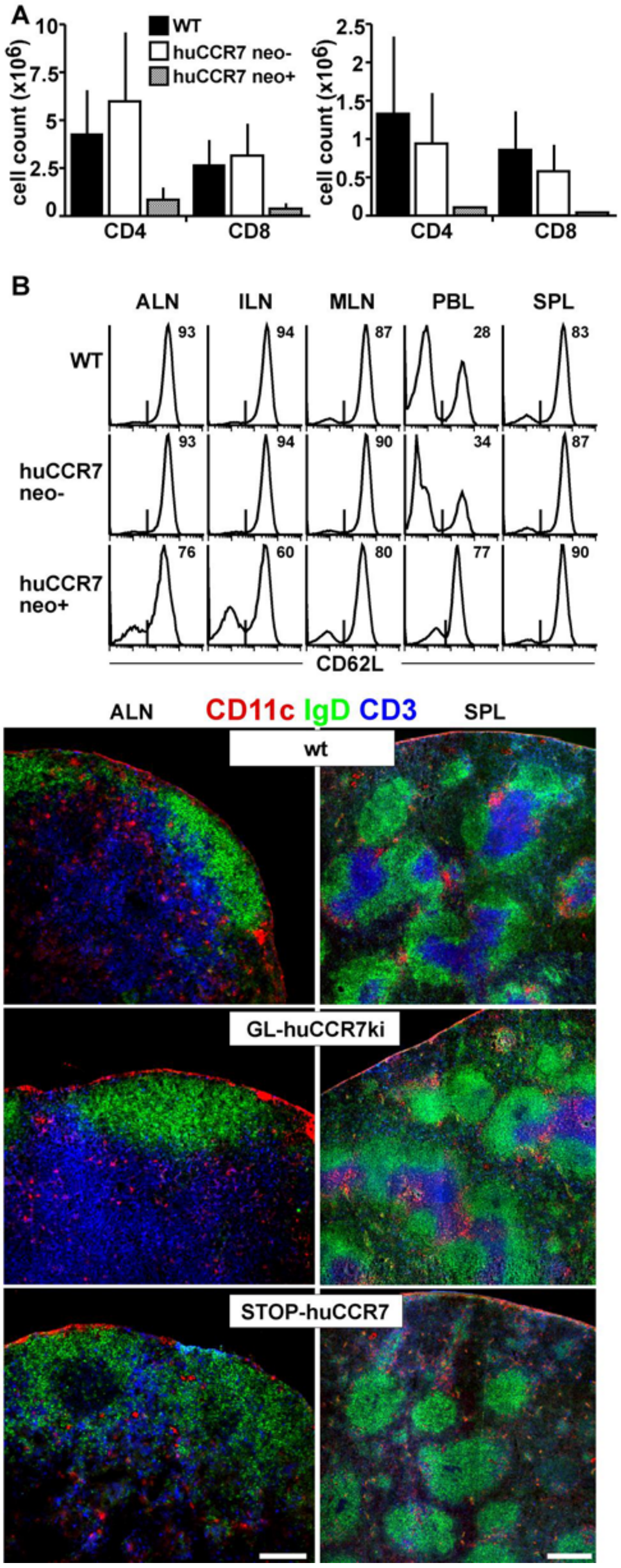
A
cell count (x10^6)
10
7.5
5
2.5
0
CD4
CD8
WT
huCCR7 neo-
huCCR7 neo+
cell count (x10^6)
2.5
2
1.5
1
0.5
0
CD4
CD8
B
ALN
ILN
MLN
PBL
SPL
WT
93
94
87
28
83
huCCR7 neo-
93
94
90
34
87
huCCR7 neo+
76
60
80
77
90
CD62L
ALN
CD11c IgD CD3
SPL
wt
GL-huCCR7ki
STOP-huCCR7

Figure 3

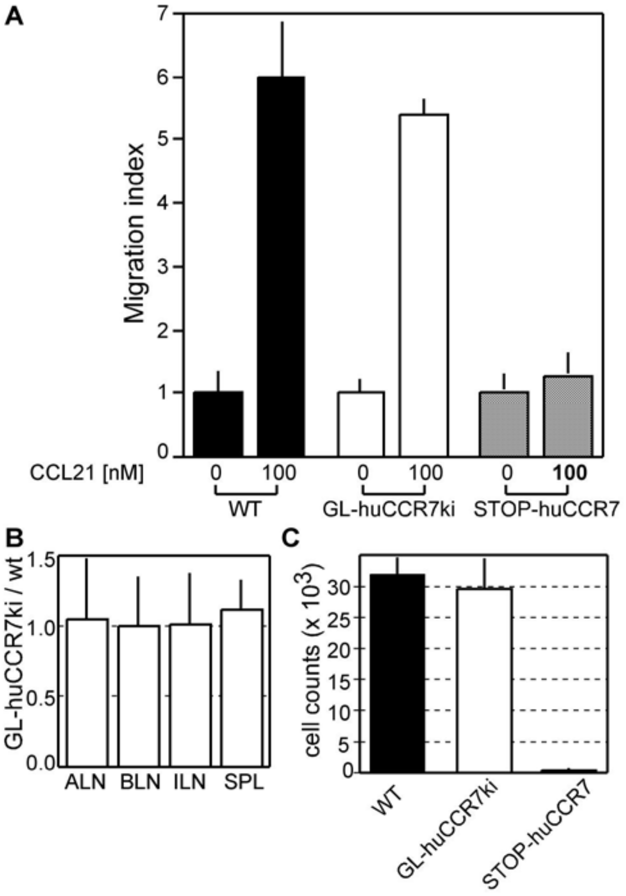
A
Migration index
7
6
5
4
3
2
1
0
CCL21 [nM]
0
100
WT
0
100
GL-huCCR7ki
0
100
STOP-huCCR7
B
GL-huCCR7ki / wt
1.5
1.0
0.5
0.0
ALN
BLN
ILN
SPL
C
cell counts (x 10³)
30
25
20
15
10
5
0
WT
GL-huCCR7ki
STOP-huCCR7

Figure 4

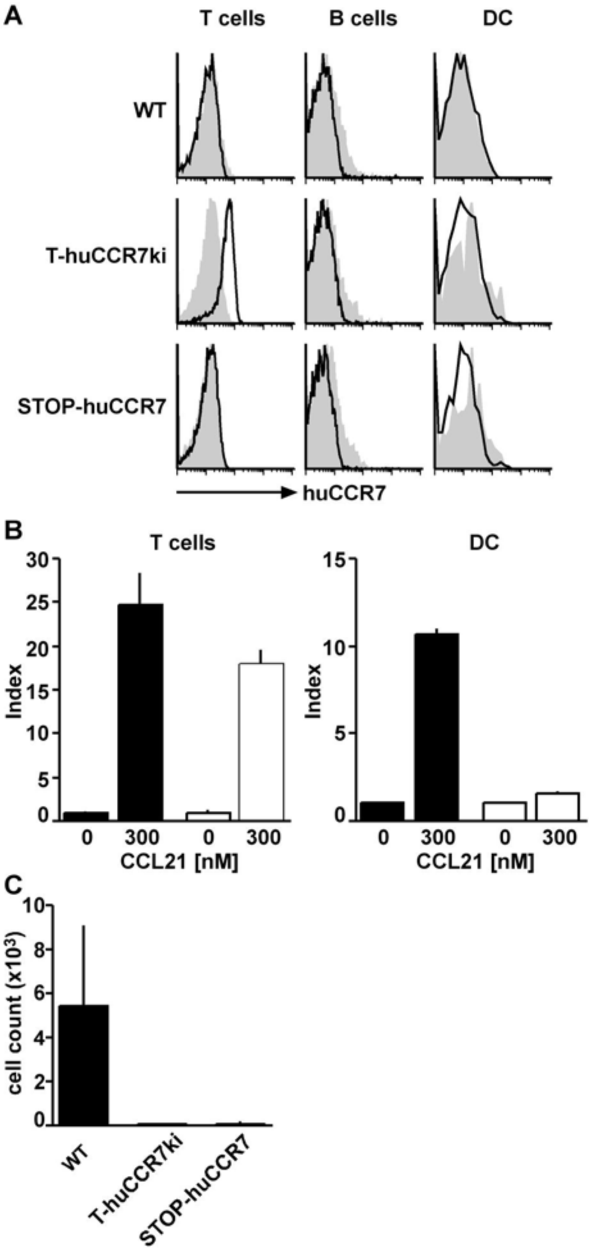
A
T cells
B cells
DC
WT
T-huCCR7ki
STOP-huCCR7
huCCR7
B
T cells
DC
Index
30
25
20
15
10
5
0
0
300
0
300
CCL21 [nM]
Index
15
10
5
0
0
300
0
300
CCL21 [nM]
C
cell count (x10^3)
10
8
6
4
2
0
WT
T-huCCR7ki
STOP-huCCR7

Figure 5

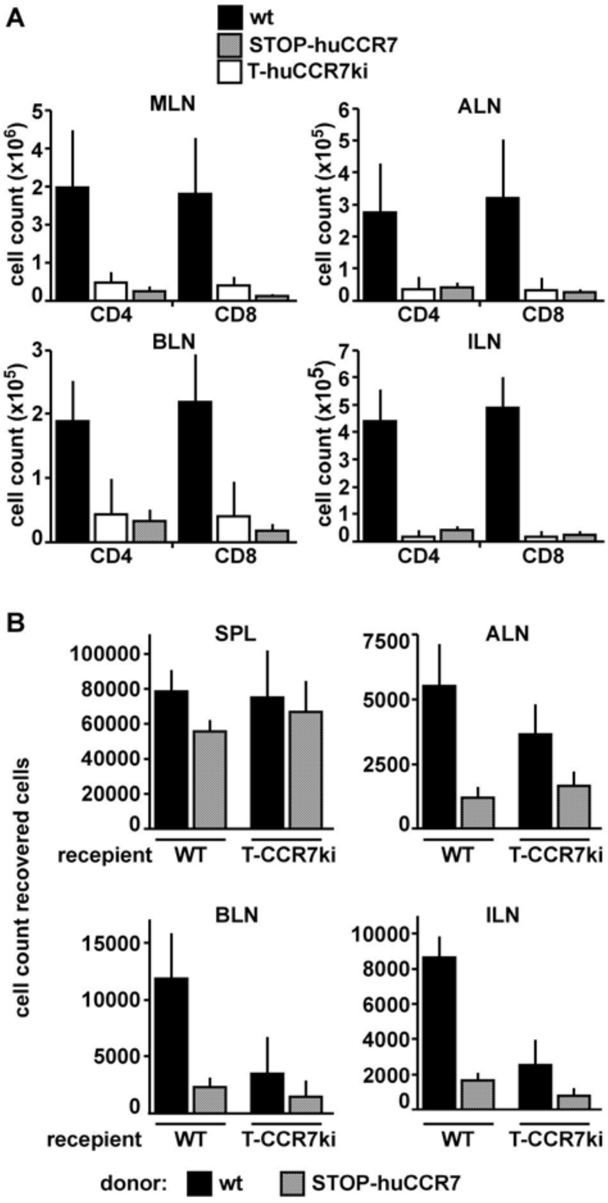
A
wt
STOP-huCCR7
T-huCCR7ki
MLN
cell count (x10^6)
5
4
2
3
1
0
CD4
CD8
ALN
cell count (x10^5)
6
5
4
3
2
1
0
CD4
CD8
BLN
cell count (x10^5)
3
2
1
0
CD4
CD8
ILN
cell count (x10^5)
7
6
5
4
3
2
1
0
CD4
CD8
B
cell count recovered cells
SPL
100000
80000
60000
40000
20000
0
recepient
WT
T-CCR7ki
ALN
7500
5000
2500
0
WT
T-CCR7ki
BLN
15000
10000
5000
0
recepient
WT
T-CCR7ki
ILN
10000
8000
6000
4000
2000
0
WT
T-CCR7ki
donor:
wt
STOP-huCCR7

Figure 6

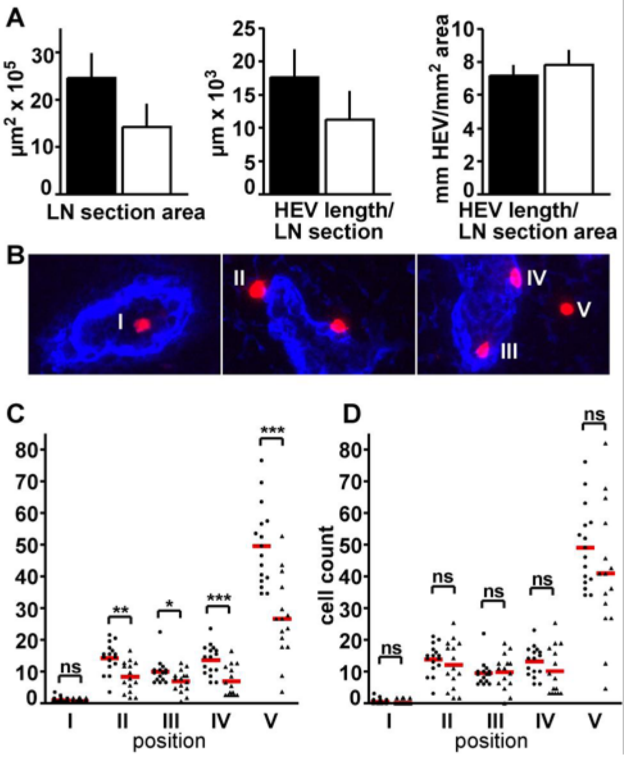
A
μm² x 10⁵
0
10
20
30
LN section area
μm x 10³
0
5
10
15
20
25
HEV length/
LN section
mm HEV/mm² area
0
2
4
6
8
10
HEV length/
LN section area
B
I
II
III
IV
V
C
0
10
20
30
40
50
60
70
80
ns
**
*
***
***
I
II
III
IV
V
position
D
cell count
0
10
20
30
40
50
60
70
80
ns
ns
ns
ns
ns
I
II
III
IV
V
position

Figure 7

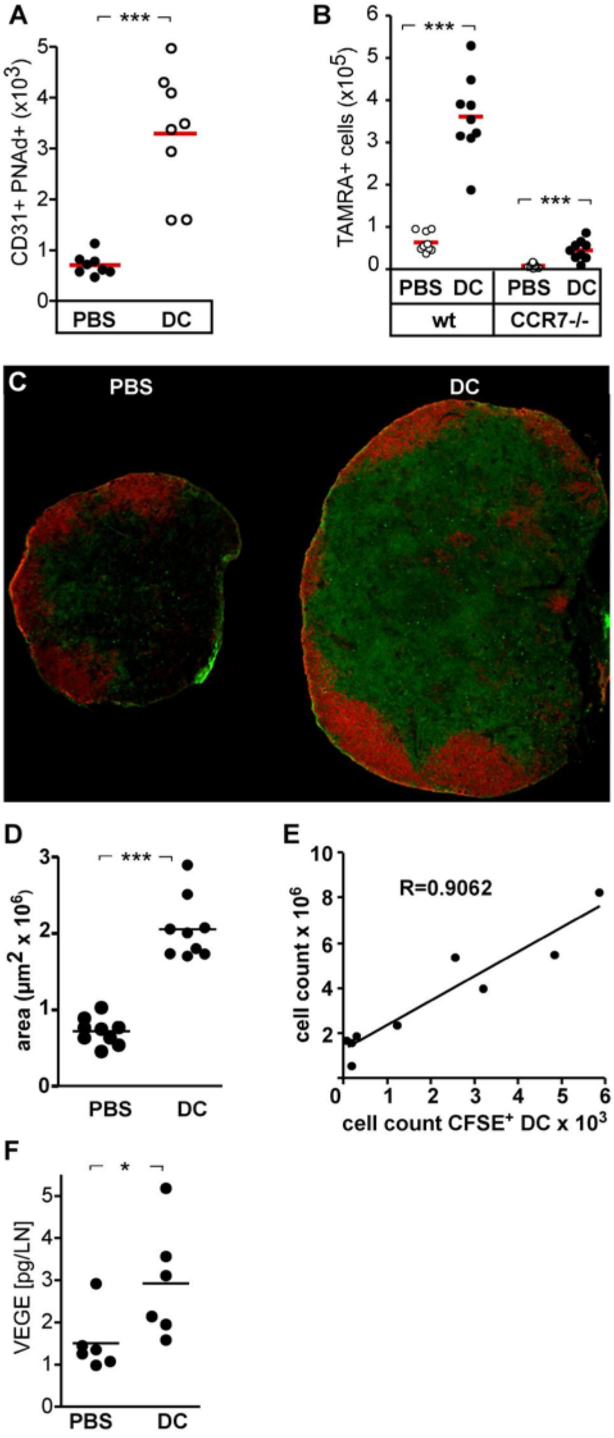
A
***
CD31+ PNAd+ (x10^3)
0
1
2
3
4
5
PBS
DC
B
***
***
TAMRA+ cells (x10^5)
0
1
2
3
4
5
6
PBS
DC
PBS
DC
wt
CCR7-/-
C
PBS
DC
D
***
area (µm^2 x 10^6)
0
1
2
3
PBS
DC
E
R=0.9062
cell count x 10^6
cell count CFSE+ DC x 10^3
0
1
2
3
4
5
6
2
4
6
8
10
F
*
VEGE [pg/LN]
0
1
2
3
4
5
PBS
DC

Figure 8

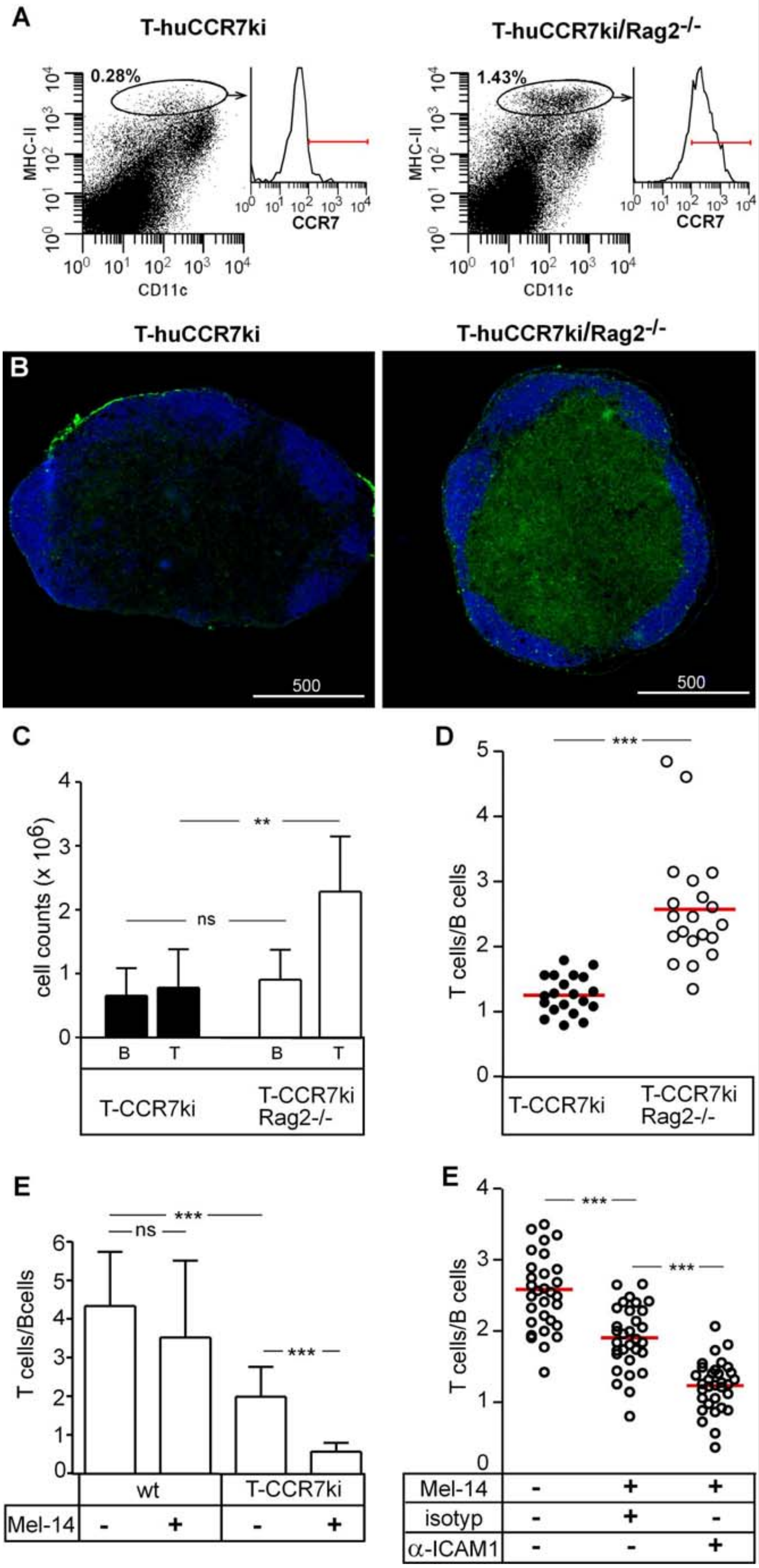
A
T-huCCR7ki
T-huCCR7ki/Rag2-/-
0.28%
1.43%
MHC-II
CD11c
CCR7
B
T-huCCR7ki
T-huCCR7ki/Rag2-/-
500
500
C
cell counts (x 10^6)
**
ns
B
T
B
T
T-CCR7ki
T-CCR7ki Rag2-/-
D
***
T cells/B cells
T-CCR7ki
T-CCR7ki Rag2-/-
E
***
ns
***
T cells/Bcells
wt
T-CCR7ki
Mel-14 - + - +
E
***
***
T cells/B cells
Mel-14 - + +
isotyp - + -
α-ICAM1 - - +

Figure 9

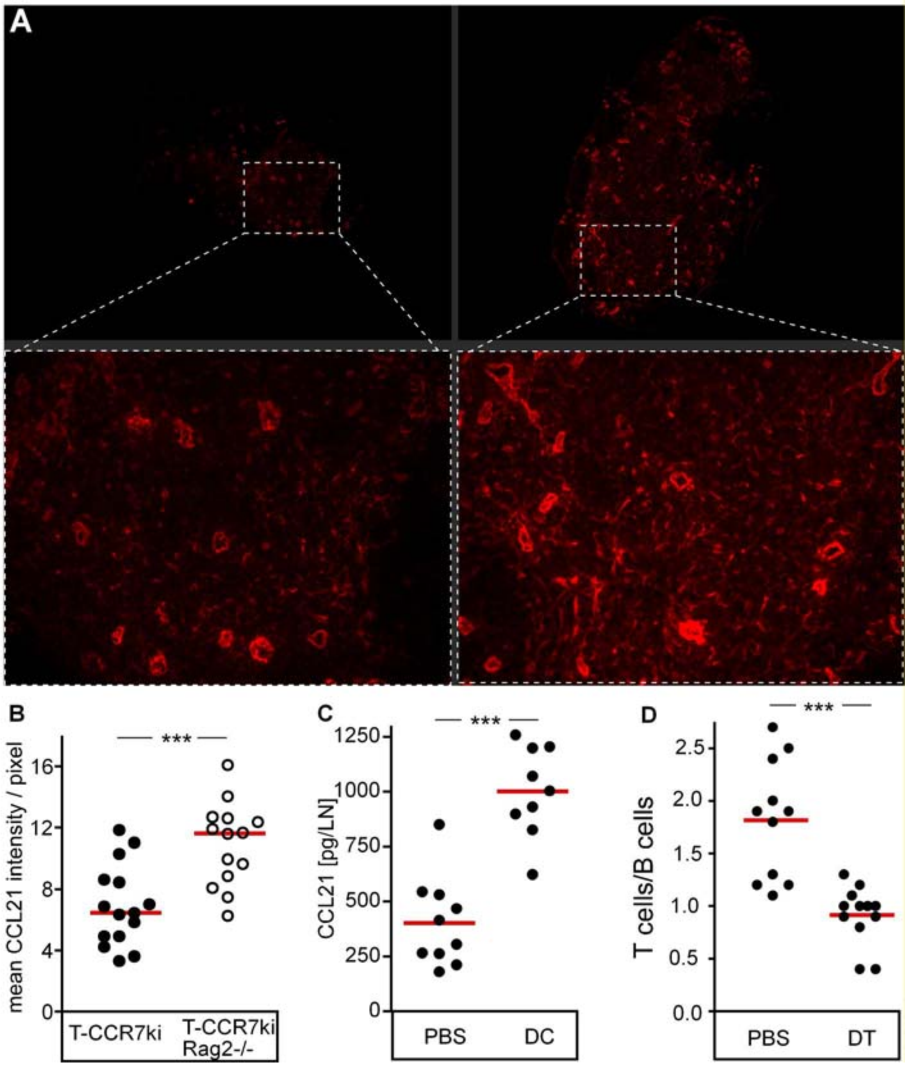
A
B
mean CCL21 intensity / pixel
0
4
8
12
16
***
T-CCR7ki
T-CCR7ki Rag2-/-
C
CCL21 [pg/LN]
0
250
500
750
1000
1250
***
PBS
DC
D
T cells/B cells
0.0
0.5
1.0
1.5
2.0
2.5
***
PBS
DT

Figure 10

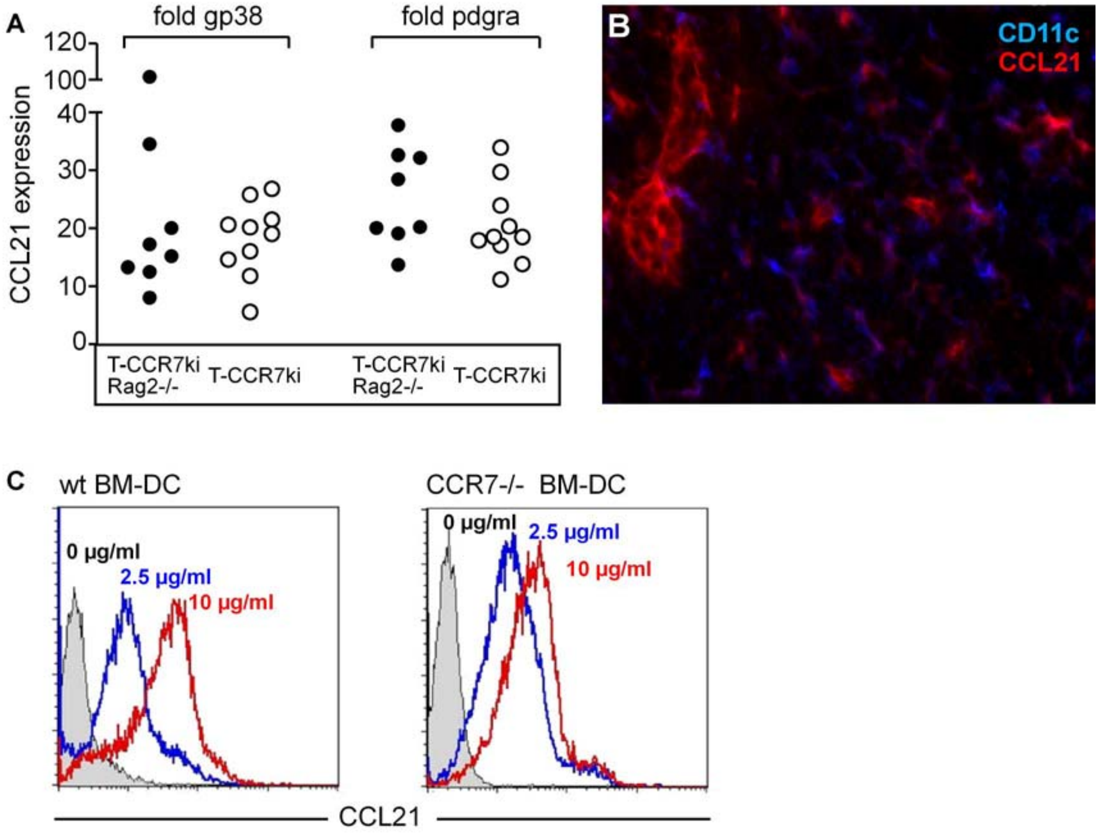
A
fold gp38
fold pdgra
CCL21 expression
120
100
40
30
20
10
0
T-CCR7ki Rag2-/-
T-CCR7ki
T-CCR7ki Rag2-/-
T-CCR7ki
B
CD11c
CCL21
C
wt BM-DC
0 µg/ml
2.5 µg/ml
10 µg/ml
CCR7-/- BM-DC
0 µg/ml
2.5 µg/ml
10 µg/ml
CCL21

Legends to figures

Figure 1.

Generation of humanized CCR7 mice

(A) Cloning strategy. The diagrams show the targeting vector with the loxP-flanked neo resistance cassette; the locus of the murine *ccr7*, and the targeted allele before and after loxP-mediated *in vivo* excision of the neo-resistance cassette. Open boxes indicate the neo-resistance cassette and the EMCV-IRES; the black box indicates human *CCR7* cDNA, while the grey boxes indicate the three exons of the murine ccr7 allele as well as the 3'-UTR. Vertical arrows mark the loxP-recognition sites. Horizontal arrow show the length of the various fragments following digestion with restriction enzymes used for the southern blot analysis. The probes p1 and p2 are used for southern blot analysis, whereas a, b, and c depict products of PCR genotype analysis. Restriction sites: E, EcoRI; B, BamHI; S, SalI; SA, SacII; X, XhoI.

(B) Southern blot analysis of recombinant embryonic stem cell DNA from 3 representative clones. DNA was either digested with BamHI and hybridized with the 5'-probe p1 or was digested with EcoRI and hybridized with the 3'-probe p2, respectively.

(C) Genotyping of tail DNA by PCR from wild-type, neomycin non-deleted heterozygous (huCCR7$^{+/-}$neo$^{+/-}$), non-deleted homozygous (huCCR7$^{+/+}$neo$^{+/+}$), neomycin-deleted heterozygous (huCCR7$^{+/-}$neo$^{-/-}$) and neomycin-deleted homozygous (huCCR7$^{+/+}$ neo$^{-/-}$) littermates applying primer-pairs specific for fragments a, b, or c as shown in (A).

(D) Flow cytometry of cells isolated from blood of wild-type (WT), huCCR7$^{+/+}$neo$^{+/+}$, huCCR7$^{+/-}$neo$^{-/-}$, and huCCR7 neo- mice and analyzed for the expression of murine CCR7 (upper row) and human CCR7 (lower row). The shaded area depicts the isotype control. Shown are representative results from 4 independent experiments.

Figure 2.

(A) Distribution of CD4 and CD8 T cells in mesenteric (left) and axilary lymph node (right). Lymphocytes were isolated from WT (black column), huCCR7 neo- (open column), and STOPhuCCR7 (hatched column) littermates and stained with antibodies against CD4 and CD8. Absolute cell counts (+SD; Pooled data including 2 to 8 mice.

(B) Flow cytometry of lymphocytes isolated from axilary (ALN), inguinal (ILN), mesenteric lymph node (MLN), peripheral blood (PBL), and spleen (SPL). Cells from WT (top), huCCR7 neo- (middle), and STOPhuCCR7 (bottom) littermates were stained with anti-CD62L and anti-CD3 m Ab. The percentage of CD62L$^+$ T cells is specified. Representative data for 5 mice/ genotype analyzed.

(C-H) Immunohistology of axilary lymph node (ALN) and spleen (SPL) of wild type (C, D), GL-huCCR7ki (E, F), and STOP-huCCR7 (G, H) mice. 8µm cryosections of 6-8 week-old mice were stained with antibodies indicated. Shown are sections representative for 6 animals analyzed per genotype.

Figure 3.

(A) Chemotaxis assay of lymphocytes towards the chemokine CCL21. Lymphoytes isolated from spleen of wild-type (WT; black columns), GL-huCCR7ki (open columns), and STOP-huCCR7 (hatched columns) mice were analyzed for their ability to migrate towards CCL21 (0 or 100 nM) within 3h. Shown is the migration index (mean of triplicates +SD) of one representative experiment of five performed.

(B) *In vivo* migration of mouse lymphocytes expressing huCCR7. Lymphocytes isolated from WT and GL-huCCR7ki mice were labeled with different fluorescent dyes (TAMRA, CFSE) and injected i.v. into WT mice. After 3 hrs cells were isolated from ALN, BLN, ILN, and SPL were stained for CD3-expression. The ratio (+SD) of recovered CD3$^+$ of GL-huCCR7ki and wt origin is shown (n=8 recipients).

(C) FITC-skinpainting. Both ears of mice with the indicated genotype were painted with FITC solution. 24h later single-cell suspensions of the ear-draining facial lymph nodes were prepared and analyzed by flow cytometry. Shown are absolute cell counts (+SD) of FITC$^+$CD11c$^+$MHCII$^+$ cells (n = 4 mice per group; representative data from one of two experiments performed)

Figure 4.

(A) Expression of huCCR7 on blood CD4$^+$ T cells and spleen CD11c$^+$ DC from wild-type (WT), T-huCCR7ki, and STOP-huCCR7.

(B) Chemotactic migration of T cells (left) and dendritic cells (DC; right) towards CCL21. Lymphocytes, isolated from peripheral lymph nodes, and mature bone marrow DC from WT (black column) and T-huCCR7ki (open column) migrated for 3h towards medium alone (0) or 300 nM CCL21 (mean +SD; n=3).

(C) FITC-skinpainting. Mice were painted with FITC solution. 24h later single-cell suspensions of the facial lymph node of WT, T-huCCR7ki, and STOP-huCCR7 mice were analyzed by flow cytometry. Shown are the cell numbers for the recovered FITC$^+$CD11c$^+$MHCII$^+$ cells (mean +SD, n = 8 lymph nodes of 4 mice/genotype).

Figure 5.

(A) Distribution of CD4$^+$ and CD8$^+$ T cells in mesenteric (MLN), axilary (ALN), brachial (BLN), and inguinal lymph node (ILN) of WT (black columns), T-huCCR7ki (open columns), and STOP-huCCR7 (hatched columns) mice. Absolute cell counts were determined for CD4+ and CD8+ T cells (mean +SD; n = 3 mice/genotype; 1 representative of 4 experiments performed)

(B) Cells isolated from peripheral lymph nodes and spleen of WT (black column) and T-huCCR7ki (hatched column) were labeled with TAMRA and CFSE, respectively. Labeled cells were i.v. transferred to WT or T-huCCR7ki recipients as indicated. 3h after injection the mice were sacrificed and lymphocytes were isolated from SPL, ALN, BLN, and ILN to recover transferred cells. Absolute cell count of recovered CD3$^+$ lymphocytes are shown (mean +SD; n = 4 recipients/group).

Figure 6.

(A) Measurement of high endothelial venule (HEV) length and lymph node (LN) section area in WT (black columns) and T-huCCR7ki (open columns) mice. ILN cryosections were stained with anti-CD31 and Meca79 mAb and DAPI and analyzed by fluorescent microscopy and morphometry. Based on DAPI staining the LN section area (left panel) has been determined. The length (µm) of the HEV has been determined on the basis of CD31$^+$Meca79$^+$ endothelial cells (middle panel). The right panel indicates the length of the HEV in relation to the section area of the LN (mean +SD; n = 16 section derived from 8 ILN per group)

(B) Adoptive transfer of WT T cells in WT and T-huCCR7ki mice. Lymphocytes were isolated from peripheral LN and spleen of WT mice, pooled, and MACS-sorted for T cells. After labeling with TAMRA, T cells were injected into the tail vein for 30 min. 8µm cryosections of the ILN of recipients were stained with anti-CD31 and Meca79 mAb. The micrographs display the positions (I to V) of labeled T cell that were analyzed in (C). I: inside HEV without obvious contact to endothelial cells; II: attached to the luminal surface of HEV; III: between HEV endothelial cells; IV: attached to the abluminal surface of HEV; V: in the LN without obvious contact to HEV.

(C) Cell count of transferred T cells in ILN of WT (dots) and T-huCCR7ki (triangles). The left panel shown Cell counts of transferred T cells are shown per LN section (left panel) or LN section area (right panel; dots and triangles indicate individual sections, and red bars mean values obtained from 16 sections of 8 ILN per genotype.)

Figure 7.

(A) Immature BM-DC were injected s.c. into the right and PBS into the left flank and foot pad of CCR7-deficient mice. 5 days later the number of CD31$^+$MECA79$^+$ cells in the popletial and inguinal LN have been determined. (B) Same as (A) but these mice additionally i.v. received TAMRA-labeled WT or CCR7$^{-/-}$ lymphocytes. After 30 min mice were killed, inguinal, brachial and popletial lymph nodes were analyzed. Dots indicate LN pairs, red bar mean values.

(C) Immunohistology of popletial LN of T-huCCR7ki mice 5 days after s.c. injection of immature BM-DC into the footpad. 8µm cryosections of 6–8-wk-old mice were stained with antibodies against CD3 (green) and B220 (red). Shown are sections representative for 6 LN analyzed per group.

(D) Analysis of the section area of popletial LN in T-huCCR7ki mice 5 days after s.c. injection of PBS (open circles) or immature BM-DC (filled circles) into the footpad. Dots indicate LN from 9 mice, red bars indicate mean values.

(E) immature BM DC were labeled with CFSE and then injected s.c. in the flank and footpad of T-huCCR7ki mice. After 5 days the cellularity of the draining LN has been determined and correlated to the number of homed DC. R indicates the correlation constant. Pooled data from 9 PLN of 3 mice. (F) Popliteal LN from mice receiving PBS or DC s.c. into the footpad were harvested at day 5 and analyzed for the expression of VGEF using ELISA.

Figure 8.

(A) Flow cytometry of cells isolated from PLN of T-huCCR7ki mice (left) and T-huCCR7ki/RAG2$^{-/-}$ (right) chimeras. The expression of huCCR7 is shown for MHC-II$^+$ CD11c$^+$ cells.

(B) Immunohistology of peripheral lymph node of T-huCCR7ki (left) and T-huCCR7/Rag1$^{-/-}$ mice. 8µm cryosections of PLN were stained with antibodies against CD3 (green) and B220 (blue).

(C) Lymphocytes were isolated from the PLN of T-huCCR7ki mice (filled circles) and T-huCCR7ki/Rag2$^{-/-}$ chimeras (open circles). The ratio of T cells to B cells is shown.

(A-C) Data of n= 10 mice and 20 PLN, respectively.

(D) Egress of lymphocytes in the PLN of WT and T-huCCR7ki mice. TAMRA labeled WT cells were transferred to WT and T-huCCR7ki mice. 24 hours later one part of the mice was killed as a control while the other part was treated with the L-selectin blocking antibody Mel 14. Another 14 hours later treated mice were sacrificed. Lymphocytes were isolated from PLN and analyzed by flow cytometry. The panel shows the ratio of T cells to B cells in antibody treated and untreated WT and T-huCCR7ki mice. Representative data of one experiment from two experiments performed with 28 mice.

(E) Egress of lymphocytes in the PLN of WT mice. The experimental setup is identical to the one described for (D) with an additional groups receiving anti-ICAM or isotype control antibodies after 24 hrs. Data from 2 independent experiments with 8 mice per group, dots represent individual LN.

Figure 9.

(A) Analysis of CCL21 expression in PLN of T-huCCR7ki mice and T-huCCR7ki/Rag2$^{-/-}$ chimeras. Crysections were stained with an antibody against CCL21 and analyzed for the expression of CCL21 (red).

(B) The panel indicates the mean of CCL21 intensity per pixel of PLN cryosection of T-huCCR7ki mice (filled circles) and T-huCCR7ki/Rag2$^{-/-}$ chimeras (open circles). Each circle represents the intensity per pixel of one PLN cryosection. (C) The amount of CCL21 present in the inguinal LN of T-CCR7ki mice 5 days after the s.c. footpad injection of PBS or DC. (D) CD11c-DTRtg mice received either PBS or DT as indicated. After 5 days animals were sacrificed skin-draining LN were isolated and analyzed for the percentage of T and B cells. Shown are T/B ratios of individual LN.

Figure 10

DC bind CCL21 (A) qRT-PCR analysis for the expression of CCL21 relative to the expression of the stromal specific gp38 and pdgra in LN from T-CCR7ki/ Rag2$^{-/-}$ and

T-CCR7ki bone marrow chimeras. (B) Co-localization of CD11c and CCL21 on Cryosections from LN of B6 mice. (C) Wild type (wt) or CCR7$^{-/-}$ bone marrow derived DC were incubated at 4°C with CCL21 at concentrations indicated. After extensive washing binding of CCL21 to DC was revealed with anti-CCL21 antibodies using flow cytometry

Reference list

1. von Andrian, U. H., and C. R. Mackay. 2000. T-cell function and migration. Two sides of the same coin. *N Engl J Med* 343:1020-1034.
2. von Andrian, U. H., and T. R. Mempel. 2003. Homing and cellular traffic in lymph nodes. *Nat Rev Immunol* 3:867-878.
3. Banchereau, J., and R. M. Steinman. 1998. Dendritic cells and the control of immunity. *Nature* 392:245-252.
4. Steinman, R. M., D. Hawiger, and M. C. Nussenzweig. 2003. Tolerogenic dendritic cells. *Annu Rev Immunol* 21:685-711.
5. Lohr, J., B. Knoechel, V. Nagabhushanam, and A. K. Abbas. 2005. T-cell tolerance and autoimmunity to systemic and tissue-restricted self-antigens. *Immunol Rev* 204:116-127.
6. Forster, R., A. Schubel, D. Breitfeld, E. Kremmer, I. Renner-Muller, E. Wolf, and M. Lipp. 1999. CCR7 coordinates the primary immune response by establishing functional microenvironments in secondary lymphoid organs. *Cell* 99:23-33.
7. Hintzen, G., L. Ohl, M. L. del Rio, J. I. Rodriguez-Barbosa, O. Pabst, J. R. Kocks, J. Krege, S. Hardtke, and R. Forster. 2006. Induction of tolerance to innocuous inhaled antigen relies on a CCR7-dependent dendritic cell-mediated antigen transport to the bronchial lymph node. *J Immunol* 177:7346-7354.
8. Ohl, L., M. Mohaupt, N. Czeloth, G. Hintzen, Z. Kiafard, J. Zwirner, T. Blankenstein, G. Henning, and R. Forster. 2004. CCR7 governs skin dendritic cell migration under inflammatory and steady-state conditions. *Immunity* 21:279-288.
9. MartIn-Fontecha, A., S. Sebastiani, U. E. Hopken, M. Uguccioni, M. Lipp, A. Lanzavecchia, and F. Sallusto. 2003. Regulation of dendritic cell migration to the draining lymph node: impact on T lymphocyte traffic and priming. *J Exp Med* 198:615-621.
10. Pappu, R., S. R. Schwab, I. Cornelissen, J. P. Pereira, J. B. Regard, Y. Xu, E. Camerer, Y. W. Zheng, Y. Huang, J. G. Cyster, and S. R. Coughlin. 2007. Promotion of lymphocyte egress into blood and lymph by distinct sources of sphingosine-1-phosphate. *Science* 316:295-298.
11. Schwab, S. R., and J. G. Cyster. 2007. Finding a way out: lymphocyte egress from lymphoid organs. *Nat Immunol* 8:1295-1301.
12. Pham, T. H., T. Okada, M. Matloubian, C. G. Lo, and J. G. Cyster. 2008. S1P1 receptor signaling overrides retention mediated by G alpha i-coupled receptors to promote T cell egress. *Immunity* 28:122-133.
13. Link, A., T. K. Vogt, S. Favre, M. R. Britschgi, H. Acha-Orbea, B. Hinz, J. G. Cyster, and S. A. Luther. 2007. Fibroblastic reticular cells in lymph nodes regulate the homeostasis of naive T cells. *Nat Immunol* 8:1255-1265.
14. Jung, S., D. Unutmaz, P. Wong, G. Sano, K. De los Santos, T. Sparwasser, S. Wu, S. Vuthoori, K. Ko, F. Zavala, E. G. Pamer, D. R. Littman, and R. A. Lang. 2002. In vivo depletion of CD11c(+) dendritic cells abrogates priming of CD8(+) T cells by exogenous cell-associated antigens. *Immunity* 17:211-220.
15. Worbs, T., T. R. Mempel, J. Bolter, U. H. von Andrian, and R. Forster. 2007. CCR7 ligands stimulate the intranodal motility of T lymphocytes in vivo. *J Exp Med* 204:489-495.
16. Webster, B., E. H. Ekland, L. M. Agle, S. Chyou, R. Ruggieri, and T. T. Lu. 2006. Regulation of lymph node vascular growth by dendritic cells. *J Exp Med* 203:1903-1913.

17. Sackstein, R. 2005. The lymphocyte homing receptors: gatekeepers of the multistep paradigm. *Curr Opin Hematol* 12:444-450.
18. Cyster, J. G. 2005. Chemokines, sphingosine-1-phosphate, and cell migration in secondary lymphoid organs. *Annu Rev Immunol* 23:127-159.
19. Rosen, H., M. G. Sanna, S. M. Cahalan, and P. J. Gonzalez-Cabrera. 2007. Tipping the gatekeeper: S1P regulation of endothelial barrier function. *Trends Immunol* 28:102-107.
20. Mandala, S., R. Hajdu, J. Bergstrom, E. Quackenbush, J. Xie, J. Milligan, R. Thornton, G. J. Shei, D. Card, C. Keohane, M. Rosenbach, J. Hale, C. L. Lynch, K. Rupprecht, W. Parsons, and H. Rosen. 2002. Alteration of lymphocyte trafficking by sphingosine-1-phosphate receptor agonists. *Science* 296:346-349.
21. Matloubian, M., C. G. Lo, G. Cinamon, M. J. Lesneski, Y. Xu, V. Brinkmann, M. L. Allende, R. L. Proia, and J. G. Cyster. 2004. Lymphocyte egress from thymus and peripheral lymphoid organs is dependent on S1P receptor 1. *Nature* 427:355-360.
22. Allende, M. L., J. L. Dreier, S. Mandala, and R. L. Proia. 2004. Expression of the sphingosine 1-phosphate receptor, S1P1, on T-cells controls thymic emigration. *J Biol Chem* 279:15396-15401.
23. Halin, C., M. L. Scimone, R. Bonasio, J. M. Gauguet, T. R. Mempel, E. Quackenbush, R. L. Proia, S. Mandala, and U. H. von Andrian. 2005. The S1P-analog FTY720 differentially modulates T-cell homing via HEV: T-cell-expressed S1P1 amplifies integrin activation in peripheral lymph nodes but not in Peyer patches. *Blood* 106:1314-1322.
24. Shiow, L. R., D. B. Rosen, N. Brdickova, Y. Xu, J. An, L. L. Lanier, J. G. Cyster, and M. Matloubian. 2006. CD69 acts downstream of interferon-alpha/beta to inhibit S1P1 and lymphocyte egress from lymphoid organs. *Nature* 440:540-544.
25. Ziegler, E., M. Oberbarnscheidt, S. Bulfone-Paus, R. Forster, U. Kunzendorf, and S. Krautwald. 2007. CCR7 signaling inhibits T cell proliferation. *J Immunol* 179:6485-6493.
26. Fischer, U. B., E. L. Jacovetty, R. B. Medeiros, B. D. Goudy, T. Zell, J. B. Swanson, E. Lorenz, Y. Shimizu, M. J. Miller, A. Khoruts, and E. Ingulli. 2007. MHC class II deprivation impairs CD4 T cell motility and responsiveness to antigen-bearing dendritic cells in vivo. *Proc Natl Acad Sci U S A* 104:7181-7186.
27. Capecchi, M. R. 1989. Altering the genome by homologous recombination. *Science* 244:1288-1292.
28. Jang, S. K., H. G. Krausslich, M. J. Nicklin, G. M. Duke, A. C. Palmenberg, and E. Wimmer. 1988. A segment of the 5' nontranslated region of encephalomyocarditis virus RNA directs internal entry of ribosomes during in vitro translation. *J Virol* 62:2636-2643.
29. Lee, P. P., D. R. Fitzpatrick, C. Beard, H. K. Jessup, S. Lehar, K. W. Makar, M. Perez-Melgosa, M. T. Sweetser, M. S. Schlissel, S. Nguyen, S. R. Cherry, J. H. Tsai, S. M. Tucker, W. M. Weaver, A. Kelso, R. Jaenisch, and C. B. Wilson. 2001. A critical role for Dnmt1 and DNA methylation in T cell development, function, and survival. *Immunity* 15:763-774.
30. Sawada, S., J. D. Scarborough, N. Killeen, and D. R. Littman. 1994. A lineage-specific transcriptional silencer regulates CD4 gene expression during T lymphocyte development. *Cell* 77:917-929.
31. Pabst, O., H. Herbrand, T. Worbs, M. Friedrichsen, S. Yan, M. W. Hoffmann, H. Korner, G. Bernhardt, R. Pabst, and R. Forster. 2005. Cryptopatches and isolated lymphoid follicles: dynamic lymphoid tissues dispensable for the generation of intraepithelial lymphocytes. *Eur J Immunol* 35:98-107.

3.4 Lebenslauf

Persönliche Daten

Name	Meike Wendland
Adresse	Roderbruchstr. 9a 30655 Hannover
Telefon	0511/9405568
E-Mail	meike.wendland@yahoo.de
Geburtsdatum, -ort	09. Dezember 1976, Burgwedel
Familienstand	verheiratet 1 Kind, Alter: 13 Monate

Hochschulausbildung

06/2002-08/2007	Promotion in der Arbeitsgruppe Prof. Dr. Reinhold Förster am Institut für Immunologie, Medizinische Hochschule Hannover zum Thema: **„Untersuchungen zum Einfluss der Chemokinrezeptoren CCR7 und CCR9 auf die Migration von Immunzellen“**
04/2002	Diplom im Fachbereich Biologie der Technischen Universität Braunschweig. Note: „Sehr gut“ Diplomarbeit am Institut für Biochemie zum Thema: **„Untersuchungen zur Funktion des Zytoskelett assoziierten Proteins Raver1“**
10/1996-05/2002	Studium der Biologie an der Technischen Universität Carolo-Wilhelmina zu Braunschweig

Schulausbildung

1996	Abitur, Note: 2,8
1989 – 1996	Gymnasium Isernhagen, Isernhagen Altwarmbüchen
1987 - 1989	Orientierungsstufe, Isernhagen N.B.
1983 - 1987	Friedrich-Dierks-Schule, Isernhagen H.B.

Hannover, Oktober 2008